Abstract

The withdrawal of the Fennoscandian ice sheet resulted in an excess of meltwater and rapid isostatic uplift in southern Scandinavia which led to the formation and continuous growth of the proglacial Baltic Ice Lake. An increasing altitudinal difference between the North Atlantic and the Baltic Ice Lake was suddenly erased in the end of Younger Dryas when the Baltic Ice Lake finally drained into the sea and dropped 25 m within 1-2 years. Lake Vättern in central southern Sweden is situated right on the edge of this dramatic event constituting the westernmost outpost of the Baltic Ice Lake before the final drainage. Furthermore, its alignment with an old graben structure makes it unusually deep resulting in a very potent sediment trap during the deglaciation. Its exceptionally thick sediment archive (>300 m) holds imprints of paleoenvironmental changes after, during and possibly before the late Weichselian glaciation. Terrestrial ice recession data to the east and particularly to the west of Lake Vättern are abundant but corresponding data from Lake Vättern itself are rare. Here we present the results from a 2012 drilling campaign in southern Lake Vättern where a composite sediment core down to 74 m below lake floor was recovered. The sediment core was analyzed to obtain physical properties, chemical properties of the sediments and chemical speciation of the pore waters. Three lithostratigraphic units were identified on the basis of these analyses and supporting seismic reflection data. These units correspond to the Late Pleistocene to Holocene evolution of Lake Vättern: A lowermost glacial clay unit (U3) accumulated during a pro-glacial Lake Vättern stage, a middle unit of post-glacial clay (U2) deposited during the Yoldia Sea stage and finally an uppermost gyttjaclay (U1) that has been deposited since Lake Vättern became isolated from the Yoldia Sea.. The transition between U3 and U2 marks the widely recognized final drainage of the Baltic Ice Lake. At 54 meter below lake floor (U3) glaciotectonized sediments indicate ice grounding attributed to the ice readvance that formed the Levene ice marginal line. Furthermore, at 33 meter below lake floor (U3) porewater chlorinity data highlight a marine incursion into the Vättern basin that is likely connected to a previously speculated drainage of the Baltic Ice Lake near the Alleröd-Younger Dryas transition.

Sammanfattning

Tillbakadragandet av den skandinaviska inlandsisen åtföljdes av stora mängder smältvatten samt en hastig landhöjning i södra Skandinavien vilka tillsammans möjliggjorde bildandet av Baltiska issjön. Allteftersom ytterligare smältvatten tillkom så ökade nivåskillnaden mellan nordatlanten och den uppdämda issjön. I slutet av Yngre Dryas tappades slutligen Baltiska issjön ut i Nordatlanten och vattennivån sjönk med 25 m på bara några år. Vättern utgjorde under många år Baltiska issjöns västligaste utpost och är som sådan en viktig länk till den dramatiska tidsperioden kring Baltiska issjöns tappning. Vättern är Sveriges näst största sjö och dess geologiska historia domineras av bildandet av den gravsänka där sjön idag återfinns. Den nästan 120 m djupa södra delen av sjön har mer än 300 m mäktiga avsättningar av bottensediment. Dessa sediment utgör ett miljö- och klimatarkiv av vilka de övre 74 m omfattar senglacial till postglacial tid. De understa delarna av bottensedimenten är troligtvis avsatta före den senaste glaciationen, det vill säga före sen Weichsel. I denna avhandling presenteras resultat från en sedimentprovtagning som hösten 2012 genomfördes från en borrplattform ankrad utanför Trånghalla i södra Vättern. Totalt erhölls 74 m av lagerföljden genom kärnprovtagning från borrplattformen med ett HQ-borrsystem anpassat för lösa sediment. Sedimentlagerföljden har beskrivits och analyserats med avseende på fysikaliska och kemiska egenskaper. Tillsammans med reflektionsseismiska data identifierades tre litostratigrafiska enheter som representerar Vätterns geologiska utvecklingshistoria i stora drag: Den undre enheten (U3) består av glaciallera, delvis med uttalade varv, avsatt framförallt när Vättern var en del av den Baltiska issjön. Den mellersta enheten (U2) utgörs av en lera avsatt i Yoldia havet och den övre enheten (U1) består av gyttjelera vilken härrör från perioden efter Vätterns isolering från övriga Östersjön. Övergången mellan U2 och U3 (24 m ner i sedimentlagerföljden) är tydlig och markerar Baltiska issjöns slutliga tappning till Västerhavet. I nedersta delen av U2 återfinns en störd sedimentsekvens med kompressionsstrukturer och mikroförkastningar daterad till >11.5 cal. ka BP. Dessa strukturer återspeglar tektonisk aktivitet i området efter den Baltiska issjöns tappning. 54 m ned i lagerföljden återfinns mycket störda sedimentstrukturer vars uppkomst förklaras med en betydande isframstöt som tryckt ihop och stört sedimenten. Vi kopplar samman denna isframstöt med den på land beskrivna israndslinje som fått namn efter orten Levene i Västergötland. Kloridjonhalten i porvattnet uppvisar ett maximum 33 m ned i sedimentsekvensen vilket är en tydlig indikation på en saltvatteninträngning i Vättern före den slutliga tappningen av den baltiska issjön och Yoldia havets begynnelse. Denna saltvatteninträngning torde härröra från den föreslagna första tappningen av den baltiska issjön mot slutet av Alleröd.

List of papers

The thesis is accompanied by the following manuscript:

Swärd, H., O´Regan, M., Ampel, L., Ananyev, R., Chernykh, D., Flodén, T., Greenwood, S. L., Kylander, M.E., Mörth, C-M., Preto, P. & Jakobsson, M. *Regional deglaciation and postglacial lake development as reflected in a 74 m sedimentary record from Lake Vättern, southern Sweden*. Submitted to GFF.

The following papers/manuscripts are not included as a part of this thesis though an outcome of the 2012, 2013 and 2014 expeditions at Lake Vättern.

i. Jakobsson, M., Björck, S., O'Regan, M., Flodén, T., Greenwood, S.L., **Swärd, H.**, Lif, A., Ampel, L., Koyi, H., & Skelton, A. *Major earthquake at the Pleistocene-Holocene transition in Lake Vättern, southern Sweden.* Geology 42, 379-382

ii. O'Regan, M., Greenwood, S.L., Preto, P., **Swärd, H.**, Jakobsson, M. *Geotechnical and sedimentary evidence for thick grounded ice in southern Lake Vättern during deglaciation.* Submitted to GFF.

iii. Greenwood, S.L., O'Regan, M., **Swärd, H.**, Flodén, T., Ananyev, R., Chernykh, D. & Jakobsson, M. *Multiple readvances of a Lake Vättern outlet glacier during Fennoscandian Ice Sheet retreat, south-central Sweden.* Submitted to Boreas.

Cover image: The barge at the drill site outside Trånghalla, southern Lake Vättern 2012. Photo: M. Jakobsson

Table of contents

1. Background

1.1. General background

The retreat of the Weichselian ice sheet in southern Scandinavia has left glaciomorphological and glacifluvial imprints in the landscape during temporary standstills or readvances of the ice margin. These imprints, hypothetically connected as ice marginal lines (Fig. 1), are to some extent readily followed on land as end moraines but are more often recorded as deltaic deposits or hummocky moraines. The NNW-SSE elongated Lake Vättern divides the Levene ice marginal line and the broader Middle Swedish End Moraine Zone (MSEMZ) enclosed by the Younger Dryas ice marginal lines (Fig. 1). This position has made the Vättern region the subject of numerous deglaciation studies. Lake sediment studies from shallow sites in northern Lake Vättern, from small lakes in the vicinity of the northwestern shoreline, and extensive terrestrial sediment studies northwest of Lake Vättern, have delineated the chronology and the pattern of the regional deglaciation (e.g. Nilsson, 1968; Björck and Digerfeldt, 1989; Strömberg, 1994; Björck et al., 2001). Onshore deglaciation studies in the southern part of Lake Vättern have mainly focused on chronology, elevated ice-dammed proglacial lake levels and readvance(s) of the ice margin in the region (e.g. De Geer, 1893; Munthe, 1910; Nilsson, 1939, 1953; Norrman 1964, 1971 and Waldemarsson, 1986).

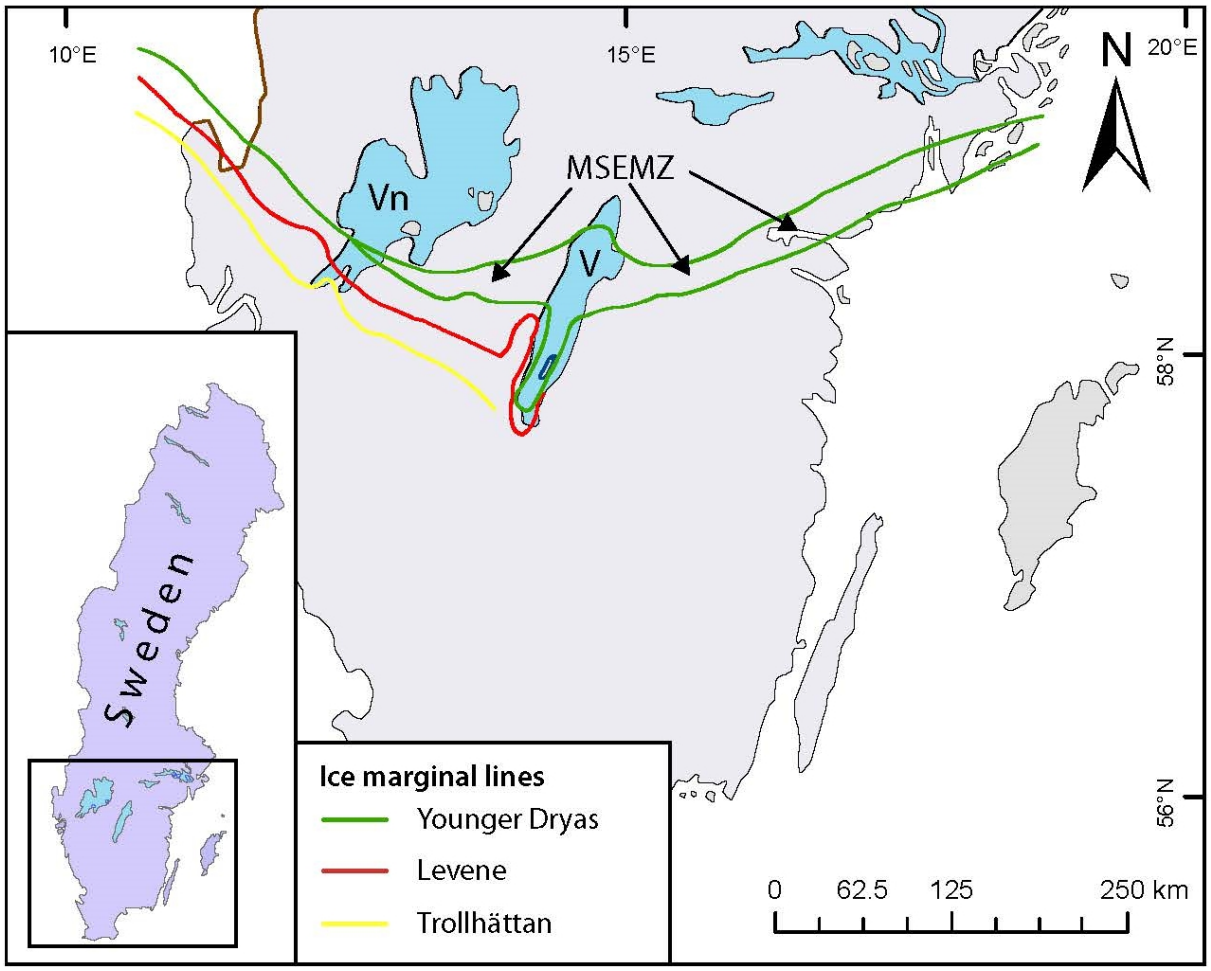

Figure 1. Ice marginal lines in southern Sweden across or close to Lake Vättern according to Lundqvist and Wohlfarth, 2000. V = Lake Vättern, Vn = Lake Vänern, MSEMZ = Middle Swedish End Moraine Zone

Scientific investigations of the deeper sediments are less numerous. Superficial (< 10 cm) sediments from the southern parts of Lake Vättern were first described by Ekman (1914) in an investigation of the bottom fauna. The sediment distribution was in part challenging to interpret with sandy sediments found at considerable depths in the middle of the lake far from any shoreline. In the 1960s the late Professor John Norrman did extensive investigations on the shore and bottom morphology of Lake Vättern including superficial (<3 m) sediment coring (Norrman, 1964; Norrman and Königsson, 1972). Norrman (1964; 1972) encountered the same challenge as Ekman (1914) with sand layers, gravel and sand on top of clays at intermediate depths far from the shorelines. These were attributed to periods of lower lake levels, areas intersected by the MSEMZ or to turbidities formed via mass wasting along the subaqueous slopes of the lake.

1.2. Initial field work 2008

In the summer of 2008 researchers from the Department of Geological Sciences (IGV) at Stockholm University together with researchers from Lund University undertook an initial marine geophysical and geological survey of southern Lake Vättern. The purpose was twofold: 1) To test a new portable multibeam echo sounder 2) To find optimal sites for sediment coring in search of quality paleoclimate archives. Subbottom profiling with a chirp sonar together with two 1.5 m gravity cores were taken to complement the multibeam data.

The gravity cores were taken in the Gränna-Visingsö strait at two spots: (i) On the subaqueous slope towards Gränna 60 m below lake surface (VA2008-2GC) and (ii) At the bottom of the deep trough east of Visingsö 108 m below lake surface (VA2008-1GC) (Fig. 2).VA2008-1GC is mainly composed of distinct sulfide laminated clay. This unit has a sharp upper boundary with a 5 cm sand layer on the core top (Fig. 3a). VA2008-2GC is composed of varved clay in the lowermost part that is overlain by faintly sulfide laminated clay (Fig. 3b). The laminated clay is intercalated by a 5 cm sand layer with sharp upper and lower boundaries. A thick (20 cm) sand layer is also found at the top of VA2008-2GC. The cores were scanned with a Multi Scan Core Logger (MSCL) at IGV to obtain bulk density,

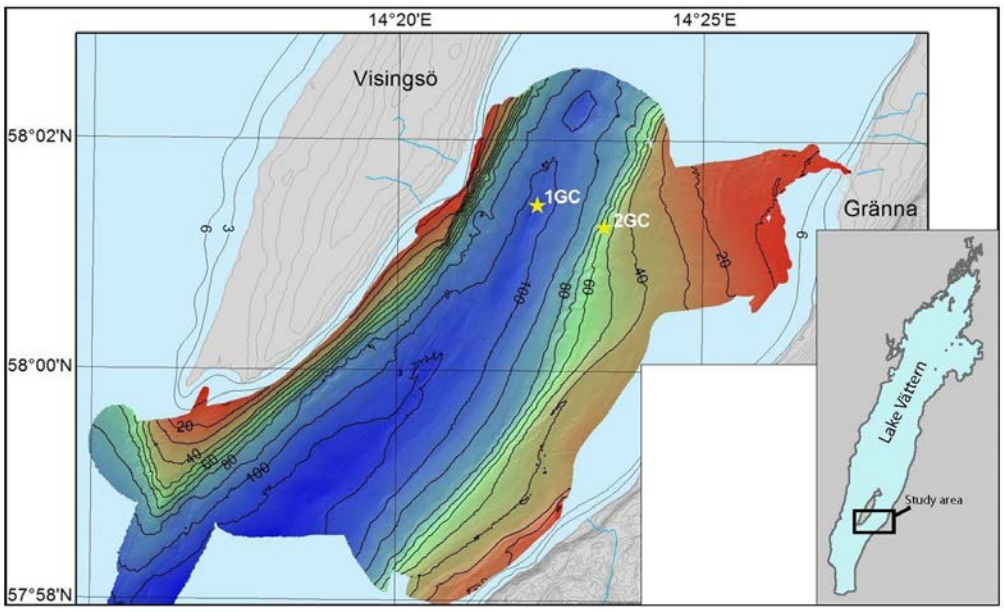

Figure 2. Locations of the VA2008 gravity cores on top of bathymetric map between Gränna and Visingsö generated from multibeam echo sounding 2008. 1GC = VA2008-1GC, 2GC =VA2008-2GC

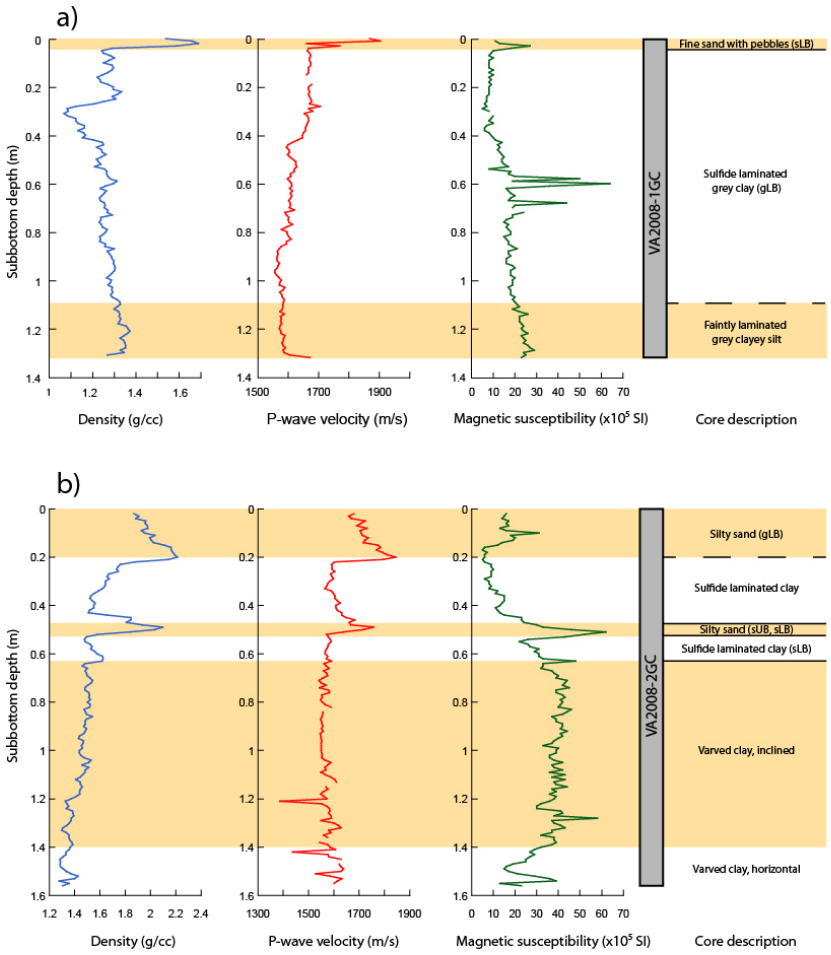

c)

POLLEN ANALYSIS OF CORE VA2008-1GC

Most common pollen types (>1%)	Percent	Concentration (grains/cm³)
Betula pubescens	25	762
Juniperus communis	16	504
Pinus sylvestris	13	413
Cyperaceae	10	295
Gramineae*	7	221
Artemisia	4	115
Salix	4	115
Betula nana	3	103
Rumex	2	53
Empetrum nigrum	2	53
Rosaceae	1	37
Chenopodiaceae	1	37
Total		3109

*Also called Poaceae. Note: 241 pollen grains counted.

Figure 3. Physical properties and core description of VA2008 gravity cores along with pollen assemblage from VA2008-1GC. sLB = sharp lower boundary, gLB = graded lower boundary, sUB = sharp upper boundary a) VA2008-1GC b) VA2008-2GC c) Pollen assemblage for VA2008-1GC from Jakobsson et al., 2014

compressional wave (P-wave) velocity and magnetic susceptibility data. The sand layers in both cores are clearly revealed in the physical properties logs as positive peaks. The sand layers on the core tops are significant, as they likely point towards ongoing surface erosion, an interpretation supported by the subbottom data (Fig. 4).

In the sulfide laminated clay sequence magnetic susceptibility and P-wave velocity data are in the same range for both cores. The bulk density range for the sulfide laminated clay in VA2008-1GC is substantially lower than the corresponding data in VA2008-2GC. If surface sediments were eroded, these differences are likely ascribed to different burial histories for these sediments (i.e how much sediment was deposited and eroded in the past). The varved clay sequence (VA2008-2GC) shows a higher level of magnetic susceptibility compared to the sulfide laminated clay. This difference likely reflects a lower amount of lithogenic material in the sulphide laminated clay sequence, and possibly a higher organic carbon content.

Dating of the sulphide laminated sediments in VA2008-1GC was performed by S. Björck using pollen analyses. A pollen assemblage corresponding to the Younger Dryas-Preboreal transition zone ~11.5 ka BP was identified throughout this interval (Jakobsson et al., 2014) (Fig. 3c).

The multibeam data collected during the 2008 survey highlight three prominent slide scars on the eastern slopes of Visingsö and collapse structures (<10 m) in the deep trough between Gränna and Visingsö (Fig. 5). The collapse structures are clearly revealed in the east-west subbottom profiles as vertical displacement structures (Fig. 4). These structures are found across the Gränna-Visingsö strait and even in the deep trough south and north of the Gränna-Visingsö strait. They are imaged along

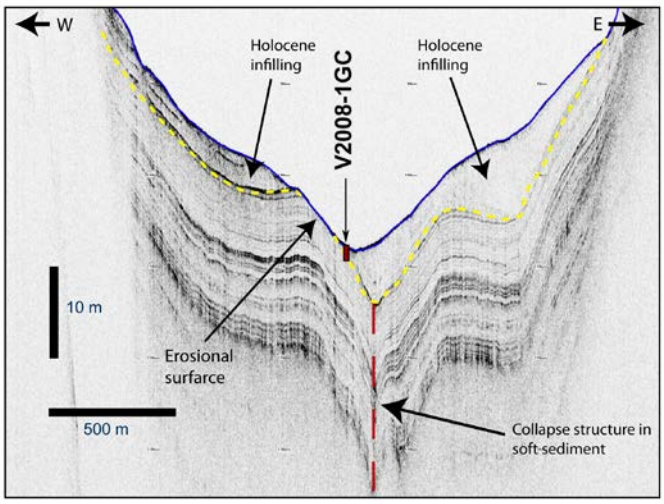

Figure 4. East-west subbottom profile in the Gränna-Visingsö strait across the gravity core sampling sites. Blue line indicates lake floor, yellow dashed line indicates the top of tectonically displaced sediments.

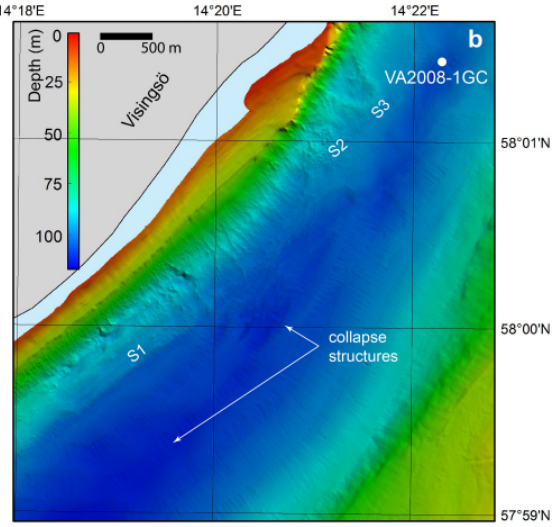

Figure 5. Slide scars and collapse structures in the Gränna-Visingsö strait. S1, S2 and S3 indicate slide scars at the subaqueous slope of Visingsö. Note the position of VA2008-1GC. From Jakobsson et al., 2014.

>80 km of the easterly deep trough, which is situated above the old fault zone (Jakobsson et al., 2014) (see section 3.2). Jakobsson et al., (2014), proposed that the collapse structures developed during neotectonic activity accompanying deglaciation. These earthquakes resulted in vertical displacements across the old fault zone. The maximum vertical displacement derived from the seismic and subbottom data is ca. 13 m, and was used to estimate the size of possible single earthquake. An estimated seismic event with a magnitude of 7.5 and a surface rupture length of 125 km place this event among the largest reported paleoseismic events in Sweden (Jakobsson et al., 2014).

The subbottom data and sediment cores collected in the Gränna-Visingsö strait provided data used to constrain the timing of the neotectonic event described above. VA2008-1GC is located on top of the collapsed soft sediment structures (Fig. 4). Because these sediments were deposited during the Younger Dryas/Preboreal transition, the neotectonic activity is interpreted as postdating the final drainage of the BIL (~11.7 cal ka BP) (Björck et al., 1996) and is contemporary with the last stages of deglaciation and the beginning of the Holocene.

The fact that very little sediment has accumulated within the deep trough between Gränna and Visingsö (Fig. 4) suggests that there is modern or prolonged (since the beginning of the Holocene) sediment winnowing in this area. Currently there is no established link between the neotectonic events at the end of deglaciation, and the mass wasting seen along the seen along the sloping lake floor.

1.3. The 2012 drilling

In 2012, a series of episodes resulted in a substantial leap for the Lake Vättern research. First of all, a mining company, Asera Mining AB, was about to prospect a possible iron ore situated ~2000 m below the surface of Lake Vättern. IGV became involved in the environmental impact assessment process that preceded the mine prospecting and this resulted in an investigation of the surficial sediment at the prospecting site in southern Lake Vättern. Five 50 cm sediment cores were recovered with a gravity corer at 91-105 m in a 1.3 km east-west stretching transect over the 2012 drill site. These cores consist of sulfide laminated olive green gyttjaclay (TOC~6%) and show no signs of a benthic fauna or bioturbation. Furthermore subbottom data from the same site indicate undisturbed and layered sediment down to 15 m below lake floor (Jakobsson et al., 2012). In connection with the environmental impact assessment the County Administrative Board Jönköping suggested that IGV should approach Asera Mining AB in order to use the drill platform including the drill equipment after the prospecting was finished. This was done, Asera Mining AB was positive to the suggestion and it became a unique opportunity to recover long cores from a more or less unexplored paleoenvironmental archive – the Lake Vättern sedimentary basin.

An initial spot coring operation from the barge was carried out in the late summer of 2012 to acquire a general picture of the deeper sediment stratigraphy. This coring was performed at the final prospecting drill site using the stationary drill equipment on the barge. In total 20 spot cores (10-50 cm in length) were recovered at depths between 14-71 meter below lake floor (mblf). Three main sedimentary regimes were encountered: (i) sulfide laminated olive grey clay/gyttjaclay between 14-26 mblf (Fig. 6a) (ii) partly disturbed pale brown varved silty clay between 29-47 mblf (Fig. 6b and 6c) and (iii) olive grey silty clay without visible varves between 50-68 mblf (Fig. 6d). The bottommost spot core at 71 mblf recovered a ~35 cm normally graded sand sequence (Fig. 6d).

During two weeks in November 2012 personnel from IGV together with staff working for Asera Mining AB drilled five closely spaced boreholes and successfully recovered lake sediment down to a depth of 74 mblf. Furthermore, two 5 m piston cores were taken from the drill platform in the summer of 2012.. The main units identified in the spot cores were captured in the 74 m composite core from the November 2012 drilling. However, the clear but partly disturbed varves found between 29-38 mblf have no equivalents in the composite core. Visible varves in the corresponding unit (U3A) in the composite core are rare (see Appendix). An additional geophysical mapping campaign in the summer of 2013 included the collection of seismic reflection data in the southern part of Lake Vättern.

The unique sediment recovery from southern Lake Vättern is a promising archive of palaeoenvironmental information in the glacial and postglacial times and may provide possible glimpses of the period preceding the late Weichselian glaciation. These data sets can help constrain the environmental setting of Lake Vättern during the regional deglaciation and inform us about the successive development stages of the Lake in relation to the evolution of the Baltic Sea. This introduction presents the background, initial results, and reflection on the key findings related to the 2012 Lake Vättern sediment drilling. It then goes on to outline the current status of planned future research that will form the basis for my PhD.

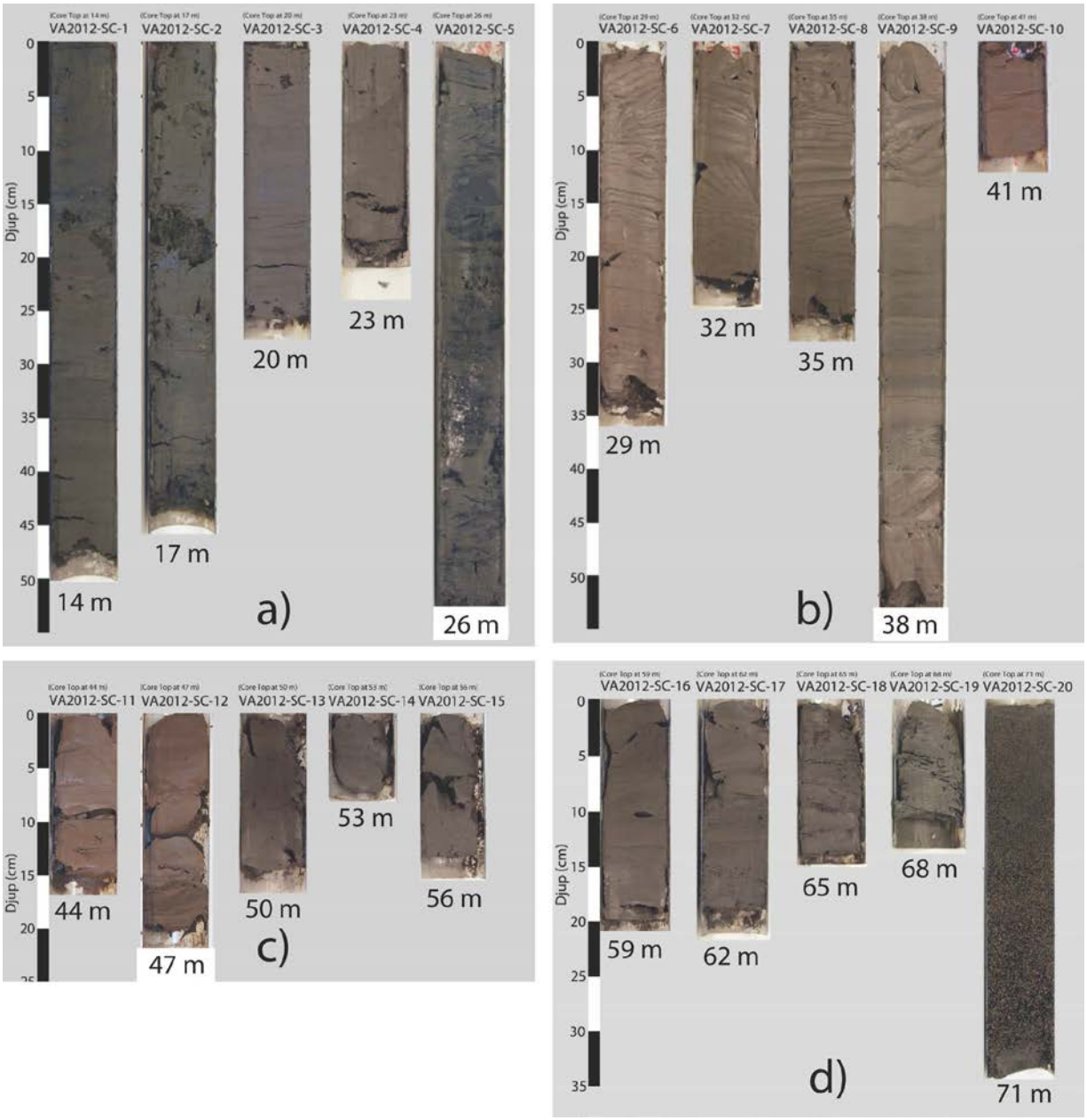

Figure 6. Spotcores from the southern Lake Vättern drill site. Numbers below each core indicate depth at core top. a) Spotcores (SC) 1-5 b) Spotcores (SC) 6-10 c) Spotcores (SC) 11-15 d) Spotcores (SC) 16-20 Photo: M. Jakobsson

2. Scientific aims

The aim of this licentiate thesis is to present a first assessment of the sediment stratigraphy and associated palaeoenvironmental interpretations in the Lake Vättern region as captured in a 74 m long sediment core. The thesis includes one manuscript that presents a general description of the sedimentary record recovered on the 2012 drilling survey. The general description will be used to further delineate aspects of the regional deglaciation. The thesis also includes core descriptions for all opened cores recovered at the drilling 2012 including the piston cores.

3. Lake Vättern – site description

3.1 Geography and relief

The NNE-SSW elongated Lake Vättern (57°46'54''- 58°52'48'' N, 14°06'37'' - 15°02'20'' E) (Fig. 7) is the second largest lake in Sweden both in terms of area (1893 km^2) and volume (77.6 km^3)(SMHI). The average depth is 40 m and the maximum depth is 119 m. The bathymetry of Lake Vättern (Fig. 8) is characterized by a deep (60-100 m) trough stretching from the southern shore up to the latitude of Karlsborg/Motala. North of this latitude the deep trench divides into two separate branches following the western and eastern shoreline. In the central western section of the lake a platform with depths between 20-40 m comprises a large area enclosed by the central western shoreline to the east and by Visingsö in the west.

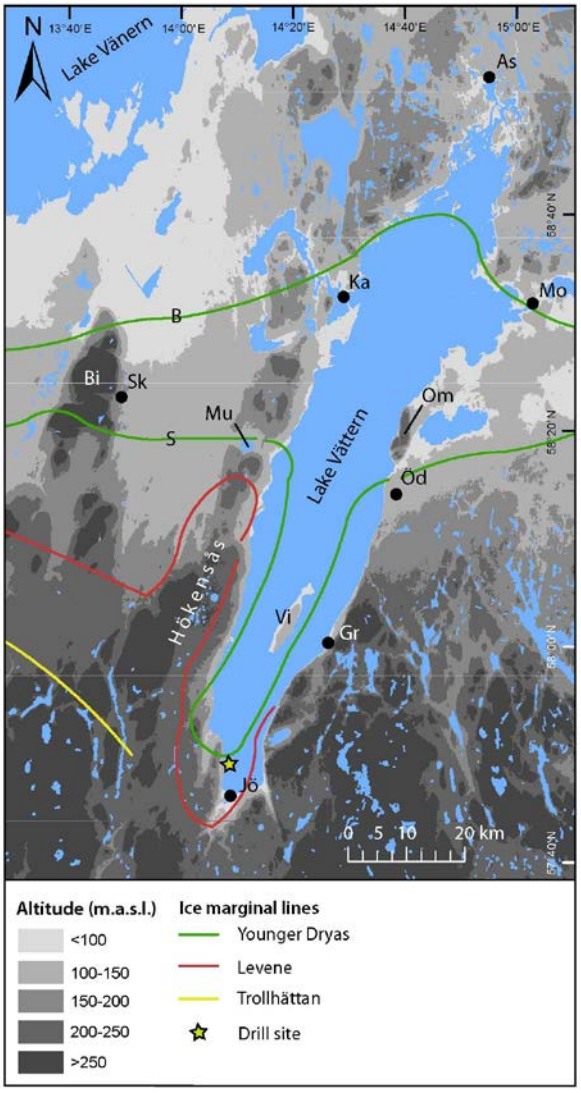

Figure 7. Topographic settings, ice marginal lines and sites referred in the text. Topography from Lantmäteriet Höjddata 50 m. Ice marginal lines from Lundqvist and Wohlfarth, 2000. As = Askersund, Mo = Motala, Om = Mt. Omberg, Öd = Ödeshög, Gr = Gränna, Vi = Visingsö, Jö = Jönköping, Mu = Lake Mullsjön, Sk = Skövde, Bi = Mt. Billingen, S = Skövde ice marginal line, B = Billingen ice marginal line

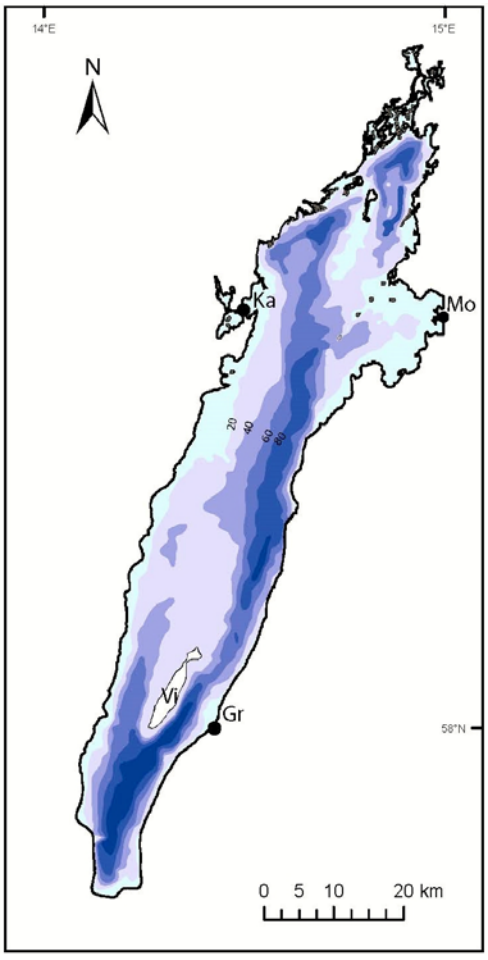

Figure 8. Bathymetry of Lake Vättern with sites referred in the text. Vi = Visingsö, Ka = Karlsborg, Mo = Motala, Gr

Lake Vättern (88 m.a.s.l.) is mainly surrounded by prominent highlands (200-300 m.a.s.l.) that are intercalated with small depressions (Fig.7). Extensive lowlands are limited to the northern and northeastern shorelines around Askersund and Motala. A prominent feature in the lowland south of Motala is the horst Mt. Omberg rising 174 m above lake level. From Ödeshög and southwards via Jönköping and up to Karlsborg on the western shore the lake is framed by the highlands of southern Sweden. As a part of these highlands the Hökensås area is an elongated ridge reaching from the southern tip up to the Karlsborg area.

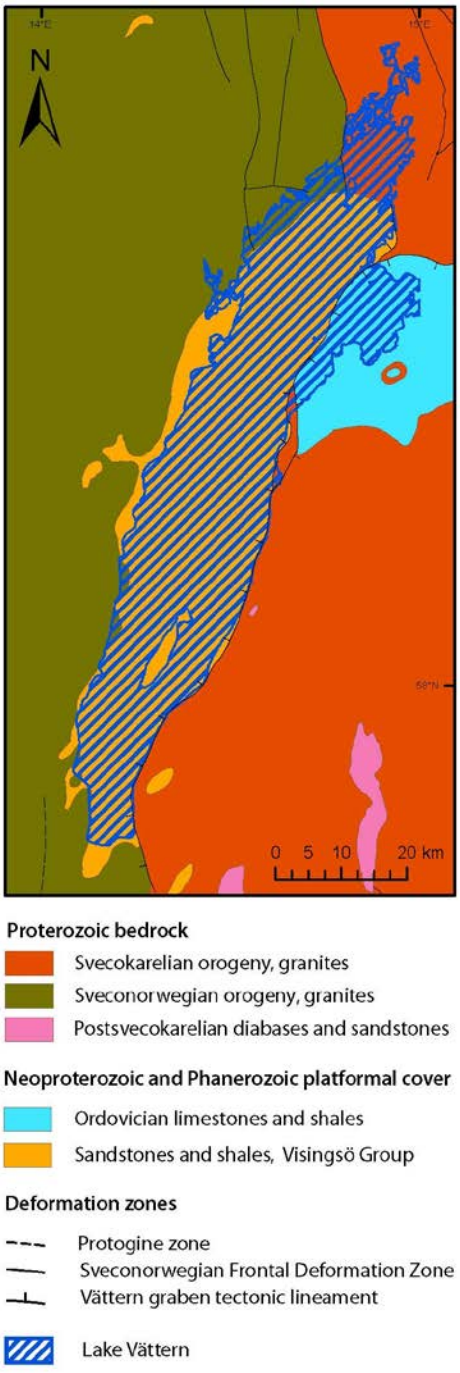

Figure 9. Regional bedrock pattern below and around Lake Vättern together with deformation zones in the specific area. From Bedrock Sweden 1M, Geological Survey of Sweden (SGU).

3.2 Bedrock geology and the origin of the Vättern basin

Located in the middle of the Transcandinavian igneous belt, Lake Vättern is mainly surrounded by granites with ages between 1.8 – 1.7 Ga (SGU, 2010) (Fig. 9). The younger granites on the western side of the lake belong to the Sveconorwegian orogeny and show a metamorphic tendency in the southwestern areas (Wik et al., 2006). East of the lake the granites belong to the Svecokarelian orogeny. In the Motala region the bedrock is composed of Ordovician limestone and shale. The Askersund area in the northernmost part of the lake constitutes a separate older granite region (~1.85 Ga).

Neoproterozoic and Phanerozoic cover of sedimentary rocks constitute the vast majority of the bedrock in the Vättern basin (Fig. 9). This regime is also found around the shorelines of Lake Vättern as well as in the Jönköping region to the south. The sedimentary bedrock, usually referred to as the Visingsö Group, is estimated to be more than 1000 m thick (Collini, 1951; Lind, 1972; Axberg and Wadstein, 1980) and was deposited between 0.8 -0.7 Ga (Lundqvist et al., 2011). The Visingsö Group consists of three vertically distributed subunits all with sandstone and shale as the dominating rock type but also including some minor occurrence of clastic conglomerates and limestone (Collini, 1951; Vidal, 1984). The Visingsö Group is interpreted as a remnant from >8000 m thick sedimentary platform that covered southeastern Sweden during the Neoproterozoic era. These thick sediments are likely derived from the weathering of the westerly Sveconorwegian mountain belt (Lundqvist et al., 2011).

Lake Vättern lies along a fault zone aligned with two deformation zones: The Sveconorwegian frontal deformation zone (SFDZ) is found north of the lake and the Protogine zone (PZ) is found south of the lake (Bingen et al., 2008) (Fig. 9). However, it is not clear whether the Lake Vättern fault zone

is a part of this zone or if it constitutes a separate tectonic lineament that partly connects with the SFDZ and the PZ (Gorbatschev, 1980; Andersson and Rodhe, 1990). The Lake Vättern basin is traditionally described as a graben structure (e.g. De Geer, 1910) but questions concerning the western fault zone made Collini (1951) suggest a half graben structure. However, seismic reflection profiling and gravitational mapping reveal the existence of a graben structure within the lake (Axberg and Wadstein, 1980; Lind, 1972). The formation of the Vättern graben is suggested to include at least two successive faulting events in the Late Precambrian and Permian (Månsson, 1996). Sedimentation of the lower and middle units of the Visingsö Group both preceded and was contemporaneous with a first faulting event at c. 0.75 Ga. The appearance of the present Lake Vättern basin is attributed to a second faulting event during the Permian (0.29-0.24 Ga) (Månsson, 1996). Sediments from the Visingsö Group within these downfaulted grabens were protected against extensive erosion.

3.3 Deglaciation and Quaternary development

The global climate amelioration during the Late Pleistocene led to a successive shrinking of the Late Weichselian ice sheet from its maximum extension: the Last Glacial Maximum ~26.5-19 ka cal. ka BP (Clark et al., 2009). The retreat of the ice sheet in southern Sweden is mapped and dated using glacial morphology, varve chronology, ^{14}C dating and glacial striations (Lundqvist et al., 2011). The general ice recession pattern is marked in the landscape by ice marginal landforms formed during temporarily readvances of the ice margin. By connecting these ice marginal landforms theoretical ice marginal lines have been constructed to reconstruct the stepwise withdrawal of the Fennoscandian ice sheet (e.g. Lundqvist and Wohlfarth, 2001). These ice marginal lines reveal a northward retreat of an east-west stretching ice margin with a convex tendency over the South Swedish highlands (Lundqvist and Wohlfarth, 2001; Lundqvist, 2009) (Fig. 1). One of these lines, the Levene ice-marginal line dated to 13.8 -13.4 cal. ka BP (Lundqvist and Wohlfarth, 2001; Larsen et al., 2012; Anjar et al., 2013) likely forms a semi-circle with glaciolacustrine and glaciofluvial deposits at the southern shores of Lake Vättern (Fig. 7) indicating an ice lobe covering the Lake in the Late Alleröd (Waldemarsson, 1986; Greenwood et al., *in review*). Earlier ice recessions and readvances in the Vättern basin captured in seismic reflection profiles, as well as in terrestrial and subaqueous geomorphology, are illustrated by Greenwood et al. (*in review*) and include up to three recession-readvance cycles, before a final readvance covered southern Lake Vättern during the emplacement of the Levene ice marginal line.

As the Late Alleröd ice lobe retreated northwards, the Vättern basin became filled with meltwater. The proglacial Lake Vättern was wedged between the ice margin in the north and the highlands to the east and west. Paleoshoreline studies aiming to describe extension and development of the proglacial Lake Vättern have been carried out since the 19th century (e.g. De Geer, 1893; Munthe, 1935; Nilsson, 1939 and 1953). Nilsson (1953, 1958) presents a detailed picture of successive extensions of the proglacial Lake Vättern that finally drained into the Baltic Ice Lake north of Ödeshög. At this time, Lake Vättern became a part of the growing Baltic Ice Lake (BIL) (Fig. 8a).

As described by Björck (1995) the growing BIL was enclosed by the highlands of southern Sweden in the south and the ice margin in the north. Thirty kilometers west of Lake Vättern the ice margin engulfed the northern tip of Mt. Billingen resulting in a wall between the sea and the BIL. As the ice retreated north of Mt. Billingen the Baltic Ice Lake drained into the sea at least twice during the last deglaciation (Björck, 1995). A first drainage in the Late Alleröd chronozone (~13.0 cal ka BP: Björck,

2008) was suggested by Donner (1969) and further stratigraphically delineated by Björck and Digerfeldt (1984, 1986) with a lowering of c. 10-20 m of BIL (Björck, 1995 and references therein; Bennike and Jensen, 2013).

During the subsequent Younger Dryas cold period (12.9 – 11.7 cal ka BP: Rasmussen et al., 2006) concomitant standstills and readvances of the ice margin left morphological imprints on the landscape on both sides of Lake Vättern, the MSEMZ (cf. Strömberg, 1969). The MSEMZ west of Lake Vättern comprises two separate ice marginal lines, the southerly Skövde line and the northernmost Billingen line extending eastward towards Mt. Billingen where they merge into a single line (Fig. 1 and 7). East of Lake Vättern the MSEMZ can be traced as deltaic depositions and thick till cover partly overlying glaciofluvial deposits (Svantesson, 1981; Lundqvist, 1988).

On the western side of Lake Vättern Lake Mullsjön is a key site for the location of the Skövde line (Fig. 7). Lake sediment analysis from Lake Mullsjön shows that the site was not overridden by ice during the Younger Dryas cold event (Björck and Digerfeldt, 1989). However, Waldermarsson (1986) connected the Öxnehaga diamicton in the Jönköping area to a Younger Dryas readvance, implying thick ice would have reached beyond the southern shores of Lake Vättern. In the vicinity of Ödeshög at the eastern shore, glaciofluvial deposits mark the most likely continuum of the Skövde line (Lundqvist, 1988). Moreover, these deposits are mostly covered by till indicating ice readvance of local character close to the shores of Lake Vättern; no contemporaneous readvance has been reported in the Linköping area to the east of the ice marginal line (Kristiansson, 1986; Brunnberg, 1995). Conclusively, an ice readvance during Younger Dryas cold period in the Vättern area should have been limited to a southward surging ice tongue linked to the Skövde ice marginal line.

The Billingen ice marginal line marks the last standstill before the drainage of the BIL. It stretches from Mt. Billingen and northeastward towards the Perstorp delta north of Karlsborg (Fig.7) where it can be traced as two subsequent deltaic deposits found before and after the final drainage of the BIL (Bergsten, 1943). This makes it possible to tie the Perstorp area to the Billingen ice marginal line. Contemporaneous ice margin deposits east of Lake Vättern are found on the Djurkälla plateau north of Motala (Bergsten, 1943) (Fig. 7). The extension of the Billingen line over the lake itself is not fully understood but glacifluvial material found on the northern shore (Bergsten, 1943) could possibly belong to the line (Lundqvist and Wohlfarth, 2001). This would imply a concave and calving ice margin over Lake Vättern in the late Younger Dryas. Conclusively, the morphology and water content of the Vättern basin comprise an environment that possibly increased the speed of the ice oscillation compared to the surrounding onshore ice movements. In colder periods the formation of an ice tongue was rapid and in warmer periods the ice tongue retreated quickly into a concave calving ice bay north of the land based retreating ice margin.

At ~11.7 cal ka BP the BIL drained catastrophically (Björck et al., 1996; cf. Andrén et al., 2011; Strömberg, 1992; Jakobsson et al., 2007) as the Fennoscandian ice sheet retreated north of Mt. Billingen. This final drainage of the BIL is estimated to have released 7800 km^3 of freshwater into the North Atlantic Ocean (Jakobsson et al., 2007) within a couple of years (Strömberg, 1992; Johnsson et al., 2013) and a lowered the BIL by 25 m (Jakobsson et al., 2007). The drainage took place during the Younger Dryas/Preboreal transition and the accompanying warmer climate and marks the beginning of a new phase in the Baltic Sea development: the Yoldia Sea (Fig. 8b).

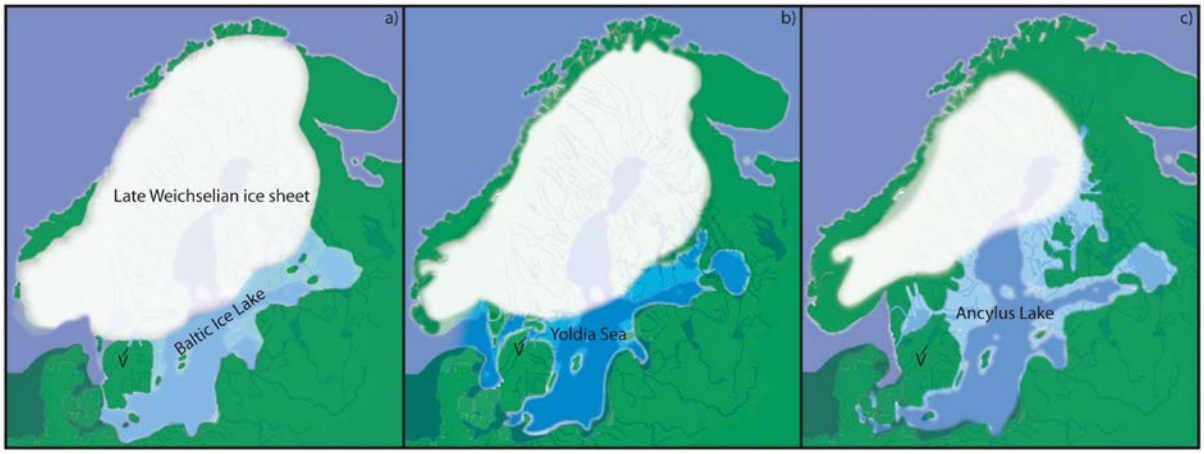

Figure 8. Lake Vättern in the first three Baltic Sea development stages during the Late Weichselian deglaciation. V = Lake Vättern a) The Baltic Ice Lake stage at the time shortly before the final drainage ca. 11.7 ka BP. b) The Yoldia Sea stage in the end of its brackish phase ca. 11.1 ka BP. c) The Ancylus Lake stage and an isolated Lake Vättern ca. 10.5 ka BP. Modified from Andrén et al., 2011.

The Yoldia Sea stage connected the Baltic basin with the North Sea for approx. 1000 years before isostatic rebound closed the Närke strait and the Baltic became an isolated lake again: the Ancylus Lake (Fig. 8c). The Yoldia Sea stage has been subdivided by Svensson (1989) into three phases: a fresh water phase that lasted ~300 years followed by a 100 -200 year brackish phase when pulses of marine water entered the Baltic basin via the Närke strait (Wastegård et al., 1995; Andrén et al., 1999) and finally another fresh water phase caused by the isostatic rebound that made the Närke strait too shallow for marine incursion from the west. Björck et al. (2001) reported the first substantial evidence of a marine incursion into Lake Vättern including the occurrence of the marine bivalve *Portlandia arctica* (Yoldia) accompanied by increased carbonate levels in the lake sediment. The marine incursion was dated to ~250 years after the final drainage of the BIL, indicating the onset of the Yoldia Sea in Lake Vättern ~50 years before any marine water reached the Baltic basin.

Paleoshoreline studies (Nilsson, 1953) led Norrman (1964) to estimate a period of 500 years between the drainage of the BIL and the isolation of Lake Vättern from the Yoldia Sea, thus in the middle of the Yoldia Sea stage. The lake isolation was a direct effect of the rapid isostatic rebound after the ice recession that lifted the Karlsborg and Motala areas above sea level. The first lake stage, Fornvättern (Ancient Lake Vättern), occupied larger areas than the present lake and had its outlet via Lake Tibon north of Askersund (Nilsson, 1953; Norrman, 1964). Due to uneven isostatic uplift along the main NNE-SSW axis in the Vättern basin the northern parts of the lake rose more rapidly than the southern parts. The lake tipped toward the south along an E-W axis through Motala and Karlsborg. Eventually, this led to a change of outlet and concomitant 5-10 m drainage of the Fornvättern into the Ancylus Lake through Motala Ström (Nilsson, 1953; Norrman, 1964). Norrman (1964) estimated that this drainage took place ~2000 years after the lake isolation.

4. Methods overview

This overview provides a broad summary of the methods used in the analysis of borehole sediments from 2012. The reader is referred to the manuscript for further details on each method. A timeline illustrates what laboratory work was done and when it was executed (Fig. 9).

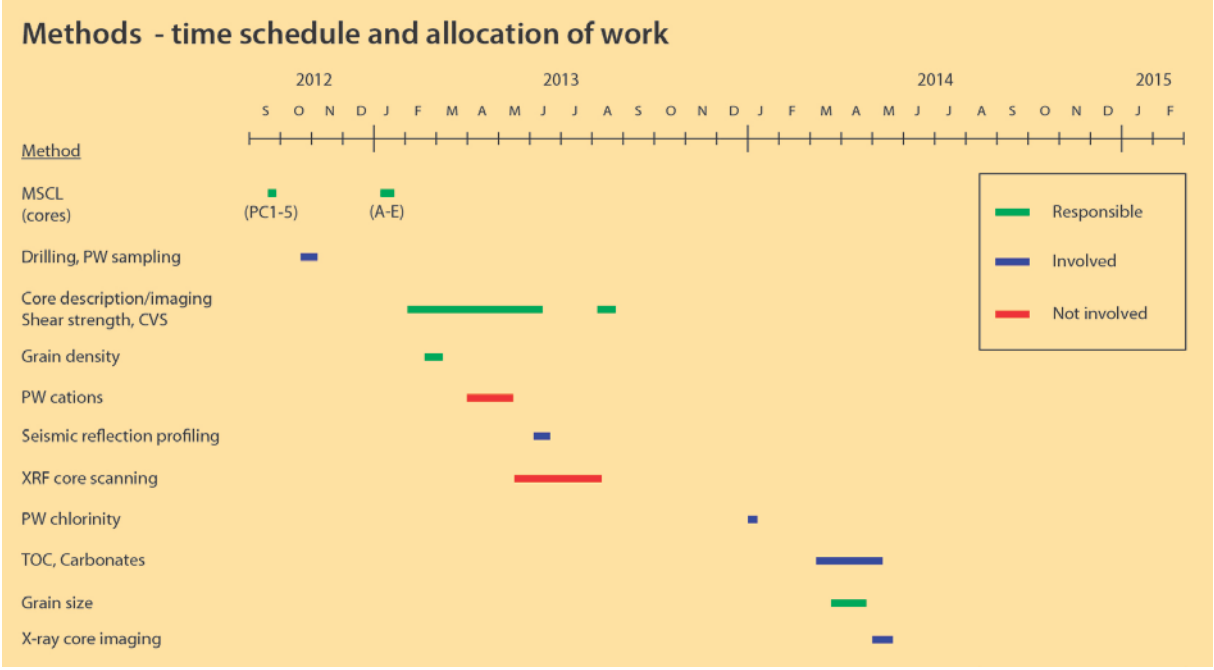

Figure 9. Timeline for the licentiate period including laboratory activities and degree of own involvement in each activity.

4.1 Drilling

Five adjacent boreholes were drilled from a barge anchored offshore north of Jönköping (Fig. 7) in southern Lake Vättern (14°11.05'E 57°50.00'N). The personnel at the barge included three drillers, a drilling supervisor and 2-3 Stockholm University scientists. Two main drilling techniques were used to maximize the sediment recovery. For the upper less compacted sediments the core barrel was pushed into the sediment without any rotation. This was done to avoid core disturbances from the rotational movement of the drilling. A minimum amount of drilling fluid was used to avoid loose sediments being flushed away. For the deeper, more compacted sediment the casing was lowered into the sediment with the core barrel inside. At specific depths the drilling started and proceeded downwards. After the recovery, each sediment core (3 m) was cut into 1.5 m sections, marked and stored in a heat controlled container (+4°C) aboard the drill platform.

4.2 Seismic reflection profiling

During the Lake Vättern survey in 2013 seismic reflection profiles were acquired in east-west direction across the drill site as a part of a more general geophysical mapping program in southern Lake Vättern. This program included multibeam swath bathymetry, chirp sonar subbottom profiling and seismic reflection profiling. These data allow insights from the analysis of the borehole sediments to be placed into a wider spatial context. Furthermore the data is used to map horizons and sedimentary features across large parts of the lake.

The basic principles behind seismic reflection (McQuillin and Ardus, 1977; Milsom and Eriksen, 2011) can be described as follows. The initiated pulse of sound (seismic wave) travels through the water column and into the sediment where it is reflected due to changes in the acoustic impedance (seismic velocity*density) between different sediment units. The reflected pulse is captured by a hydrophone resulting in the detection of the two way travel time (twt) which is used as the depth scale in the seismic profiles (see manuscript Fig. 9). The amount of reflection mirrors the amplitude of the acoustic impedance change i.e. a strong reflection infer a large change in density between to sediment layers.

4.3 Laboratory work

4.3.1 Porewater sampling and analysis

Rhizon samplers (Dickens et al., 2007) were used for offshore collection of porewater samples (Fig. 10). Subsampling was made evenly at 3 locations per 1.5 m section resulting in a ~50 cm resolution. Major cations were detected using the Inductively Coupled Plasma Optical Emission Spectrometer (ICP-OES) at the Department of Geological Sciences (IGV). The ICP-OES uses radio frequency induced argon plasma to dry, vaporize and excite the injected samples into gaseous atoms and ions. When the excited particles relax into ground state, element specific photons are emitted that can be detected and quantified (Huo and Bradley, 2000). The broad range of detected ions included Al, Be, Ca, Co, Cr, Cu, Fe, K, Li, Mg, Mn, Mo, Na, Ni, P, Pb, S, Si, Sr, Ti, V and Zn. The uncertainty of the porewater data is ±5%.

Figure 10. Pore water sampling in the field laboratory on the barge, Lake Vättern, November 2012. Photo: Martin Jakobsson.

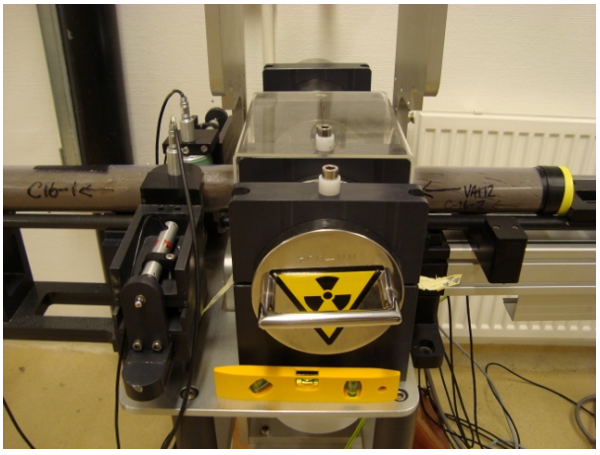

Figure 11. Multi scan core logging of a Lake Vättern sediment core in the core laboratory at the Department of Geological Sciences.

Downhole profiles of the major cations (Na, K, Ca and Mg) revealed synchronous peaks at ~24 c-mblf, and was initially interpreted as evidence for an abrupt saline water incursion into the Lake. This imprint aligned well with the BIL/Yoldia sea transition and was therefore seen as a direct aftermath of the drainage of the BIL (see manuscript Fig. 8). However, when trying to estimate the salinity of the porewater, it was found that the use of cations was complicated due to their tendency to exchange with different clay minerals in the sediment (e.g. Sayles and Mangelsdorf, 1977). The classic way to determine salinity in marine waters is to use the chloride concentration (chlorinity). This method is also applied in deep sediments porewaters (e.g. Adkins and Schrag, 2003) due to the

conservative behavior of the chloride ion. Consequently, chlorinity analysis was initiated and executed using a Dionex IC20 Ion Chromatograph connected to an anion-exchange column containing positively charged groups. The porewater samples are injected and the anions are separated due to charge and size when passing through the column. Each anion is detected and plotted as a curve where the area below the curve is proportional to the concentration. The chlorinity is determined with precision of two decimals.

4.3.2 Multi-Sensor Core Logging (MSCL)

Multi-Sensor core logging (MSCL) at IGV included the generation of bulk density and magnetic susceptibility data with a downcore resolution of 1 cm (Fig. 11). After core opening the half-cores were imaged by the Geotek Line scanning camera connected to the MSCL. The following information concerning the general principles of the MSCL is taken from http://www.geotek.co.uk/products/magsusc .

The MSCL consist of an active conveyer track on which the cores are pushed through (i) a gamma-ray attenuation porosity evaluator (GRAPE) (ii) a compressional P wave sensor and (iii) a magnetic susceptibility loop sensor. The GRAPE provides determination of bulk density using gamma-rays that penetrates the sample. During the penetration some gamma-rays are absorbed, some are scattered while some passes the sample unaffected. The detector counts the unaffected gamma-rays and calculates the energy loss and attenuation which in turn are proportional to the bulk density of the sample. A sample specific attenuation coefficient is determined by measuring a predefined standard. The standard consists of an aluminum rod with five different diameter gradations contained in liner filled with distilled water. This two-phase system represents the mineral and the interstitial water respectively. The counts for each Al diameter is plotted against the bulk density*liner thickness to receive a calibration curve for further use in the actual measurements. An applied magnetic field in the loop sensor will respond to the degree of magnetization of the sample by deliver a range of positive data. The loop sensor is absolutely calibrated towards a stable iron oxide by the manufacturer and do not need any further calibration. Digital RGB data was generated automatically from the core images.

The MSCL data was used to correlate cores from the 5 boreholes, and to produce a single continuous composite section. This was done by aligning MSCL and RGB data from the overlapping intervals in the boreholes. Furthermore, the depth scale was revised to compensate for incomplete recovery and/or expansion of recovered sediment.

4.3.3 Core description and accompanying laboratory tests

The cores were split into halves and subsequently described. The colors were determined according the Munsell color chart. The shear strength of the sediment was acquired using the Swedish fall cone test (Hansbo, 1957) and a pocket penetrometer. The fall cone test is based upon the insight that the undrained shear strength of a sediment sample will be reflected by the amount penetration of a falling device. The ISO-TS-17892-6 (Swedish Standards Institute) standardize this insight and states that a fall cone of determined mass and cone angle are to be locked in the upper position of the fall cone apparatus and then adjusted so that the tip of the fall cone just touches the surface of the sample vertically. The fall cone is then released to penetrate the sample for 5±1 s after which is

locked and the penetrated depth can be read. Constant volume sampling (CVS) was carried out twice at each section to retrieve wet bulk densities. A 10 cm^3 steel cylinder was pushed into the sediment to capture the CVS. The CVS samples were weighed, dried and reweighed to obtain the water content of the sediments. The dried samples were later used for grain density measurement using a helium displacement pycnometer.

4.3.4 XRF core scanning

The archive core halves were scanned at IGV using an ITRAX XRF Core Scanner from Cox Analytical Systems. Elemental data (Si, K, Ca, Ti, Mn, Fe, Zn, Rb, Sr, Y, Zr) as well as radiograph images were obtained with a resolution of 1 mm. The general X-ray fluorescence technique uses the fact that the energy at the atomic level is elemental specific quantized. Irradiation with x-rays on a sediment surface will result in the excitation of electrons in the atoms of the sediment and the subsequent reemission of element specific wavelength of less energy (fluorescence). This reemission is detected and converted into peak areas proportional to the concentrations of the measured elements. The ITRAX XRF core scanning is sometimes called micro-XRF due to its ability of capturing elemental changes down to submillimeter scale (Kylander et al., 2011). This is of great use in a palaeoenvironmental context where you want to capture short term changes.

4.3.5 Grain size and TOC/TC

Subsampling for grain size and total organic carbon/total carbon (TOC/TC) was made at least twice every 1.5 m section. Grain size analysis included the removal of carbonates and organic compounds. Finally the samples were run in a laser diffraction particle size analyzer (Malvern Mastersizer 3000) to retrieve the grain size distribution data. As the laser irradiates the dispersed sample the light is scattered with various angle due to particle size. Large particles have a smaller angular scattering compare to small particles. The scattering is detected through a series of detectors and the grain size distribution is calculated from the total measured scattering pattern (http://www.malvern.com/en/products/technology/laser-diffraction/).

The TOC/TC samples were separated and the TOC samples were treated with acid to remove carbonates. The final analysis of the TOC/TC samples was made through a stable isotope analysis using a Carlo Erba NC2500 analyzer coupled to a Finnigan MAT Delta V mass spectrometer. A summary of the method is extracted from Carter and Barwick (2011) and presented below. The elemental analyzer combust the dry samples in an oxygen atmosphere between 600-1800°C and produces CO_2, N_2 and H_2O. While water is trapped the other gases are separated and then transported to the mass spectrometer by the carrier gas (Helium). An electron beam ionizes the gases which then are accelerated by an electrical field into a magnetic field. The magnetic field deflects the ions with respect to mass-charge ratio and the different isotopes are finally detected. The sum of the carbon isotopes (^{12}C and ^{13}C) constitute the TOC or TC depending on the sample injected.

5. Summary of manuscript

The 74 m composite sediment core was divided into three lithostratigraphic units (Fig. 12) based on the core descriptions, the physical properties (bulk density and magnetic susceptibility) and discrete sediment analyses. U3 (25-74 c-mblf) comprises red to brown varved silty clays deposited in a proglacial lake, U2 (15-25 mblf) contains grey sulfide laminated clays defined as postglacial clays and U1 (0-15 mblf) consists of greenish gyttjaclay deposited after the isolation of Lake Vättern. The main lithostratigraphic units are further divided into subunits due to changes in color, grain density, bulk density and magnetic susceptibility (Fig. 12). The general lithostratigraphy reveals a retreating ice margin (upward decrease in varve thickness and detrital carbonates), non-biogenic sediment (very low amounts of TOC and no signs of bioturbation or fossils) and the development of Lake Vättern in close relation to the Baltic Sea development stages (a sharp BIL/Yoldia Sea sedimentary transition). Important paleoenvironmental events are highlighted below.

5.1 Imprints of ice grounding

The sediments below 54 c-mblf (U3C) are composed of highly deformed clays with intercalating silt and sand layers (Fig. 13). This is accompanied by distinct increases in the downhole bulk density, magnetic susceptibility (Fig. 12) as well as a rapid shift in color reflectance. A series of consolidation tests were run that proved the underlying sediments were indeed overconslidated (O´Regan et al., *in review*). We interpret this as an ice grounding event (cf. O'Regan et al., *in review*) related to a readvance of the ice margin most likely attributed to the Öxnehaga diamicton described by Waldemarsson (1986) and associated with the Levene ice marginal line accumulated at 13.8 – 13.4 cal. ka BP (Lundqvist and Wohlfarth, 2000; Greenwood et al., *in review*) (see section *6 for further discussion*). No glaciotectonic imprints are found above the 54 c-mblf level which indicates that only one single ice readvance is recorded in the 74 m sediment core at the drill site.

5.2 The final drainage of the BIL

We attribute the sharp U3/U2 transition to the catastrophic drainage of the Baltic Ice Lake at ~11.7 cal ka BP (Björck et al., 1996; cf. Andrén et al., 2011), which is recognized as the onset of Holocene. A distinct color change in the sediment from red clay towards gray clay has been attributed to the final drainage of the BIL in other studies of sediments from the area (e.g. Strömberg, 1992, Brunnberg, 1995 and Andrén et al., 2002). This transition is found in the Lake Vättern sediment at 24 c-mblf (U3/U2) together with a distinct 2 cm thick sand layer. Sand layers in sediment have also been found in Lake Mullsjön (Fig. 7) by Björck and Digerfeldt (1989) also a part of the BIL before the final drainage. They attributed these coarse layers to the rapid lowering of the lake levels and the subsequent rapid erosion of areas formerly situated below the lake surface. It is reasonable to attribute the sand layer at the U3/U2 transition to a comparable episode. Above 24 c-mblf laminations and sulfide bands within the sediments are highly deformed with numerous micro-faults and compressional structures (Fig. 13). We interpret these as imprints of the major earthquake event (> 11.5 cal ka BP) that followed the final drainage of the BIL (Jakobsson et al., 2014).

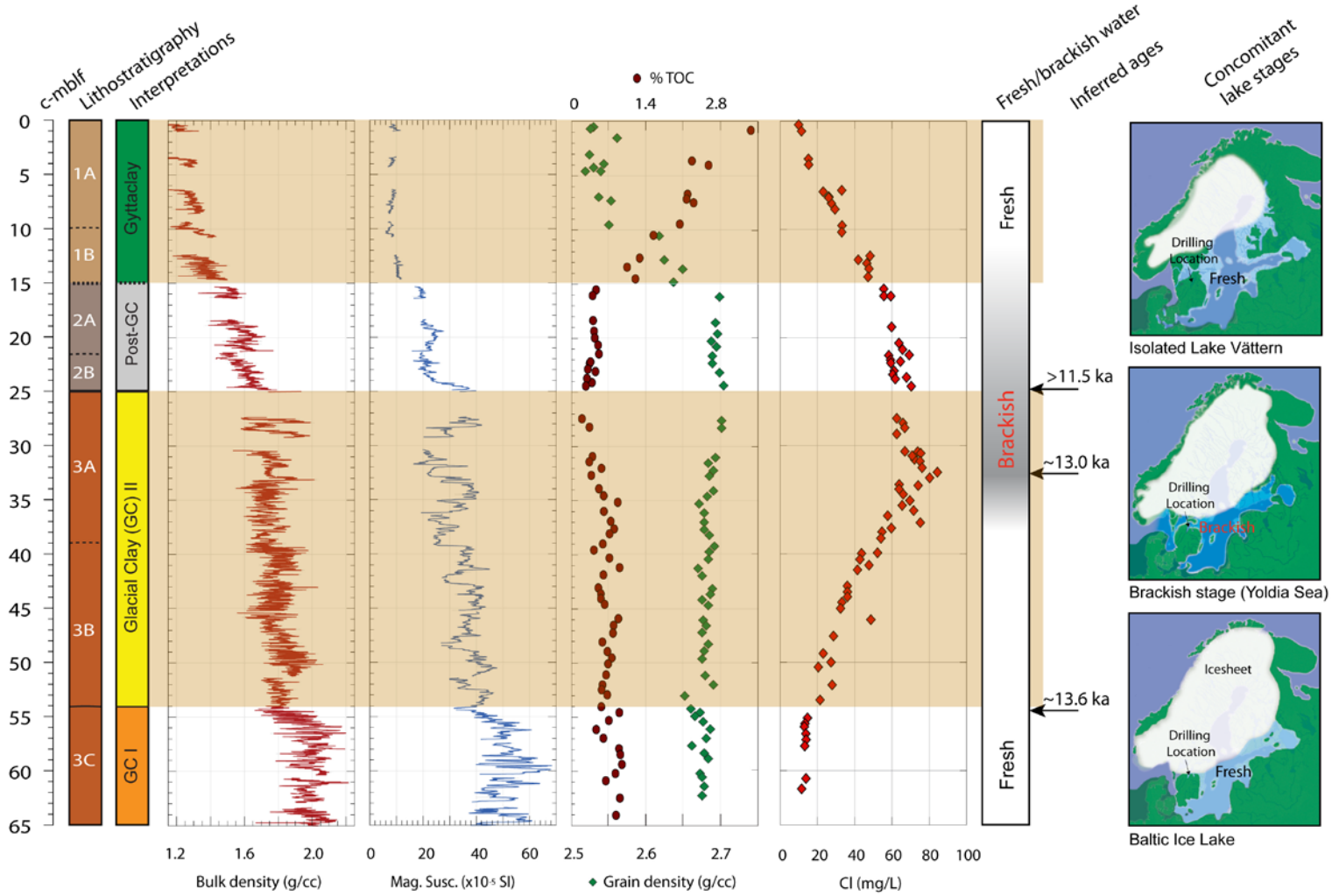

Figure 12. Lithostratigraphy and interpretations along with bulk density, magnetic susceptibility, grain density, total organic carbon (TOC) and porewater chlorinity. Inferred ages for the sediment and the concomitant Lake Vättern development stages in relation to the Baltic Sea development stages. Maps modified from Andrén et al., 2011.

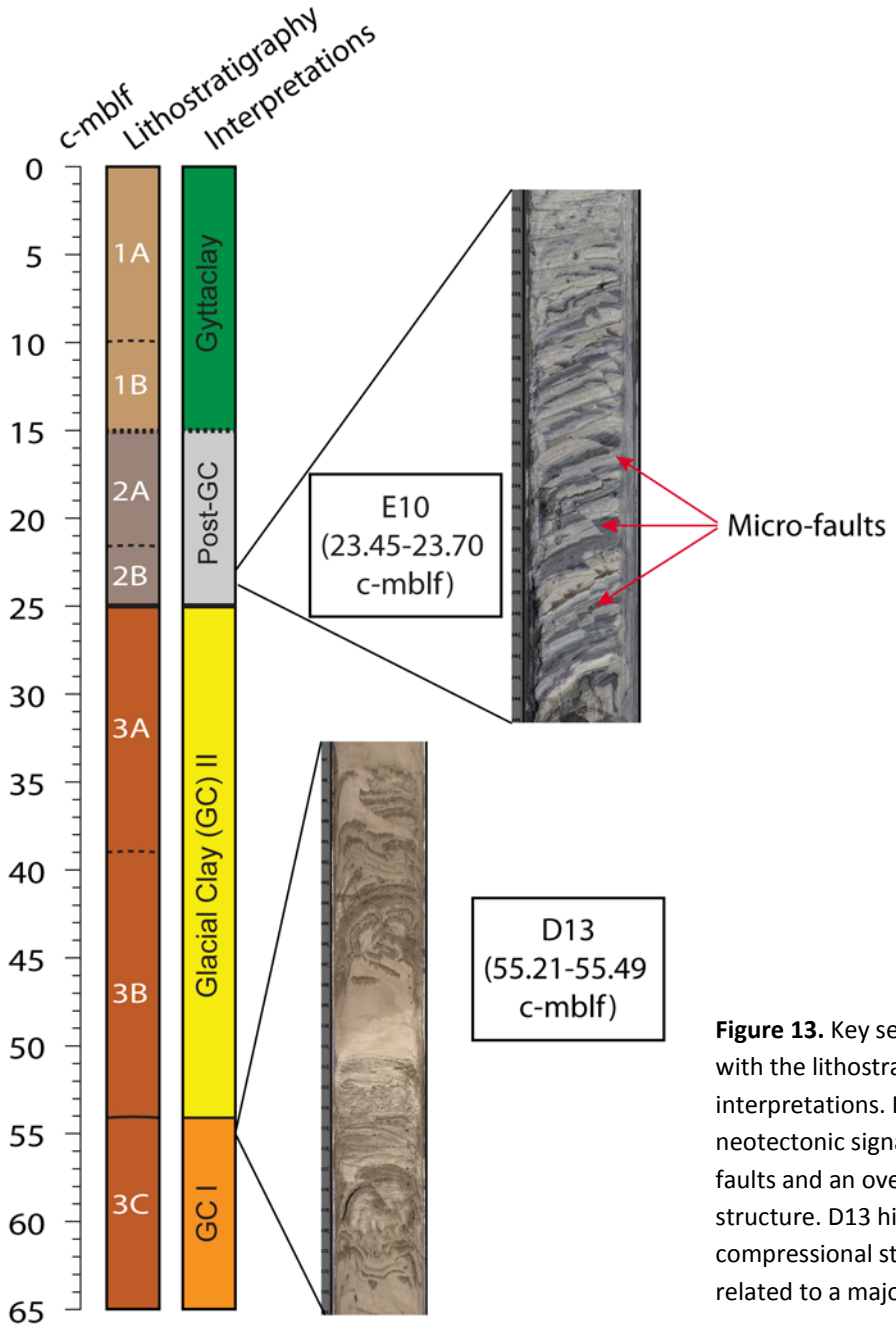

Figure 13. Key sediment cores along with the lithostratigraphic units and interpretations. E10 highlights neotectonic signatures such as micro-faults and an overall compressional structure. D13 highlights the compressional structures that are related to a major ice grounding event.

5.3 Marine incursions into the Vättern basin

The porewater dataset exhibits a peak in chlorinity at 33 c-mblf attributed to a marine incursion into Lake Vättern (Fig. 12). The chlorinity peak is located below the Younger Dryas/Preboreal transition (24 c-mblf) and the concomitant final drainage of the BIL, but well above the level of ice grounding (54 c-mblf). We associate this marine incursion to the first known drainage of the Baltic Ice Lake at the very end of the Alleröd chronozone (~12.8 cal. ka BP) first suggested by Donner (1969) and later stratigraphically delineated by Björck and Digerfeldt (1984, 1986). The porewater data provide fresh chemical evidence of a first drainage of the BIL and should exclude the possibility of a subglacial first drainage of the BIL (Björck, 1995). The porewater chlorinity is affected by diffusion as can be seen in the broad appearance of the peak (Fig. 12). Although there is a peak at 33 c-mblf the data also have a

platformal appearance at 18-35 c-mblf possibly indicating more than one marine incursion during that period.

In addition, the timing of the ice grounding (see section *5.1*) could be further constrained by the occurrence of the marine incursion. The chlorinity peak at 33 c-mblf is tied to the first drainage of the BIL (~12.8 cal. ka BP) and is therefore preceding the Younger Dryas cold period (~12.8-11.7 cal. ka BP). Of the two possible ice marginal lines that could have affected the sediment in southern Lake Vättern at this stage, the Skövde ice marginal line (Fig. 7) is attributed to the Younger Dryas cold period (Lundqvist and Wohlfarth, 2000) and should therefore have left its sedimentological imprint *above* 33 c-mblf. A Younger Dryas age of the ice grounding at 54 c-mblf is therefore hard to imagine. We therefore assume that the ice grounding at 54 c-mblf is attributable to the Levene ice marginal line or possibly an even older readvance. Evidence for a Younger Dryas ice readvance in the southernmost part of the Vättern basin should be found in the recovered sediments at any stage between the marine incursion and the Younger Dryas/Preboreal transition (U3/U2). Lenses of coarser material and dropstones are found intermittently at 24-33 c-mblf possibly indicating a thin floating ice tongue or the presence of ice bergs derived from a calving ice margin in the northern part of the lake.

6. Discussion

Lake Vättern and its surroundings are traversed by the Levene line (~13-.4-13.8 cal ka BP: Lundqvist & Wohlfarth 2001; Larsen et al 2012; Anjar et al 2013) and the subsequent Younger Dryas MSEMZ both indicating readvances and/or standstills of the retreating Scandinavian ice sheet (Fig. 7). The general, slightly convex, east-west stretching pattern of the ice marginal lines in southern Sweden (Fig. 1) is interrupted in the Lake Vättern area where the ice margin has oscillated significantly resulting in south stretching ice lobes in the Vättern basin and its proximity (Lundqvist and Wohlfarth, 2001; Lundqvist, 2009). Berglund´s (1979) summary of the research conducted on deglaciation of southern Sweden displays a prominent first lobe connected to the Levene line (Older Dryas chronozone) south of Lake Vättern and a second minor lobe reaching to the middle of the lake. This pattern was revised by Waldermarsson (1989) who made extensive lithostratigraphic investigations in the Jönköping area. The general lithostratigraphy revealed two separate subglacial till units both overlying glaciotectonized proglacial lake deposit which were interpreted as two glacial readvances (Rosenlund and Öxnehaga glaciers) with preceding, intermediate and subsequent proglacial lake stages. Although no dating of the lithostratigraphic units was performed Waldermarsson (1986) tentatively tied the last glacial readvance to the Younger Dryas – Skövde line. In their comprehensive work on late Weichselian ice marginal lines in southern Sweden Lundqvist and Wolfarth (2001) adopted Waldemarsson´s (1986) interpretation and describe two subsequent Lake Vättern ice lobes loosely connected to the Levene line and the Younger Dryas – Skövde line both overriding the southern shoreline of Lake Vättern stretching between 8-30 km south of Jönköping.

During the withdrawal of the Scandinavian Ice sheet the northern tip of Mt. Billingen has been pointed out as a threshold for two possible drainages of the Baltic Ice Lake. The first drainage is connected to the warmer period in the Late Alleröd (~13.0 cal ka BP; Björck, 2008) (Björck and Digerfeldt, 1984, 1986). As the ice retreated north of Mt. Billingen the BIL drained into the North Atlantic with subsequent shoreline displacement around the Baltic basin (Björck, 1995 and references therein; Bennike and Jensen, 2013). Oxygen isotope imprints relating to a meltwater

emanation subsequent to this event have been found in marine clays on the Swedish west coast (Bodén et al., 1997). However, direct evidences (e.g. stratigraphic or morphologic) for a first drainage are few, possibly due to a subsequent overriding ice (Björck, 2008). Furthermore, varve studies in the area (Strömberg, 1992) do not reveal any signs of a late Alleröd ice margin retreat east of Mt. Billingen. The absence of morphological and stratigraphic evidence of a first drainage of the BIL made Björck (1995) suggests a slow subglacial drainage north of Mt. Billingen to the west.

Evidences of a second and final drainage of the BIL are more abundant (e.g. Johansson, 1937; Strömberg, 1992; Andrén et al., 2002; Johnson et al., 2010), and tied to the Younger Dryas/Preboreal transition (~11.7 cal ka BP: Andrén et al., 1999; Björck, 2008). The final drainage is described as a catastrophic event, with ca. 7800 km^3 of fresh water released into the North Atlantic within 1-2 years and resulting in a 25 m drop of the water surface in the Baltic basin (Jakobsson et al., 2007; Andrén et al., 2002; Johnson et al., 2013). This was followed by the Yolda Sea stage in the Baltic, where marine waters from the North Atlantic invaded the basin. The BIL drained trough Lake Vättern and towards Mt. Billingen through the Karlsborg strait on its western flank. A widespread stratigraphic sign of the final drainage in the clays of the Baltic basin is the change from a diatact to a symmict clay mainly referred to as a change from freshwater to marine water depositional environment (e.g. Caldenius, 1940; Strömberg, 1994; Brunnberg, 1995; Johnson et al., 2013). This facies change includes less distinct varves, increased amount of silt, decreased amount of clay and a color change from reddish-brown to dark grey (Strömberg, 1994; Andren et al., 2002).

Large volumes of meltwater from the retreating ice sheet is thought to have hindered marine water to enter the Baltic basin via the Örlen and Viken valleys but as the Närke strait, north of Lake Vättern, became ice free (~11.2 cal ka BP: Björck et al., 2001) marine waters entered the Baltic basin (e.g. Wastegård et al., 1995; Brunnberg, 1995; Andrén et al., 1999). A subsequent ~100-150 year saline phase of the Yoldia Sea is reported from various sites in the central Baltic proper (e.g. Svensson, 1991; Brunnberg, 1995; Andrén, 2002). The only reported marine incursion from the Vättern basin is based on findings of the marine bivalve mollusk (Portlandia Arctica) in a symmict clay sequence from a shallow sediment core at Sjöboda in northern Lake Vättern (Fig. 14). This finding was accompanied by a distinct (1.6%) $CaCO_3$ peak related to an influx of saline water through the Örlen and Viken straits (Björck et al., 2001) (Fig. 23). The regional varve chronology (Strömberg, 1994; Björck et al., 2001) places this marine incursion ~300 years after the final drainage of the BIL but 100 year before the opening of the Närke strait. Later Andrén et al (2002) reported the earliest known marine incursion in the Baltic proper (northwestern Baltic Sea) only 15 years after the Lake Vättern event. These events are interpreted as subsequent signals of the same marine water pulse (Andrén et al., 2002) thus indicating an open Närke strait at this time. Consequently, the reported marine incursion into the Lake Vättern basin would most likely occurred from the north via the Askersund area (Fig. 23).

The integrated results of this thesis provide some intriguing new insights to the above history. The U2/U3 (24 c-mblf) records a change from a reddish-brown diatact clay to a grey sulfide banded symmict clay including an intermediate sand layer. Together with the timing (>11.5 cal ka BP, so far based on correlation with a core in the Visingö-Gränna straight) this transition clearly marks the final drainage of the BIL. Furthermore, if the facies change implies a marine environment during deposition, as suggested by several authors, this result suggests a rapid marine incursion as soon as the water level of the catastrophically draining BIL reached sea level. Limited sequences of symmict

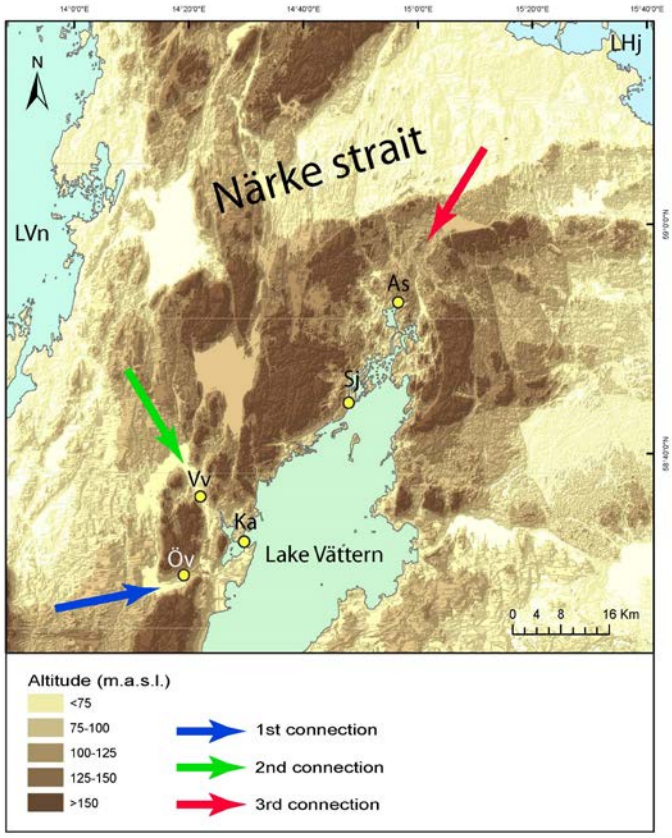

Figure 14. Possible marine water entrances into the Vättern basin during the Scandinavian ice sheet recession. The arrows indicate a stepwise opening of the Vättern basin (BIL) as the ice retreated northwards. LVn = Lake Vänern, Öv = Örlen valley, Vv = Viken valley, Ka = Karlsborg, As = Askersund, Sj = Sjöboda sediment coring site (cf Björck et al., 2001).Topographic data from Lantmäteriet höjddata

clays tied to the period after the final drainage of the BIL have been found in the Örlen and Viken valleys (Strömberg, 1994). These valleys composed narrow straits that constituted the only westward connections from the Vättern basin at this time (cf Jakobsson et al., 2001) (Fig. 14). It is therefore likely that pulses of marine waters entered the Vättern basin and that a smaller part of these waters was kept in the narrow straits. The main part of a marine water pulse would have flowed to the deeper part of the Vättern basin creating a halocline due to its comparatively high density (cf Björck et al., 2001).The broad plateau (Fig. 12) in the porewater chlorinity data encompasses this transition, and does support a marine incursion at the U2/U3 transition.

The peak in porewater chlorinity at 33 c-mblf is distinctly separated from the BIL/Yoldia Sea transition at 24 c-mblf. The only known event that can explain this clear saline effect is the proposed first drainage of the BIL. This is the first evidence for a marine incursion into the Baltic Ice Lake and it supports the retreat-readvance-retreat model suggested by Björck and Digerfeldt (1984, 1986). This model implies the successive opening-closing-opening of the threshold at the northern tip of Mt. Billingen with subsequent drainages (first and final) during the opening phases. Furthermore, a marine incursion into Lake Vättern requires an ice marginal retreat at the western flank of Lake Vättern to a position north of the Örlen valley (Fig. 14). The suggested subglacial drainage theory (Björck, 1995) would likely not allow a marine incursion as a dammed BIL with an elevated water level would add considerable pressure on the draining water mass thereby hinder any influx of water to the BIL. Although, no dating of this sediment sequence is made its strong connection with the first drainage of the BIL infer an age of ~13.0 cal ka BP (Björck, 2008).

The ice grounding event at 54 c-mblf is the only evidence of prominent ice readvances in the 74 m composite core from southern Lake Vättern. Due to its position well below the Younger Dryas sediment sequence (~33-25 c-mblf) the ice grounding event is attributed to the terrestrial Levene ice marginal line (~13.6 cal ka BP). Of the two major ice readvances described by Waldemarsson (1986) only one is captured in the 74 m composite sediment core of southern Lake Vättern. The absence of one major readvance suggests that the sedimentary imprint of the first readvance (Rosenlund glacier) is located below the recovered sediment sequence. Consequently, the second readvance (Öxnehaga glacier) seems to be the cause of the ice grounding event, and this was not during the

Younger Dryas, but earlier. Due to lack of evidence for a Younger Dryas ice lobe in southern Lake Vättern a return to the classical description (Berglund, 1979) of the Lake Vättern ice lobes seems convenient. That description includes a major Levene ice margin ice lobe stretching from the northern part of Hökensås to the south of Jönköping, and a minor Younger Dryas ice lobe that stretched from its base at the Younger Dryas-Skövde line and <10 km southwards.

7. Conclusions

The following conclusions can be drawn from the analysis of the 74 m composite sediment core recovered in southern Lake Vättern 2012:

- The lithostratigraphy reveals three distinct sedimentary units. The lower lithostratigraphic unit (U3) is deposited during one or more proglacial lake stages including the Baltic Ice Lake. The middle lithostratigraphic unit (U2) is deposited after the final drainage of the BIL. The upper lithostratigraphic unit (U1) derives from the modern isolated lake.

- Disturbed sediment together with significant increase in bulk density and magnetic susceptibility strongly suggests a compressional process associated with an ice grounding at 54 c-mblf. We tie this ice grounding to the terrestrial Levene ice marginal line formed by an ice readvance ~13.6 cal. ka BP.

- The broad peak in porewater chlorinity at 33 c-mblf reveal one (or more) marine incursion(s) into the Vättern basin before the final drainage of the BIL. The marine incursion is likely associated with the suggested first drainage of the BIL at ~12.8 cal. ka BP.

- The sharp U2/U3 transition with a distinct change from red to gray silty clay in the sediment column is connected to the final drainage of the BIL and the onset of Holocene. This transition is dated with pollen analysis from a correlatable core to >11.5 cal. ka BP.

- Compressional structures and micro-faults are found in the lower part of U2. These structures are interpreted as neotectonic features that reflect the major earthquake event described by Jakobsson et al. (2014).

8. Ongoing and future work

8.1 Geochemical imprints of a changing palaeoenvironment

The Lake Vättern sediments recovered in 2012 provide a wide range of opportunities for further palaeoenvironmental research. An in-depth study of the high-resolution elemental data acquired from the Itrax XRF core scanning has already begun. The elemental imprint of the sediment is the sum of a wide range of different processes including source rock composition, catchment weathering, atmospheric deposition, transport efficiencies, sedimentation and post-depositional processes (Boyle, 2001). The aim of this study is to identify the significance of various regional palaeoenvironmental events and processes to the elemental variations captured in the recovered sedimentary record during deglaciation.

Important palaeoenvironmental events that may be reflected in the elemental data by a significant change in sediment composition include the Levene ice marginal readvance with the accompanying ice grounding, the final drainage of the BIL and the isolation of the Vättern basin from the Yoldia Sea. These events have likely had a large effect on the elemental imprint due to their influence on the hydrological regime, rock source for weathering and catchment area.

As a start we have divided the composite sediment core into three possibly different geochemical regimes marked by the above mentioned palaeoenvironmental events: U3C (deposited before the ice grounding we postulate is contemporaneous with the levene moraine empalcement), U3A+B (deposited before the drainage of the BIL) and U2 (deposited before lake isolation from the Yoldia Sea) (Fig. 15).

The elemental data (K, Ti, Rb, Fe, Zr, Si, Mn, Sr and Ca) from ITRAX-XRF scanning is presented as peak areas vs. mblf in the composite sediment core (Fig. 15). However, in a palaeoenvironmental context it is the downhole change in the peak areas, rather than the peak area itself, that is of interest. The study of elemental changes will also include other proxies such as bulk density, magnetic susceptibility, $\delta^{13}C$, grain size, and carbonate content, all available from the laboratory analyzes of the Lake Vättern sediment cores. This kind of multiproxy approach increases the possibility of robust interpretations of the geochemical changes.

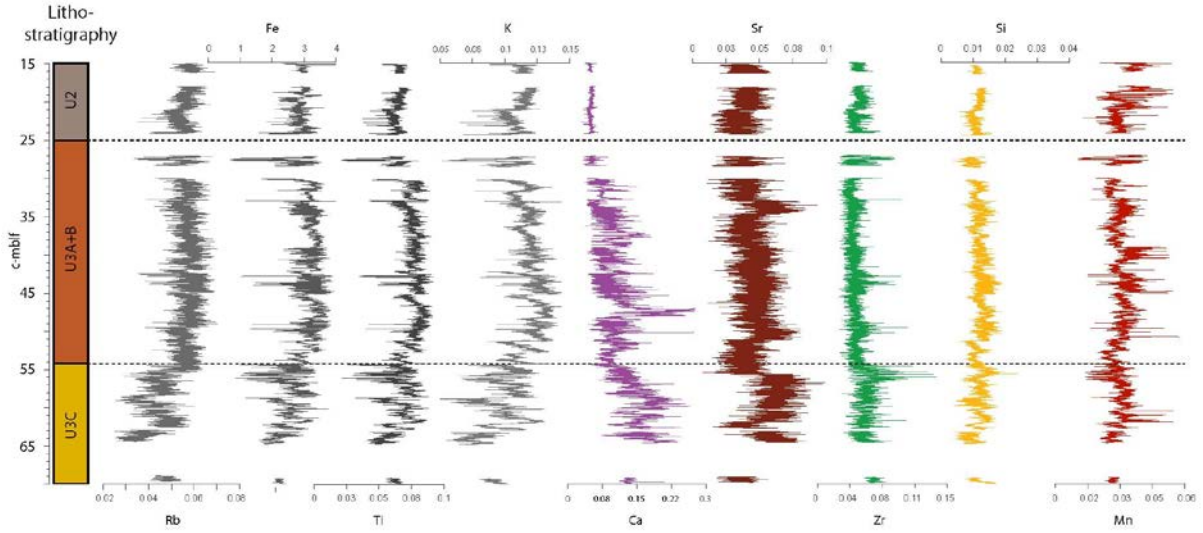

Figure 15. High resolution elemental data (Rb, Fe, Ti, K, Ca, Sr, Zr, Si and Mn) from XRF-core scanning along with the selected units of the composite sediment core.

Principal factor analysis (PFA) was performed on the scattering normalized elemental data to find groups of element that exhibit the same downhole behavior (Reimann et al., 2008). Each unit (U3C, U3A+B and U2) was assigned four factors (F1-4) that cumulatively explained >85 % of the total variance in the dataset for each unit. The preliminary results confirm the strong visual correlation between Ti, K, Rb and Fe in all units (F1)(Tab. 1). These elements (except Fe) are commonly referred to as conservative lithogenic elements not affected by biogeochemical reactions (Kylander et al., 2011). In a general limnological context Fe is often seen as an active redox element correlated with Mn (Davison, 1993) but this correlation is only present in U3C (Tab. 1). Changes in Ca are commonly related to either changes in lake precipitation of carbonates or to changes in source rock composition

(Cohen, 2003). In the Lake Vättern sediment variation in Ca seems to be independent of the lithogenic elements in the glacial clay while it is strongly correlated to the lithogenic group (F1) during the Yoldia Sea stage (U2). Sr and Zr are generally acting independently. Further work will aim to highlight substantial changes in each factor (F1-F4) and try to explain these changes in terms of regional palaeoenvironmental changes.

Associated factor	U2	Variance explained by each factor (%)	U3A+B	Variance explained by each factor (%)	U3C	Variance explained by each factor (%)
F1	*K, Ti, Rb, Fe and Ca*	42	*K, Ti, Rb, Fe*	36	*K, Ti, Rb, Fe and Mn*	48
F2	*Si and Zr*	26	*Ca*	18	*Ca*	16
F3	*Sr*	14	*Sr*	15	*Zr*	15
F4	*Mn*	13	*Zr*	15	*Sr*	12

Table 1. Result of Principal Factor Analysis together with the variance explained by each factor. Cumulative variance explained > 85%. F1 = Factor 1, F2 = Factor 2, F3 = Factor 3, F4 = Factor 4.

During periods with similar depositional environments, the elemental proportions should remain stable. Changes in the proportion of elements are a common way to identify different depositional environments within sediment cores. For the Lake Vättern sediments, we have used the results from the PFA, to identify elements from different factors, and used a cross-plotting technique to identify potential differences within or between the lithologic units (Fig 16). The initial results suggest a higher degree of clustering in the U2 interval, compared with the underlying glacial clays where there is a greater spread in the data. The data distribution in the Zr vs Rb plot is the same for all units but the concentration point has shifted towards the left for U3C. In the Ca vs Rb plot both the spread and shape varies for each unit. The discrepancy between U3C and U3A+ B is intriguing, as both units are glacial clays. The difference may reflect either a sediment source change due to different glacial source regions, or because of a grain size change due to closer proximity to the ice margin. Further work will focus on explaining the differences in the chemical composition of sediments between units, and the implications for the paleoenvironmental interpretation.

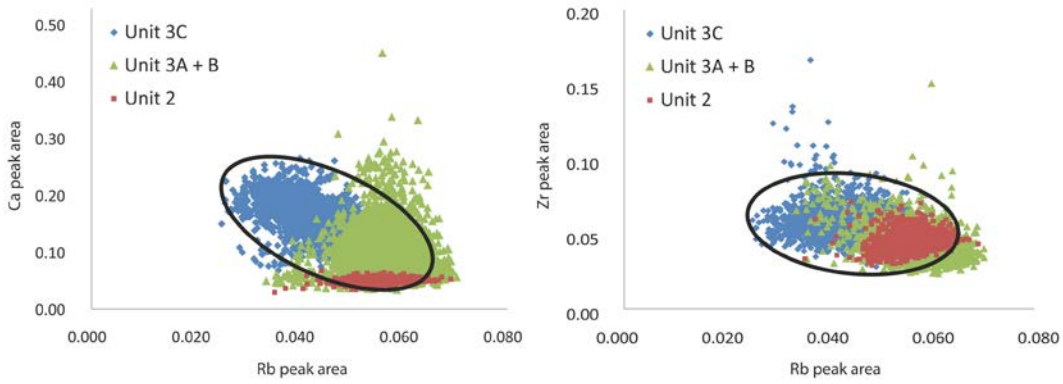

Fig. 16 Biplots of unit separated elemental data. Red data points = U2, Green data points = U3A+B, Blue data points = U3C. Black ellipse indicates the full extent of U3C data points. Rb represents the F1 elements whereas Ca and Zr represent factors uncorrelated to F1. a) Ca vs Rb b) Zr vs Rb

8.2 Porewater modeling

The next step in my PhD project is to further delineate the marine incursion(s) in Lake Vättern presented in this thesis. This will enhance the understanding of the southwest Swedish ice retreat including various possible BIL drainage scenarios. The broad chlorinity peak (20-35 c-mblf) indicates the influence of diffusion acting on the porewater and its content but could also hide the presence of more than one marine incursion. To be able to unravel this issue a comprehensive dating of the sediment cores is of great importance. My future work will therefore include a dating campaign including palynological studies, ^{14}C dating and an attempt to correlate the glacial varves found in the Lake Vättern sediment with the Swedish Time Scale (summarized in Wohlfarth and Possnert, 2000).

A reliable chronology is a foundation for the next line of research: a reconstruction of palaeosalinities in Lake Vättern. Reconstructions of palaeosalinities using the chlorinity in sediment porewater profiles have been obtained using a one-dimensional inverse models (Adkins and Schrag, 2003; Insua et al., 2014). These reconstructions have been used to reconstruct Pacific bottom water salinity during the Last Glacial Maximum. A similar approach will be adopted to fit the palaeoenvironment of the Vättern basin. To model the palaeosalinity of Lake Vättern we will use *COMSOL Multiphysics* software, which enables the use of a one-dimensional diffusion model designed with pre-defined partial differential equations. Important variables in such a model are the sedimentation rate, which determines changes in the concentration gradient, and sediment porosity (compaction) that changes the diffusion coefficient through time.

The diffusion model will be developed and run to match the current chlorinity profile using various drainage scenarios for the BIL with the aim to find the best match of the palaeosalinity and duration of incursion to the current chlorinity profile. The final model will not only help us to constrain the timing and sequence of events related to the catastrophic drainage of the BIL but also provide a more general sedimentation – compaction – diffusion model that can be applied to other geological processes. If successful, it may be possible to apply this technique to a wider data set collected during the recent Integrated Ocean Drilling Programs Baltic Sea Expedition.

Acknowledgments

First of all I want to express my deepest gratitude to my supervisors and scientific loadstars Matt O'Regan and Martin Jakobsson. Thank you for this opportunity. It has been a true joy. For further scientific advice I thank Sarah Greenwood, Malin Kylander, Richard Gyllencreutz and Carl-Magnus Mörth. Pedro Preto and Tina Varga are thanked for invaluable assistance in the core laboratory. The excellent technical staffs at IGV and ITM is hereby acknowledged: Carina Johansson for running the ITRAX, Heike Siegmund and Malin Söderman at for the TOC and isotope analyses and Pär Hjelmqvist for the chlorinity analysis.

This licentiate thesis is part of the Research School focusing on Natural Hazards at IGV. Alasdair Skelton and Hildred Crill have done a meritorious job in arranging the research school and are hereby greatly acknowledged. Jag vill i detta sammanhang också tacka min arbetsgivare Jönköping kommun samt min dåvarande rektor Ove Tunhaw som utan något som helst mankemang gjorde det ekonomiskt och praktiskt möjligt för mig att delta i forskarskolan för lärare med inriktning mot naturkatastrofer. Att vara lärarforskare är ju en smula ovanligt i den akademiska världen och därför har det varit ovärderligt att få ha 12 kollegor i samma båt vilka alltid varit redo att penetrera problem och glädjeämnen i livet och arbetslivet.

Tack Sven och Ingmarie för mat, husrum och omsorg under långa Stockholmsvistelser. Far – tack för all den tid som du lagt ner som barnvakt under dessa år inklusive dryga resor till Jönköping i stort sett varje vecka. Mor – tack för att du släppte iväg honom. Tack Elin för att du uppmuntrade mig att, trots min egen tvekan, söka till forskarskolan. Du har sedan dess stöttat mig även när oväntade akademiska vindar blåst åt ett håll som gjort det betydligt jobbigare för dig än vad som var tanken från början.

S.D.G.

References

Adkins, J.F. and Schrag, D.P., 2003. Reconstructing Last Glacial Maximum bottom water salinities from deep-sea sediment pore fluid profiles. Earth and Planetary Science Letters 216, 109-123.

Andrén, T., Björck, J., Johnsen, S., 1999. Correlation of Swedish glacial varves with the Greenland (GRIP) oxygen isotope record. Journal of Quaternary Science 14, 361-371.

Andrén, T., Lindeberg, G., Andrén, E., 2002. Evidence of the final drainage of the Baltic Ice Lake and the brackish phase of the Yoldia Sea in glacial varved from the Baltic Sea. Boreas 31, 226 - 238.

Andrén, T., Björck, S., Andrén, E., Conley, D., Zillén, L. & Anjar, J., 2011. The development of the Baltic Sea basin during the last 130 ka. *In*: Harff, J., Björck, S. & Hooth, P. (eds.): The Baltic Sea Basin, 75–98. Springer-Verlag, Berlin, Heidelberg.

Bennike, O. & Jensen, J., 2013. A Baltic Ice Lake lowstand of latest Allerod age in the Arkona Basin, southern Baltic Sea. Geological Survey of Denmark and Greenland Bulletin 28, 17-20.

Berglund, B. E., 1979. The deglaciation of southern Sweden 13,500-10,000 BP. Boreas 8, 89-118.

Bergsten, K.E., 1943. Isälvsfält kring norra Vättern. Fysisk-geografiska studier. Meddelanden från Lunds Universitets Geografiska Institution, Avhandlingar VII, 245 pp.

Bingen, B., Andersson, J., Söderlund, U. & Möller, C., 2008. The Mesoproterozoic in the Nordic countries. Episodes, v. 31, p. 29–34.

Björck, S. and Digerfeldt, G., 1984. Climatic changes at Pleistocene/Holocene boundary in the Middle Swedish endmoraine zone, mainly inferred from stratigraphic indications. *In:* Mörner, N.-A. and Karlén, W. (eds), Climatic Changes on a Yearly to Millenial Basis, pp. 37-56. Reidel, Dordrecht.

Björck, S. and Digerfeldt, G., 1986. Late Weichselian – Early Holocene shore displacement west of Mt. Billingen, within the Swedish end-moraine zone. Boreas 15, 1-18.

Björck, S., Digerfeldt, G., 1989. Lake Mullsjön - a key site for understanding the final stage of the Baltic Ice Lake east of Mt. Billingen. Boreas 18, 209-219.

Björck, S., 1995. A review of the history of the Baltic Sea, 13.0-8.0 ka BP. Quaternary International 27, 19-40.

Björck, S., Kromer, B., Johnsen, S., Bennike, O., Hammarlund, D., Lemdahl, G., Possnert, G., Rasmussen, T.L., Wohlfarth, B., Hammer, C.U. & Spurk, M., 1996. Synchronized terrestrial-atmospheric deglacial records around the north Atlantic. Science 274, 1155–1160.

Björck, S. 2008. The late Quaternary development of the Baltic Sea basin. *In*: Assessment of climate change for the Baltic Sea Basin Edited by: The BACC Author Team. 398–407. Springer-Verlag Berlin Heidelberg

Bodén, P., Fairbanks, R.G., Wright, J.D., Burckle, L.H., 1997. High-resolution stable isotope records from southwest Sweden: The drainage of the Baltic Ice Lake and Younger Dryas Ice Margin Oscillations. Paleoceanography 12 (1), 39–49.

Brunnberg, L., 1995. Clay-varve chronology and deglaciation during the Younger Dryas and Preboreal in the easternmost part of the Middle Swedish Ice Marginal Zone. Quaternaria, Stockholm University, A, Vol. 2, 94 pp.

Caldenius, C., 1944. Baltiska issjöns sänkning till Västerhavet. En geokronologisk studie. Geologiska föreningens i Stockholm förhandlingar 66, 366-382.

Carter, J.F. & Barwick, V.J., 2011. Good practice guide for isotope ratio mass spectrometry, Forensic Isotope Ratio Mass Spectrometry Network (FIRMS). 41 pp.

Cohen, A. S., 2003. Paleolimnology: The History and Evolution of Lake Systems. Oxford University Press: Oxford.

Davison, W., 1993. Iron and manganese in lakes. Earth and Science Reviews 34, 119–163.

De Geer, G., 1893. Om strandlinjens förskjutning vid våra insjöar. Geologiska Föreningen i Stockholm Förhandlingar 15, 378-394.

De Geer, S., 1910. Map of landforms in the surroundings of the great Swedish lakes. SGU. Ba 7.

Dickens, G.R., Koelling, M., Smith, D.C., Schnieders, L., 2007. Rhizon Sampling of Porewaters on Scientific Drilling Surveys: An Example from the IODP Survey 302, Arctic Coring Survey (ACEX), Scientific Drilling, pp. 22-25.

Donner, J.J., 1969. A profile across Fennoscandia of Late Weichselian and Flandrian shore-lines. Societas Scientarum Fennica. Commentationes Physico-Mathematicae 36, 1-23.

Ekman, S., 1914. Sedimentering, omsedimentering och vattenströmningar i Vättern. Ymer 34, Stockholm

Greenwood, S.L., O'Regan, M., Swärd, H., Flodén, T., Jakobsson, M., Multiple readvances of a Lake Vättern outlet glacier during Fennoscandian Ice Sheet retreat, south-central Sweden. (*in review*)

Gorbatschev, G. 1980. The Precambrian development of southern Sweden. Geologiska Föreningen i Stockholm Förhandlingar 102:2, 129-136.

Hansbo, S. 1957. A new approach to the determination of the shear strength of clay by the fall-cone test. Swedish Geotechnical Institute Proceedings, Stockholm. No. 14, 46 pp.

Insua, T. L., Spivack, A. J., Graham, D., D'Hondt, S. and Moran, K., 2014. Reconstruction of Pacific Ocean bottom water salinity during the Last Glacial Maximum. Geophysical Research Letters 41, 1-7.

Jakobsson, M., Björck, S., Alm, G., Andrén, T., Lindeberg, G., Svensson, N.-O., 2007. Reconstructing the Younger Dryas ice dammed lake in the Baltic Basin: Bathymetry, area and volume. Global and Planetary Change 57, 355-370.

Jakobsson, M., Ampel, L., Junghahn, K., Lif, A., 2012. Undersökning av bottensediment i sydvästra Vättern. Rapport från Institutionen för geologiska vetenskaper, Stockholms Universitet

Jakobsson, M., Björck, S., O´Regan, M., Flodén, T., Greenwood, S.L., Swärd, H., Lif, A., Ampel, L., Koyi, H., Skelton, A., 2014. Major earthquakes at the Pleistocene-Holocene transition in Lake Vättern, southern Sweden. Geology 42, 379-382.

Johansson, S., 1937. Senglaciala och interglaciala avlagringar vid ändmoränstråket i Västergötland. Geologiska föreningens i Stockholm förhandlingar 59, 379–454.

Johnson, M.D., Ståhl, Y., Larsson, O. & Seger, S., 2010. New exposures of Baltic Ice Lake drainage sediments, Götene, Sweden. GFF. 132 (1), 1-12.

Johnson, M.D., Kylander, M.E., Casserstedt, L., Wiborgh, H., Björck, S., 2013. Varved glaciomarine clay in central Sweden before and after the Baltic Ice Lake drainage: a further clue to the drainage events at Mt Billingen. GFF 135, 293-307.

Kristiansson, J., 1986. The ice recession in the south-eastern part of Sweden. A varve-chronological time scale for the latest part of the Late Weichselian. University of Stockholm, Department of Quaternary Research, Report 7, 149 pp.

Kylander, M.E., Ampel, L., Wohlfarth, B. & Veres, D., 2011. High-resolution X-ray fluorescence core scanning analysis of Les Echets (France) sedimentary sequence: new insights from chemical proxies. Journal of Quaternary Science 26(1), 109-117.

Lind, G., 1972. The Gravity and Geology of the Vättern area, Southern Sweden. Geologiska Föreningen i Stockholm Förhandlingar 94:2, 245-257.

Lundqvist, J., 1988. Late glacial ice lobes and glacial landforms in Scandinavia. *In:* Goldthwait, R.P., Matsch, C.L. (eds.), Genetic Classification of Glacigenic Deposits. A.A. Balkema, Rotterdam, 217-225.

Lundqvist, J., Vilborg, L., 1998. Lokaler i Sverige. *In:* Andersen, S., and Pedersen, S. S., (eds.), Israndlinier i Norden, Nordisk Ministerråd. København , 182-185.

Lundqvist, J., Wohlfarth, B., 2000. Timing and east–west correlation of south Swedish ice marginal lines during the Late Weichselian. Quaternary Science Reviews 20, 1127-1148.

Lundqvist, J., 2009. Weichsel-istidens huvudfas. In: Fredén, C., (ed.), Berg och Jord, 124-135, Sveriges Nationalatlas. Norstedts kartor. Bromma

Lundqvist, J., Lundqvist, T., Lindström, M., Calner, M., Sivhed, U., 2011. Sveriges geologi från urtid till nutid, 3rd ed. Studentlitteratur, 628 pp.

Milsom, J. & Eriksen, A., 2011. Field Geophysics. John Wiley & Sons, Ltd. 229-239.

Munthe, H., 1910. Studies in the late Quaternary history of south Sweden. Geologiska föreningen i Stockholm förhandlingar 32, 1197-1293.

Munthe, H., 1935. Till frågan om Vätterns senkvartära historia, Geologiska Föreningen i Stockholm Förhandlingar 57:1, 29-46.

MqQuillin, R. & Ardus, D.A., 1977. Exploring the Geology of Shelf Seas. Graham & Trotman Ltd. 233 pp.

Nilsson, E., 1939. Huvuddragen av Vättertraktens geografiska utveckling under senkvartär tid. Mäster Gudmunds gilles årsbok, 11-38, Jönköping.

Nilsson, E., 1953. Om södra Sveriges senkvartära historia. Geologiska Föreningen i Stockholm Förhandlingar 75, 155-246.

Nilsson, E., 1958. Issjöstudier i södra Sverige, Geologiska Föreningen i Stockholm Förhandlingar 80:2, 166-185.

Nilsson, E., 1968. Södra Sveriges senkvartära historia. Geokronologi, issjöar och landhöjning. Kungliga Svenska Vetenskapsakademiens Handlingar, Fjärde Serien. Bd. 12:1. 117 pp.

Norrman, J.O., 1964. Vätterbäckenets senkvartära strandlinjer. Geologiska föreningen i Stockholm förhandlingar 85, 391-413.

Norrman, J.O., 1971. Skallhultsplatån, en supraakvatisk deltayta bildad innanför inlandsisens rand under isavsmältningen i Vätterbäckenet. Geologiska Föreningen i Stockholm Förhandlingar 93, 215-224.

Norrman, J.O., Königsson, L-K., 1972. The Sediment Distribution in Lake Vättern and some Analyses of Cores from its Southern Basin. Geologiska Föreningen i Stockholm Förhandlingar 94:4, 489-513.

O'Regan, M., Greenwood, S., Preto, P., Swärd, H., Jakobsson, M., Geotechnical and sedimentary evidence for thick-grounded ice in Southern Lake Vättern during deglaciation. (in review)

Rasmussen, S. O., Andersen, K. K., Svensson, A. M., Steffensen, J. P., Vinther, B. M., Clausen, H. B., Siggaard-Andersen, M. L., Johnsen, S. J., Larsen, L. B., Dahl-Jensen, D., Bigler, M., Röthlisberger, R., Fischer, H., Goto-Azuma, K., Hansson, M. E., Ruth, U., 2006. A new Greenland ice core chronology for the last glacial termination. Journal of Geophysical Research 111, D06102

Reimann, C., Filzmoser, P., Garret, R., Dutter, R., 2008. Statistical Data Analysis Explained: Applied Environmental Statistics. John Wiley & Sons Ltd.

Sayles, F.L. & Mangelsdorf Jr, P.C., 1977. The equilibration of clay minerals with sea water: exchange reactions. Geochimica et Cosmochimica Acta 41, 951-960.

SGU (Geological Survey of Sweden), 2010. Bedrock Sweden 1:1 000 000 Electronic resource]: https://maps.slu.se/get/

Strömberg, B., 1992. The final stage of the Baltic Ice Lake. Sveriges Geologiska Undersökning, Series, Ca 81, 347–353.

Strömberg, B., 1994. Younger Dryas deglaciation at Mt. Billingen, and clay varve dating of the Younger Dryas/Preboreal transition. Boreas 23, 177-193.

Svantesson, S.-I., 1981. Beskrivning till jordartskartan Hjo. Sveriges Geologiska Undersökning Aa 44, 101.

Vidal, G., 1984. Lake Vättern. Geologiska Föreningen i Stockholm Förhandlingar 106:4, 397-397.

Waldemarson, D., 1986. Weichselian lithostratigraphy, depositional processes and deglaciation pattern in the southern Vättern basin, south Sweden. LUNDQUA Thesis, Vol. 17, 128pp.

Wastegård, S., Andrén, T., Sohlenius, G. & Sandgren, P. 1995. Different phases of the Yoldia Sea in the north-western Baltic Proper. Quaternary International 27, 121–129.

Wik, N-G., Andersson, J., Bergström, U., Claeson, D., Juhojuntti, N., Kero, L., Lundqvist, L., Möller, C., Sukotjo, S., & Wikman, H. 2006. Beskrivning till regional berggrundskarta över Jönköpings län. SGU, K 61, 60 pp.

Wohlfarth, B., Possnert, G., 2000. AMS Radiocarbon measurements from the Swedish varved clays. Radiocarbon 42:3, 323–333.

Hou, X., & Jones, B. T., 2000. Inductively Coupled Plasma/Optical Emission Spectrometry *In*: Encyclopedia of Analytical Chemistry, Meyers, R. A., (Ed.), John Wiley & Sons Ltd, Chichester, 9468-9485.

Regional deglaciation and postglacial lake development as reflected in a 74 m sedimentary record from Lake Vättern, southern Sweden

Henrik Swärd[1], Matt O´Regan[1], Linda Ampel[1], Roman Ananyev[2], Denis Chernykh[3], Tom Flodén[1], Sarah L. Greenwood[1], Malin Kylander[1], Carl Magnus Mörth[1], Pedro Preto[1] & Martin Jakobsson[1]

[1] *Department of Geological Sciences, Stockholm University, Stockholm*

[2] *P.P.Shirshov Institute of Oceanology, Russian Academy of Sciences, 36 Nahimovski prospekt, Moscow, 117997, Russia and National Research Tomsk Polytechnic University, 30 Lenin Avenue, Tomsk, 634050, Russia*

[3] *Russian Academy of Sciences, Far Eastern Branch, Pacific Oceanological Institute, 43 Baltiiskaya Street, Vladivostok 690041, Russia and National Research Tomsk Polytechnic University, 30 Lenin Avenue, Tomsk, 634050, Russia*

Abstract

Lake Vättern and its basin have been in the center of the highly dynamic retreat history of the Late Weichselian ice sheet in south central Sweden. This part of the deglacial history is described from an abundance of terrestrial studies but no complimentary long sediment cores from the lake have been available. Here we present the results from a unique borehole in southern Lake Vättern that recovered Late Pleistocene to Holocene sediments down to 74 meters below the lake floor. Physical and chemical analysis of the sediment and pore waters, together with geophysical mapping, displays glacial as well as post-glacial imprints implying an oscillating ice sheet margin, neotectonic activities and one or more marine incursions into the Lake. We suggest that glaciotectonic deformation of the sediments at 54 meters below the lake floor can be connected to the terrestrial Levene ice marginal line (~13.4 cal. ka BP), and that after this episode, grounded ice did not cover southern Lake Vättern again. Potential readvances, including at the Younger Dryas, were likely restricted to a more northerly position in the basin and delivered coarse sediments and dropstones to the south of the lake. We identify the final drainage of the Baltic Ice Lake, but find evidence for an earlier marine incursion into the Vättern basin (~12.8 cal. ka BP), indicating water exchange between the ocean and the Baltic Ice Lake during the late Alleröd.

Introduction

Lake Vättern, the second largest lake in Sweden, is elongated in a NNE-SSW direction and situated in the central southern part of the country (Fig. 1a). It occupies an area of approximately 1900 km^2 and stretches 135 km with a maximum width of 35 km. The main axis of the lake aligns with two major north-south stretching tectonic lineaments; the Protogine Zone (PZ) in the south and the Sveconorwegian Frontal Deformation Zone (SFDZ) in the north (Fig. 1a) which together constitute the eastern border of the Sveconorwegian orogeny (Gorbatchev, 1980, Bingen et al., 2008). The formation of the Vättern half-graben started 700-800 Ma during a phase of extensional faulting (Andréasson and Rodhe, 1990; Månsson, 1996). A surface expression of this fault system is seen in the lake bathymetry in the form of a deep channel that runs along the eastern part of the lake (Fig 1b). The deepest stretch of Lake Vättern reaches 119 m and is found in this channel to the east and south of the island of Visingsö.

The retreating Late Weichselian Ice sheet in southern Sweden is marked in the landscape by a set of ice marginal landforms (Lundqvist and Wohlfarth, 2001). Of these, the Levene moraine extends towards the southernmost part of Lake Vättern (Fig. 1b). An embayment in the ice margin is suggested to have existed, around the highland of Hökensås (200 m above the present lake level), which captured an abundance of glaciofluvial sediments from the surrounding thicker ice lobes (Lundqvist

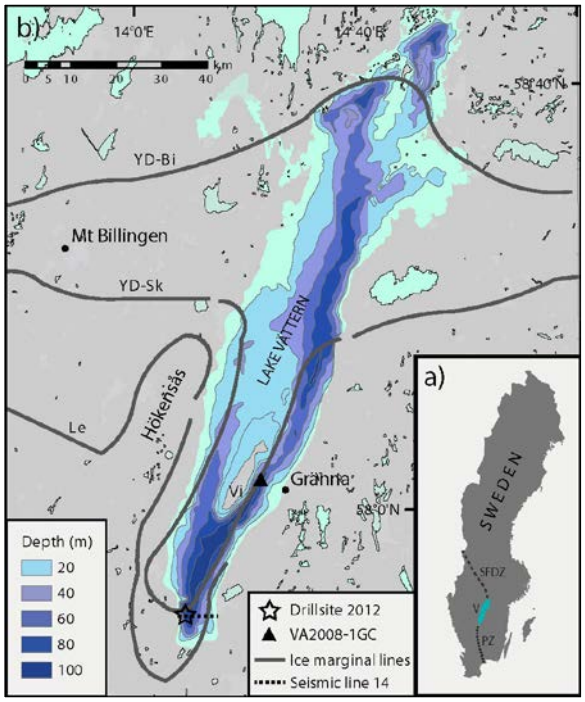

Fig. 1 a) Lake Vättern in southern central Sweden with connecting tectonic lineaments. V = Lake Vättern, PZ = Protogine Zone, SFDZ = Sveconorwegian Frontal Deformation Zone. b) Lake Vättern with drill sites and location of seismic line 14 that crosses the drilling site. Bathymetry adapted from Norrman, 1964 and ice marginal lines from Lundqvist and Wohlfarth, 2000. YD-Sk = Younger Dryas-Skövde moraine, YD-Bi = Younger Dryas-Billingen moraine, Le = Levene moraine, Vi = Visingsö Island.

and Wohlfarth, 2001). East of this embayment, an ice lobe extending southwards in the deep lake basin is inferred from mapped striae (Waldermarson, 1986) and thick glaciofluvial and glaciolacustrine deposits south of the present lake shore (Lundqvist and Wohlfarth, 2001). From evaluation of published dating results constraining the Levene moraine, Lundqvist and Wohlfarth (2001) concluded that it was formed before or around 13.4 cal. ka BP. This implies that the Late Weichselian Ice Sheet margin was located at the southern tip of Lake Vättern at about this time. Two prominent moraines, the Skövde and Billingen moraines lie north of the Levene moraine towards the western shore of Lake Vättern (Fig. 1b). They represent the halt in the general ice retreat during Younger Dryas cold period and they continue east of the lake across Sweden in a northeasterly direction (e.g. Strömberg 1969; Björck and Digerfeldt, 1981). The chaotic interior structure of these moraines led Björck and Digerfeldt (1984) to suggest a major re-advance of the ice sheet during the early coldest part of Younger Dryas.

During the latest deglaciation, Lake Vättern originally formed as an isolated proglacial lake. It became connected to the larger Baltic Ice Lake (BIL) when the ice front retreated north of the south eastern highlands of the Vättern basin at <14 cal. ka BP (Björck, 1995). The (re)advances of lobes of ice in Lake Vättern into these proglacial water bodies are therefore closely coupled to the history of the Baltic. When the ice margin eventually retreated north of Mt Billingen (Fig. 1b), the Baltic Ice Lake catastrophically drained 25 m of its level towards the contemporary sea in the west (Björck and Digerfeldt, 1984). The outburst is estimated to have involved 7800 km^3 water (Jakobsson et al., 2007) over a time period of less than a year (Johnson, 2013). At the final drainage of the BIL Lake Vättern became a part of the Yoldia Sea for a period estimated to be shorter than 1000 years due to the regional isostasy that finally isolated the lake from the Baltic Sea (Björck, 1995).

We would expect the deglaciation history of south central Sweden to be captured in the bottom sediment of Lake Vättern. The general bottom surface sediment distribution in the lake was described by Norrman (1964) and Norrman and Königsson (1972). The upper meters of the sediment stratigraphy below the lake floor from sites north of Visingsö, consists of a top layer of brown clay with an underlying varved grey clay layer. Some of the cores had a sand layer at the very top, suggesting ongoing winnowing and erosion of modern and Holocene sediments (Norrman 1964). For the deeper parts south and east of Visingsö sediments showed a heterogeneous stratigraphy with interbedded intervals of silty clay, silty gyttja-clay and silt. Norrman and Köunigsson (1972) suggest that the silt content derives from redeposition or eroded deposits from the subaqueous platform west of Visingsö Island. The interbedded layers could also be a result of mass wasting

processes from the steep subaqueous slopes that are common in the southern part of the lake (Norrman and Köunigsson, 1972). Recent geophysical mapping in the southern part of the lake confirm the frequent presence of mass wasting processes, possibly linked to neotectonic activity generating shallow earthquakes (Jakobsson et al., 2014). The Vättern basin is believed to hold a deep sediment archive, which would have the potential to provide a detailed record of the deglacial and Holocene sedimentary regimes and environmental conditions in the basin. It should therefore help to constrain the dynamics of ice sheet retreat and Baltic Sea development.

In October/November 2012, five closely spaced boreholes (A-E) were drilled using a drilling system from a barge anchored offshore from Tranghalla in southern Lake Vättern (Fig. 1b). The deepest recovered sediments were from 74 meters below the lake floor (c-mblf). Sediment cores from these boreholes, including earlier spot cores, were supplemented with two 5 meter piston cores taken from the lake surface beside the barge.

Here we provide an initial synthesis of the drilling results, focusing on the physical properties of the recovered sediments and how they relate to the deglacial and Holocene environmental conditions in Lake Vättern. The acquired seismic reflection profiles across the drill site allow us to place the drill core stratigraphy in a regional context. We identify three major lithologic units in the 74 m of penetrated sediments and tentatively correlate these to the widely recognized Baltic Sea development stages. This record provides a valuable new resource for constraining deglacial and postglacial environments at a high temporal resolution in south-central Sweden.

Methods

Drilling and sediment core processing

Drilling in Southern Lake Vättern was performed in October and November of 2012 at a water depth of 90 – 95 meters (E 14:11:03; N 57:50:00) (Fig. 1b). The drilling rig, provided by Asera Mining AB, was fitted with an HQ wire line drilling system with HQ-3 plastic liners (length 3 m, inner ∅ 63 mm and outer ∅ 65 mm) (Fig. 2). When cores were brought onto deck, the liners were pulled from the core barrel and cut into 1.5 m sections, curated and stored in a heated container (> 4°C) to prevent freezing. The sediment recoveries for the five boreholes (A-E) are reported in Figure 3a together with the stratigraphic depths, here reported in

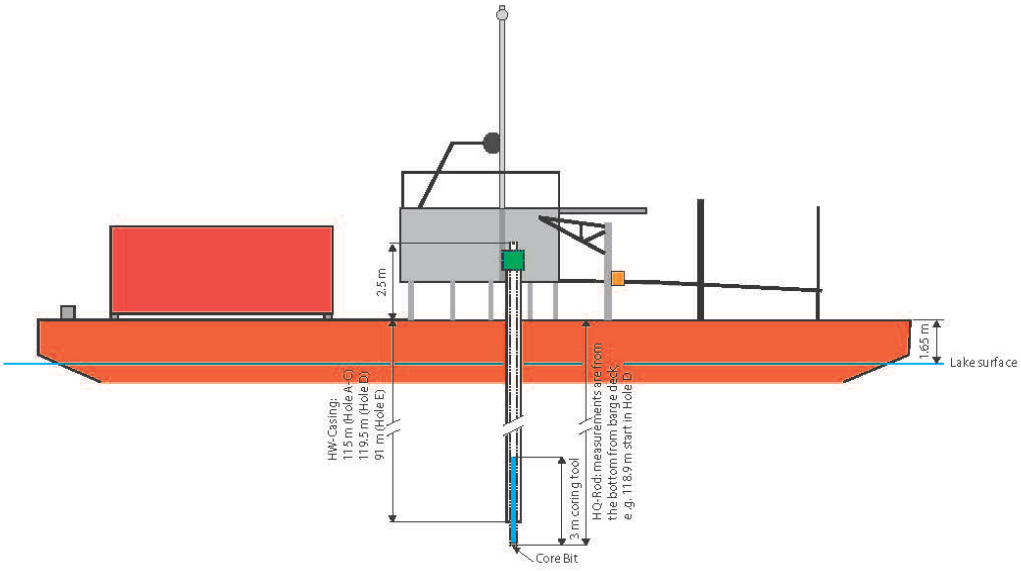

Fig. 2 Sketch of the drill rig used in the 2012 drillings, southern Lake Vättern

reference to 'meter below lake floor' (mblf). When drilling was complete, the cores were transported to the Department of Geological Sciences (IGV), Stockholm University and stored in a refrigerated room at 4°C.

On the barge, subsampling of the cores was limited to pore water sampling. Pore waters were collected with Rhizon samplers, syringes attached to a porous wire of glass fiber that are inserted into soft sediments (Dickens et al., 2007).The porous glass fiber had a length of 10 cm and the syringe was a 12 cm PVC/PE tube with a female luer lock and a tip with bulb (∅ 2.8 mm). To acquire high resolution pore water data, sections were sampled at three positions, using 1 – 4 Rhizon samplers. The pore water used for dissolved metal ions was acidified before being sealed in a jar.

At IGV, a GEOTEK Multi Sensor Core Logger (MSCL) was used for non-destructive measurements of bulk density, compressional wave velocity and magnetic susceptibility (MS). The MSCL data have a down core resolution of 1 cm. After logging, most of the cores were split, except for some of the shorter cores from Holes A and B, and those sections reserved for more advanced geotechnical tests.

One half of each core was preserved as an archive. These were described and digitally imaged using the MSCL. The archive halves were scanned at IGV using an ITRAX XRF Core Scanner. The working halves were used for destructive measurements. Constant volume samples for determining the index properties (grain density and water content) were taken at a resolution of 1-2 per section. Separate samples for grain size, total organic carbon (TOC) and carbonate content were taken at the same resolution. Undrained shear strength measurements were acquired using a fall cone device and a hand held penetrometer. Finally, pore water analysis was performed using inductively coupled plasma - atomic emission spectroscopy (ICP-OES) and ion chromatography in order to acquire concentrations of major cations and chloride ions respectively.

Multi-Sensor Core Logging

Gamma-ray attenuation derived bulk density measurements were performed with a Cs-137 radiation source having energy of 0.662 MeV with a resolution of 1 cm. The MSCL was calibrated daily using and aluminum standard in a liner filled with distilled water (Blum, 1997). The obtained calibration curves were used to convert measured intensity of gamma rays passing through the sediment to bulk density. Magnetic susceptibility was measured with a MS2C Bartington loop (∅ 100 mm) with a resolution of 1 cm. MSCL data were manually processed to remove outlying data points. The MSCL data were cleaned by removing bulk density measurements outside the range of 1.1 – 2.5 g/cm^3 and MS data outside of 0 – 100 SI x 10^{-5}.

Digital core imaging

High resolution (1 mm) images of the archive core half were obtained using the GEOTEK imaging system on the MSCL. The camera was calibrated daily. Digital RGB (Red-Green-Blue) data were extracted from the digital images using the MSCL image analysis software.

XRF data

An ITRAX XRF core scan produces a micro-radiographic (x-ray) digital image as well as micro-XRF elemental profiles with a theoretical elemental range from Al to U. The XRF analyses were made using a Mo tube set at 30 kV and 28 mA with a resolution of 5 mm and a dwell time of 25 s. After a detector upgrade core B8 and B11 were analysed using the Mo tube set at 30 kV and 50 mA with a resolution of 5 mm and a dwell time of 8 s. For more technical information on the ITRAX the reader is referred to Croudace et al. (2006).

Index properties

Constant volume samples were taken at a frequency of 1-2 per section. After weighing, the samples were dried in an oven at 105°C for >24 hours. Dried samples were weighed and crushed with a pestle in a mortar to a fine powder. The powder was inserted in a Micromeritics helium displacement

pycnometer (Accupyc1340) to obtain the grain density. Water content (w_c, %) was calculated using the equation

$$w_c = \frac{m_{wet} - m_{dry}}{m_{wet}} \times 100$$

Grain size

Grain size sampling was performed with a resolution of two samples every 1.5 meters. To remove organic material and carbonates the samples were prepared with 30% H_2O_2 and 10% HCl under calm heating until no bubbles evolved. Thereafter 3 ml Calgon (1% solution of Sodium hexametaphospate) were added followed by 1-minute ultrasonication for a thorough deflocculation. Grain size measurements were performed using a Malvern Mastersizer 3000 laser diffractometer. The relative error for the accuracy of the grain size data was < 1%.

Total organic carbon (TOC) and carbonates

Two samples every 1.5 meters were taken for TOC and carbonate analysis. Separate treatments were used to prepare Total carbon (TC) and Total organic carbon (TOC) analyses from the sediment. HCl was added to the TOC samples to remove carbonates. The samples were combusted with a Carlo Erba NC2500 analyzer and measured with a Finnigan MAT Delta V mass spectrometer. As output data stable isotope $\delta^{13}C$ was detected in both TC and TOC samples. The relative error was <1% for both measurements. The carbonate content was determined from the difference between TC and TOC.

Undrained shear strength (S_u)

Two types of apparatus were used to obtain the undrained shear strength (S_u); the fall-cone and a penetrometer (Geotester pocket penetrometer). Shear strength measurements were only performed in regions where split sediments visually appeared to be intact.

The fall-cone test was performed according to ISO-TS-17892-6 (Swedish Standards Institute) at a downcore resolution of approximately 20 cm. For softer sediments (0 – 31.25 c-mblf) we used a 60°/182 g cone. For sediment below 31.25 c-mblf we used a 30°/205 g cone. The undrained shear strength (S_u) is derived from

$$S_u(kPa) = Kg\,(\frac{Q}{h})^2$$

where *K* is the proportional constant, *g* is the gravity constant (m/s^2), *Q* is the cone weight (g) and *h* is the cone penetration into the sediment (mm). *K* is 0.80 for cones with 30° tip and 0.27 for cones with 60° tip.

The penetrometer was pressed 6 mm into the sediment at two separate spots on each section (1.5 m). Two different sizes of tips were used at each location. Combinations of 10 mm/15 mm and 10 mm/20 mm were the most common. The measured penetration force (kg force) were converted to unconfined compressive strength (UCS, kg/cm^2)

$$UCS = K_1 \times penetration\ force$$

where K_1 is the conversion factor (0.1718) given in the Geotester pocket penetrometer manual. The undrained shear strength (kPa) was calculated from UCS by

$$S_u = \frac{UCS \times g}{2}$$

where *g* is the gravity constant in dm/s^2

Pore water analysis

Downhole chloride concentration was measured with a Dionex IC20 Ion Chromatograph connected to an AS22 column. The sample volume injected was 10 µl and a 4.5 mM Na_2CO_3/1.4 mM $NaHCO_3$ eluent was used with a flow of 1.2 ml/min. For details on the method see European standard EN-ISO 10304-1:2009. The cation concentrations were determined with a Thermo ICAP6500 Duo ICP-OES containing a micro concentric spray chamber and a particle nebulizer. The nebulizer flow was set to 0.45L Ar/s and the integration time used was 3 s.

Seismic reflection profiling

Geophysical mapping, including multibeam swath bathymetry and subbottom/seismic reflection profiling, was carried out in the drill site area in 2013. Results from this mapping

are previously reported in Jakobsson *et al.* (2014), although with a specific focus on neotectonic features. At present we describe the acoustic stratigraphy of the seismic reflection profiles directly crossing the coring site acquired using a ~0.3 l (20 cu in) Bolt PAR airgun and 18 m long hydrophone single channel streamer, on the 10 m long vessel *Hamnen*. Positions were received with a Hemisphere VS100 GPS and corrected using SBAS (Satellite Based Augmentation System). The seismic reflection data were acquired using software from Meridata and interpreted in Kingdom Suite provided by IHS through an academic license agreement to Stockholm University. Suppressions of multiple reflections in the seismic reflection profiles were done using the RadExPro seismic processing software.

Synthetic seismogram

A synthetic seismogram was compiled using the composite bulk density measurements (Fig. 3) and p-wave velocity data from the MSCL. Sediment recovery was rather poor in intervals of the upper c. 30 m of the stratigraphy resulting in several gaps where no MSCL data was acquired. To minimize the effect of the coring gaps in the synthetic seismic record, linear interpolation of the velocity and density data was performed across these data gaps. Convolution with a wavelet extracted from seismic Line 14 crossing the coring site was carried out using Kingdom Suite software.

Results

Developing a composite section

MSCL and RGB data from boreholes A-E (Fig. 3a-c) were used to construct a composite sequence using a hole-to-hole correlation approach. As is routinely done on deep sea drilling expeditions, a composite sedimentary column was constructed by splicing together material from the 5 closely spaced holes, as well as the two shallow (5 m) piston cores. Hole-to-hole correlation was facilitated by using the software Splicer (version 2.2), available on www.ldeo.columbia.edu.

Before a composite sequence was spliced together, the MSCL data were used to align cores from different holes to account for potential errors in the recorded mblf depth scale, derived from the drillers' logs. These errors commonly arise from 1) the incomplete recovery of cored intervals, where the recovered material is assumed to be from the top of the drilled interval, 2) differential expansion or compression of cores during recovery, which can sometimes result in recovered sequences being longer than the cored interval (or vice versa) and 3) material falling into the base of the borehole between cores that may not have a stratigraphic significance. Where recovery was sometimes greater than the drilled sequence (usually by only a few centimeters) the top of the underlying core was set at the base of the overlying core in the composite depth scale. This revised depth scale is called the 'composite meters below lake floor' (c-mblf).

Offsets for each core in the composite depth scale are given in the supplementary material. Once cores from each hole were aligned in the depth domain, a composite section was spliced together. This was done from the lake floor down, taking the most intact cores (or intervals of cores), and identifying tie points to overlapping cores in neighboring holes that extended deeper into the composite depth domain. Where no overlapping recovery existed, the underlying core was appended to the spliced record, and a gap exists in the composite section.

MSCL Data

To a first order, the bulk density and volume specific magnetic susceptibility increase

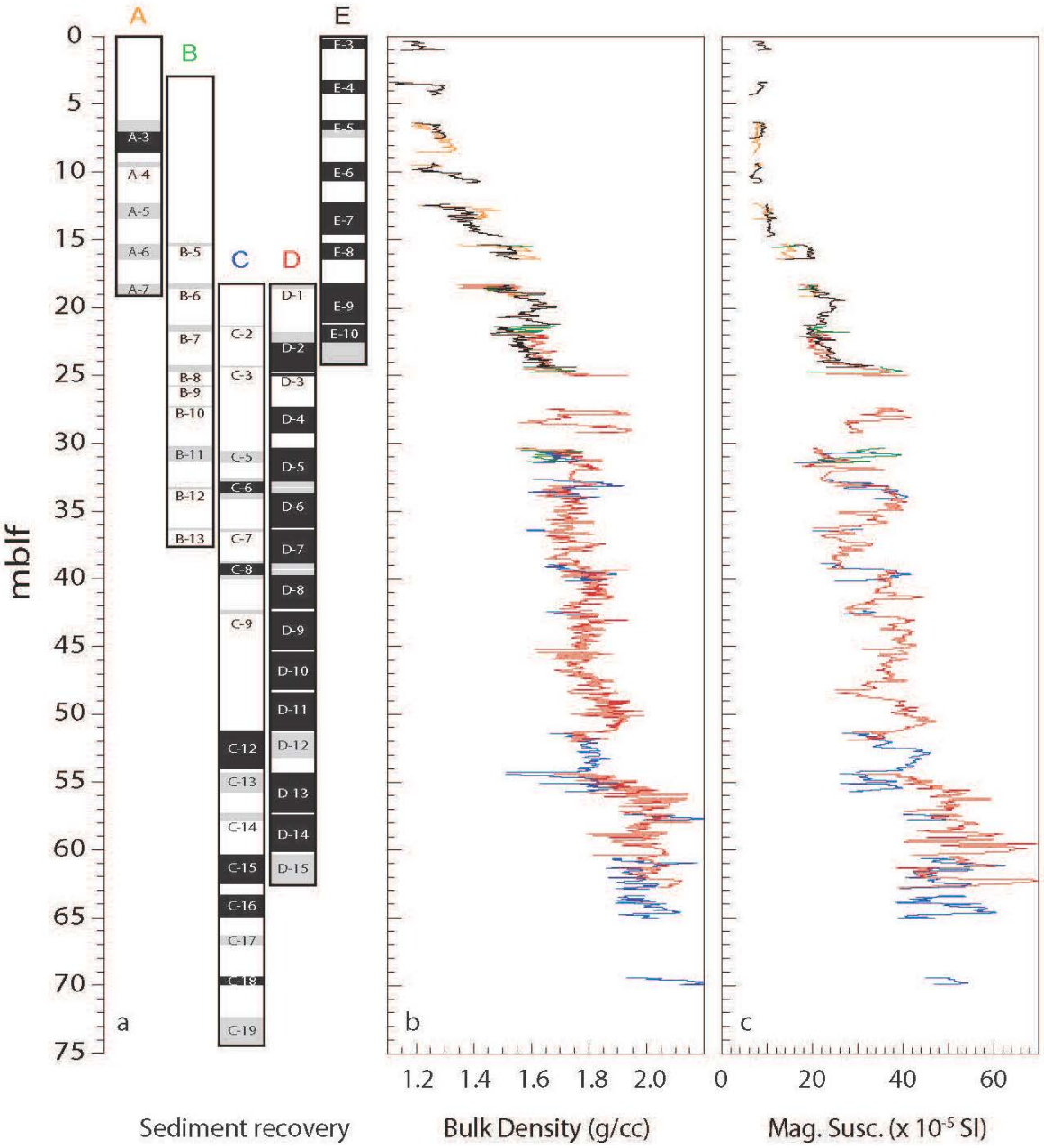

Fig. 3 a) Sediment recovery plots for holes A – E. Black and grey boxes indicate recovery for each core. Data from the black sections were used for constructing the composite section. b) Bulk density and c) magnetic susceptibility data from the Multi sensor core logger in the `meter below lake floor` (mblf) domain. The colour annotates the origin of the data with respect to holes A – E.

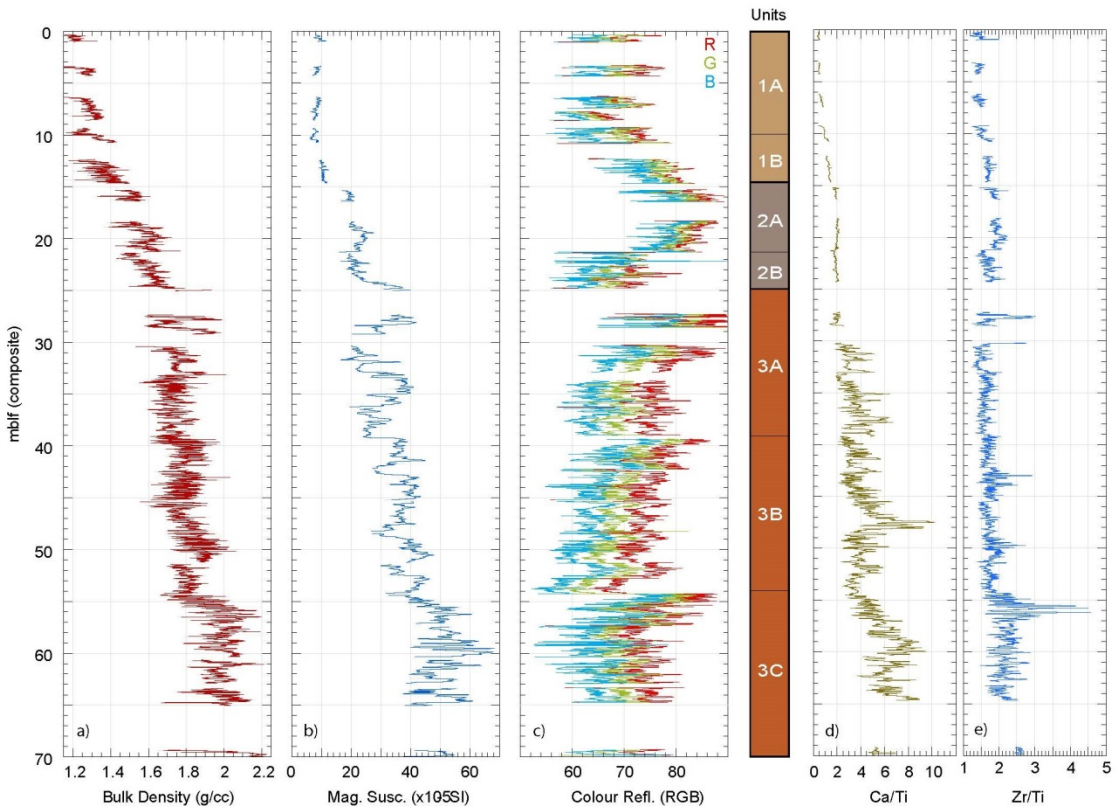

Fig. 4 Spliced composite section of MSCL and XRF-scanning data together with the lithostratigraphic units. a) Bulk density (3cm, 3pt smoothed) b) Magnetic susceptibility (3 cm, 3pt smoothed) c) RGB data (5cm, 51pt smoothed) d) Major lithostratigraphic units defined in this study, e) Ca/Ti XRF data, f) Zr/Ti XRF data. Unit 1 = Gyttjaclay (Late lake deposits), Unit 2 = Postglacial clay (Yoldia stage deposits), Unit 3 = Glacial clay (Baltic Ice Lake deposits).

downhole, with the most notable offsets occurring at 15, 25 and 55 c-mblf (Fig. 4a-b). These changes reflect large-scale shifts in sediment lithology. The average bulk density at 65 – 55 c-mblf has an average of 2.0 g/cm^3 while the average MS is 50 $\times 10^{-5}$ SI at the same interval, although with large amplitudes. A clear decrease in the bulk density, as well as in the MS, occurs at 55 c-mblf. From 55 c-mblf and up to 25 c-mblf the bulk density and MS exhibit a modest rate of increase, upon which is superimposed a significant amount of small scale variability. A closer look reveals prominent variations in bulk density occurring on centimeter to decimeter scales, revealing a pronounced cyclicity with a variable downhole frequency. Average values of 1.8 g/cm^3 and 35 $\times 10^{-5}$ SI are found in this interval. The MS data reveals more pronounced variation compared to the bulk density data, but the overall trend is similar. At 25 – 15 c-mblf the average bulk density decreases to 1.6 g/cm^3 and the average MS to 23 $\times 10^{-5}$ SI, and from 15 c-mblf and upwards the average bulk density is 1.3 g/cm^3 and the average MS is 9 $\times 10^{-5}$ SI. A step decrease in both parameters occurs at 15 c-mblf, and for the MS data the amplitude of the variations decreases considerably around this level.

RGB data

The digital colour data (red, green and blue [RGB]) that were extracted from the archive half images, are reflecting major downhole changes in sediment composition, as well as high frequency cyclic variations within these intervals. A high reflectance indicates brighter color of the sediment compared to sediment with low reflectance. The 3 color bands align well with each other (Fig. 4c). The reflectance starts to increase at 59 c-mblf up to 54 c-mblf where there is a significant and direct dip in the RGB reflectance. From 54 c-mblf and upwards there is a relatively smoothly

increasing trend for the reflectance that reaches its maximum at 39 c-mblf. Lower reflectance between 39 and 33 c-mblf is followed by an increase in reflectance from 33 up to 27 c-mblf. At 25 – 22 c-mblf the reflectance is low followed by a rapid increase at 22 c-mblf to a peak between 16 – 17 c-mblf followed by a decrease up to 10 c-mblf. The reflectance of the upper 10 meters of the core indicates only minor changes.

XRF data

Based on analytical performance (counting statistics), reliable data were acquired for Si, K, Ca, Ti, Mn, Fe, Rb, Sr, Y and Zr. All data were normalized to the incoherent + coherent scattering to remove various instrumental effects, and then smoothed using a 10-point running mean to capture the main shifts. To avoid problems associated with variable matrices (i.e., differences in organic and minerogenic contents within a sequence) which can affect such XRF analyses, it is common practice to work with elemental ratios. This circumvents the problem of having a relative concentration measurement (thereby eliminating the units) and can reveal changes that might otherwise go unseen in single element profiles. The elemental profiles were normalized by Ti because it was analytically reliable (counting statistics above measurement background) and this conservative element (i.e., commonly found in weathering resistant minerals) does not play a role in biological processes (Croudace et al., 2006; Koinig et al., 2003; Kylander et al., 2013).

Here we present the Ca/Ti and Zr/Ti downhole plots (Fig. 4e-f) and recognize the three major divisions found in the MSCL and RGB data. Below 55 c-mblf, Zr/Ti, which can be used as a proxy for grain size, is elevated. High frequency variability in Ca/Ti and Zr/Ti is apparent up to 25 c-mblf. Furthermore, we

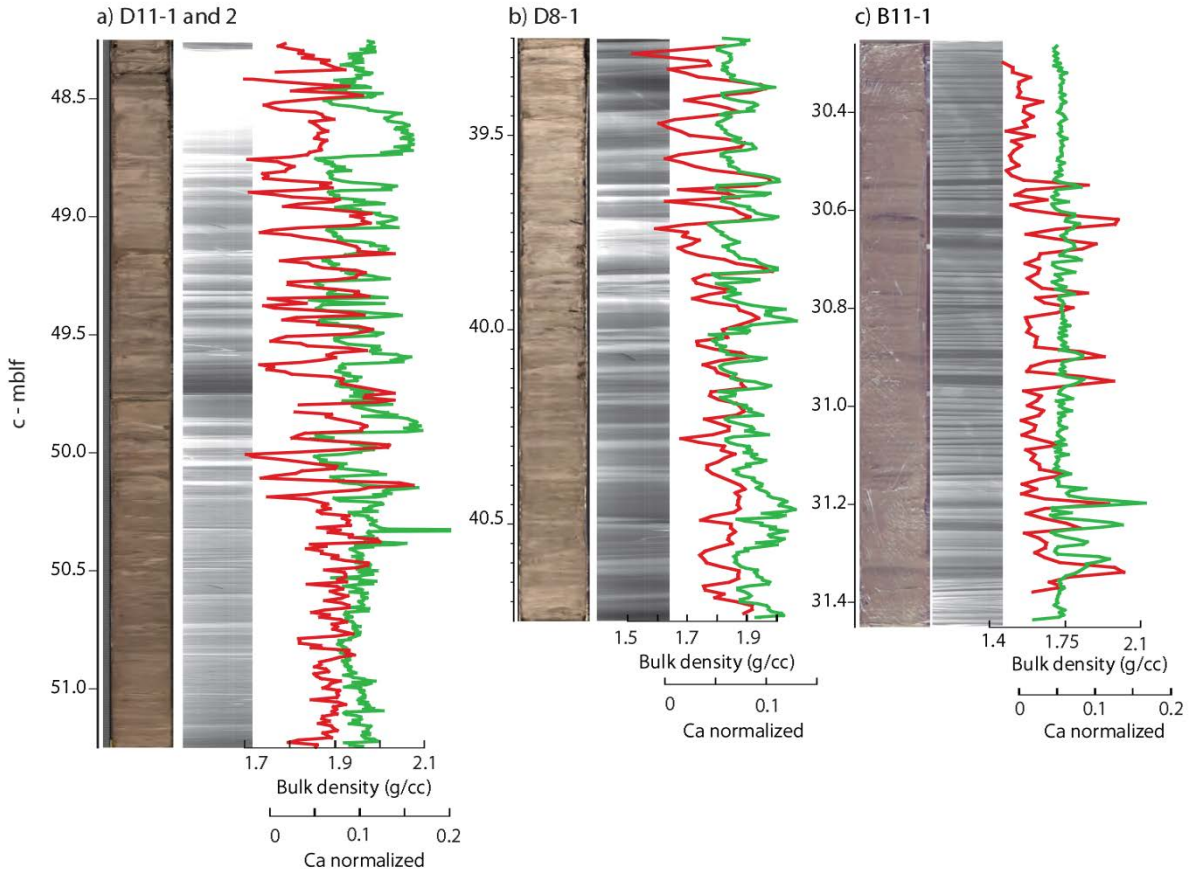

Figure 5. Digital x-ray images with overlying bulk density and normalized Ca together with digital images from the glacial clay. a) Hole D core 11 section 1 and 2 (unit 3C at 48.25-51.25 c-mblf), b) Hole D core 8 section 1 (unit 3B at 39.25-40.75 c-mblf), c) Hole B core 11 section 1 (unit 3A at 30.25-31.45 c-mblf).

present single Ca data only normalized to the incoherent + coherent scattering together with bulk density data when looking for varves in the glacial clay (Fig. 5).

Grain Density and Water Content

To a first order, a downhole decrease in water content is expected as sediments compact under increasing levels of overburden. At depths where the sediment composition changes, the rate of downhole change in the water content, and absolute magnitudes of the water content, are also expected to change. Grain density measurements provide a reliable indication for large-scale compositional changes in the sedimentary column. For example, the grain density of organic matter is usually low, around 1.2 g/cm^3, while quartz (sand) has a grain density of 2.65 g/cm^3 and most clay dominated sediments exhibit higher grain densities ranging between 2.68 and 2.71 g/cm^3.

The water content decreases rapidly between 0 - 20 c-mblf from ~70% at the lake floor to ~ 35% at 20 c-mblf (Fig. 6a). Between 0 - 10 c-mblf the grain density is relatively stable, and exhibits only minor downhole increase (Fig. 6a). With an average value of 2.54 g/cm^3, it suggests a significant contribution from organic and or biosiliceous material. However, between 10 and 15 c-mblf, there is a clear increase in the grain density from 2.61 g/cm^3 to 2.64 g/cm^3, likely reflecting either a greater abundance of terrigenous material, or increased occurrence of heavy authigenic minerals. Between 15 - 20 c-mblf, the grain density stabilizes between 2.69 - 2.70 g/cm^3, as would be expected for more terrigenous dominated marine and lacustrine sediments. These large changes in grain density between 10 and 20 c-mblf, suggest a compositional control on the rapid decrease in water content through this same interval.

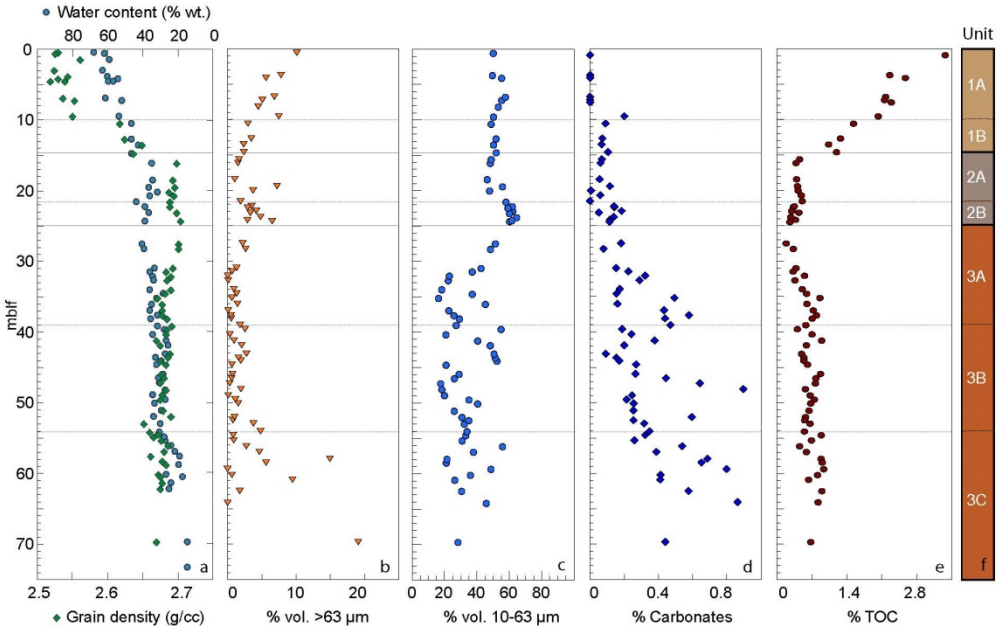

Figure 6. Downhole plots from discrete sample analyses of a) grain density and water content, b) coarse fraction content (>63 um), c) sortable silt content (10-63 um), d) % carbonates e) % TOC e) Major lithostratigraphic units defined in this study.

At 20 c-mblf, a sharp increase in the water content occurs. This is followed by a relatively smooth downhole decrease to ~55 c-mblf. At 55 c-mblf, the water content decreases rapidly to ~ 15 - 20%, with higher values (~ 60 c-mblf) in intervals with elevated sand and silt contents. Below 20 c-mblf, compaction processes likely drive the downhole reduction

in water content, as the grain density data reveals only a slight reduction through this interval.

Grain size

The highest abundance of sand sized material occurs in sediments below 55 c-mblf, although the distribution is highly variable (Fig. 6b and c). From 55 to 25 c-mblf, the sand sized content remains below 5% volume, increasing slightly between 25 and 20 c-mblf. From 20 c-mblf to the surface, the volume of sand sized material increases. This increase is likely related to the presence of biosiliceous material (diatom valves) that were not removed by our pre-treatment (Vaasma, 2008).

TOC and carbonates

The total organic carbon content remains relatively low (~0.7%) between 75 and 15 c-mblf (Fig. 6e). From 15 c-mblf to the surface, TOC increases to where it reaches a maximum value in near surface sediments of 3.5%. The carbonate content is highly variable in sediments from 75 c-mblf to 25 c-mblf (0.1 – 0.9%) (Fig. 6d). Between 25 – 10 c-mblf the carbonates are low and stable (0.05 – 0.1%) and above 10 c-mblf no carbonates are detected.

Undrained shear strength

The undrained shear strength (S_u) can be defined as the maximum value of shear stress the sediment can withstand in an undrained condition (Duncan and Wright, 2005). S_u data from both penetrometer and fall cone agreed fairly well (Fig. 7). However, at 21 - 24 c-mblf the fall cone data was generally higher than the penetrometer data. As expected, S_u increases downhole, but two distinct regimes in are distinguished. The lower segment (25 - 75 c-mblf) has a more pronounced increase of S_u with depth compare to the upper sequence (0 - 25 c-mblf). The scattering of data increases down hole and is most pronounced below 55 c-mblf. These high frequency changes in shear strength are likely related to the coarser grained intervals found below this level, as is recorded by the direct grain size measurements and Zr/Ti ratios.

Pore water chemistry

Pore water speciation in the sediment cores will ideally reflect changes in the chemical composition of the water mass at the time of deposition. The chloride ion is conservative in deep sea sediments (Sayles and Mangelsdorf Jr, 1977) which makes it useful when estimating palaeosalinities (McDuff 1985, Adkins and Schrag 2001). The pore water data from the Lake Vättern sediment is given as concentrations (in mg/L) of detectable ions. Chloride concentrations (chlorinity)are used to calculate pore water salinity in parts per thousand using the older definition of salinity (STANDARDS, 1966) where,

$$Salinity = 1.80655 \times Cl^{-}\ ‰$$

A brackish phase in the history of Lake Vättern is clearly revealed (Fig. 8). The chlorinity increases from fresh water levels (~10 mg/L) at the core top steadily down to 22 c-mblf where a broad plateau exists between 22 - 33 c-mblf, with a chloride ion concentrations of 60 - 75 mg/L (Fig. 8a). This corresponds to a pore water salinity of 0.10 - 0.12 ppt. The

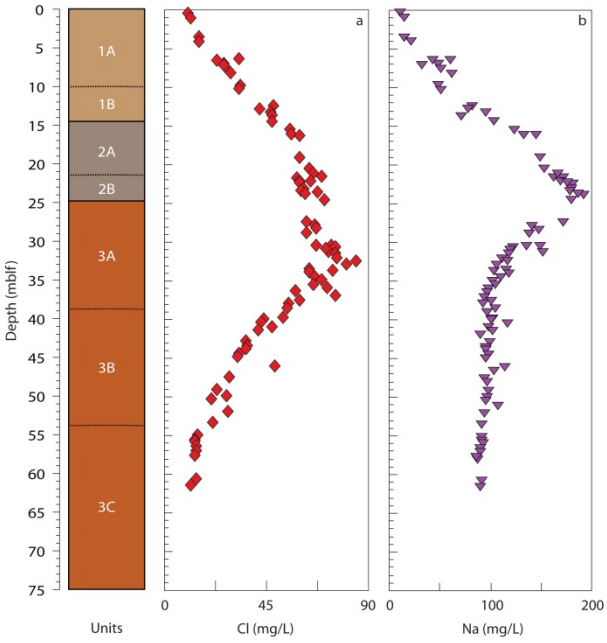

Fig. 8 Pore water chemistry represented by Na and Cl concentrations together with lithostratigraphic units.

highest chlorinity is found at 33.4 c-mblf (84 mg/L) and corresponds to a pore water salinity of ~0.15 ppt. From 33.4 c-mblf, the chlorinity starts to decrease smoothly to 55 c-mblf where it stabilizes at ~0.025 ppt (13.5 mg/L). This level indicates slightly higher pore water salinities than the modern fresh bottom lake waters. The concentration of major monovalent and divalent cations (Na, K, Mg, Ca) display a similar downhole pattern and will here be represented by Na concentration data (Fig. 8b). The concentration of Na shows low levels at the core top with increasing concentrations down to a clear peak between 23 - 24 c-mblf. There is a less distinct peak in the cation concentration between 22 and 33 c-mblf. Generally, there is a downhole decrease in the Na concentration below 23-24 c-mblf, but a secondary peak in concentration is evident around 31 c-mblf. Below 31 c-mblf, the Na concentration decreases down to 35 c-mblf where it stabilizes around levels slightly higher than the present lake Na concentration.

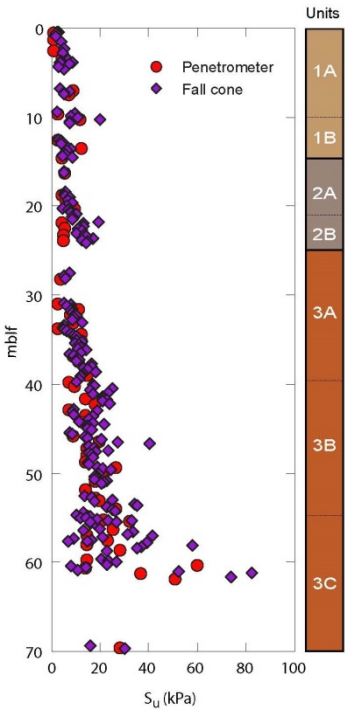

Fig. 7 Undrained shear strength, S_u, derived from fall cone test and penetrometer test along with the lithostratigraphic units.

Acoustic stratigraphy and core-seismic integration

Seismic reflection Line 14 runs in an east to west direction across the lake basin and through the drill site (Fig 1b, 9). A trough outlined by the prominent reflector R1 is seen in Line 14. This trough coincides with the deep bathymetric channel and can be followed in all seismic profiles crossing Lake Vättern presented by Jakobsson et al. (2014). There are no clear visible acoustic structures below R1 in this trough as the energy of the seismic pulse is not enough to penetrate further. However, on the shallower eastern flank unconformable reflectors, marked RU in Fig 8, are identified below R1. The bottom of the deepest part of the trough is situated at about 0.4 sec TWT (Two-Way-Travel Time) below the lake surface. The trough is filled here with approximately 0.25 sec TWT sediments. Above reflector R1, an acoustic unit is identified that is characterized by an internal chaotic structure. A clear upper limit of this unit is not straightforward to identify across the entire

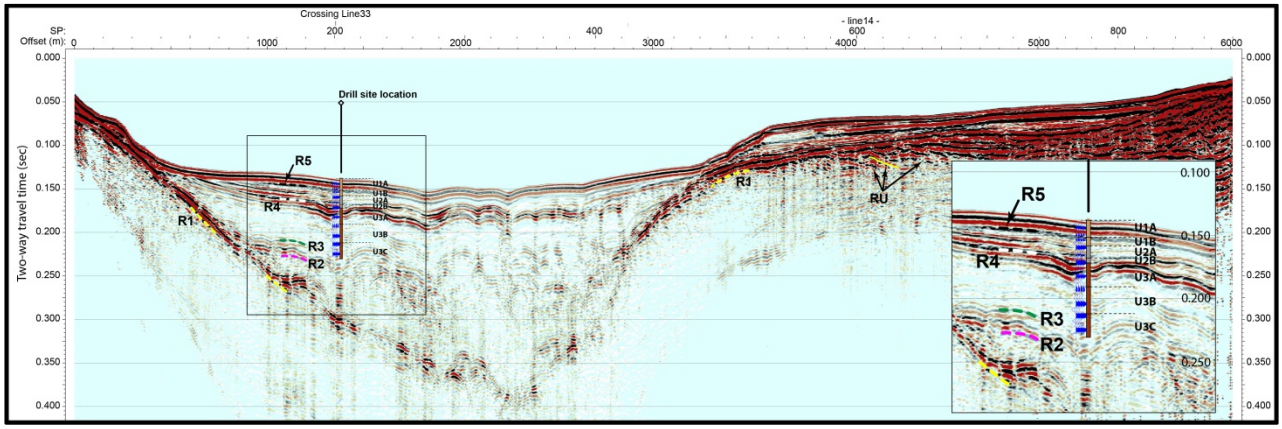

Fig. 9 Seismic profile of line 14. R1, R2, R3, R4 and R5 are seismic reflectors (1-5). RU = unconformable reflector below R1 (= trough reflector).

trough. It is, however, here defined by R2 on the western side (Fig. 9). R2 is followed upwards by a set of conformable rather strong reflectors. The uppermost of these reflectors is defined as R3. From R3 follows a nearly acoustically transparent unit with only occasionally visible conformable internal reflectors. In the following section we use the physical properties reported above to define three major lithostratigraphic units in the recovered sediments (Fig. 4). Reflector R4 correlates to the transition between Unit 3 and 2 in the lithostratigraphy. The stratigraphic boundaries between Unit 2A/1B and 1B/1A seems at first to correlate well with generated reflections in the synthetic seismogram. However, a closer inspection of the composite bulk density records also shows that core gaps are located close to these boundaries. Finally, reflector R5 is defined to constrain an uppermost conformable unit of which the upper limit comprises the lake bottom topography.

General lithostratigraphic table

Sediment Unit	Interval (mblf)	General lithology	Period
1	0-15	Gyttja clay	Present lake formation
1A	0-10	Fine sulfide laminated silty gyttja clay	Isolated lake
1B	10-15	Silty (gyttja) clay	Lake transition
2	15-25	Post-glacial silty clay	Yoldia sea
2A	15-21	Post-glacial homogenous silty clay	Late Yoldia sea/Lake transition
2B	21-24	Sulfide laminated post-glacial silty clay	Early Yoldia sea
3	25-74	Glacial silty clay/clayey silt	BIL
3A	25-39	Glacial silty clay	BIL
3B	39-54	Glacial silty clay	BIL
3C	54-74	Glaciotectonized clayey silt	BIL

Table. 1 Lithostratigraphic units with general lithology and development stages of Lake Vättern.

Discussion

Lithostratigraphic Units

The lithology of the sediment cores together with the physical properties are used to define three major lithostratigraphic units, which describe the recovered sequence of Late Pleistocene to Holocene sediments of southern Lake Vättern (Tab. 1 and Fig. 4).

Unit 3 (25 – 70 c-mblf), Glacial Clay

The sediments in Unit 3 comprise reddish- to greyish- brown silty clays with interleaving coarser lenses. This unit contains the highest carbonate content and has relatively low TOC contents (Fig. 6d and e). The large variability in the carbonate content is captured at a much higher resolution by the Ca/Ti ratios (Fig. 4d). The variability arises from high frequency cyclic changes in sediment texture and composition. Darker, higher density sediments are coarser (>Zr/Ti) and contain more Ca than the lighter sediments. These cyclic changes are typical of varved glacial clays (De Geer, 1940). The thickness of the varves changes substantially throughout the unit. For example, decimeter scale varves are clearly seen between 49 – 50 c-mblf (Fig. 5a). At 40 c-mblf the thickest varves are < 5 cm (Fig.5b) while at the top of unit 3 the varves are in the mm range and not captured by the current measurement resolution of the MSCL (1 cm) or XRF (5 mm) data, though they are clearly visible in digital x-ray images (Fig.5c).

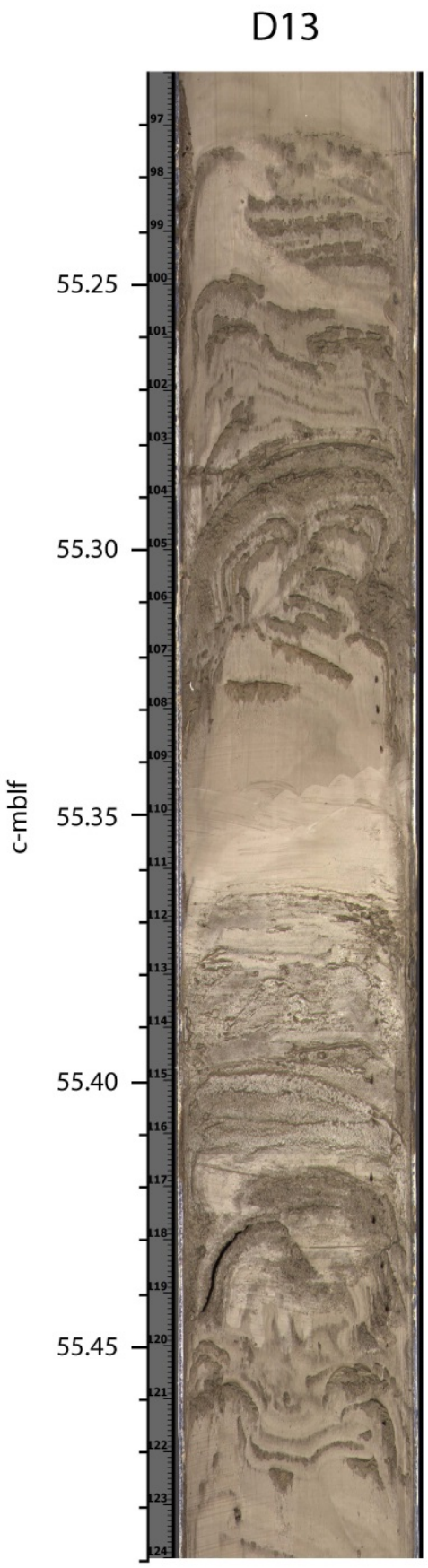

Fig. 10 . Glaciotectonized sediment at 55.21-55.49 c-mblf (Hole D core 13 section 1)

Subunit 3C (54 – 74 c-mblf)

Three subunits are recognized within Unit 3. The lowermost one, subunit 3C (54 – 70 c-mblf) contains a significant amount of coarser material concentrated in centimeter scale sand layers, as well as numerous pebbles and sand/silt inclusions. The uppermost part of subunit 3C (54 – 57 c-mblf) comprises dark greyish brown (10 YR 4/2) to greyish brown (2.5 Y 5/2) clayey silt to silty clay and is highly deformed (Fig. 10). A significant upward decrease in the undrained shear strength (Fig. 7) and bulk density (Fig. 4a) occurs at the top of subunit 3C, and combined with the visible deformation structures, these are attributed to a grounding of glacial ice at the drilling location. This interpretation is supported by a high degree of overconsolidation, determined through oedometer tests on intact samples (O'Regan et al., in prep). The smooth reduction in shear strength and bulk density seen within subunit 3B and 3A, suggest that there are no other periods of significant erosion or glacial loading in the recovered sequence. The top of subunit 3C marks the last time that glacial ice was in contact with the lake floor at this location. While the top of subunit 3C is manifested by a strong reflector in the synthetic seismogram, an equally prominent reflector is not clearly identified in the seismic Line 14 (Fig. 9). There is, however, a faint reflector in Line 14 located slightly above the upper boundary of subunit 3C. This reflector increases in strength towards the east in Line 14.

Subunit 3B (39 – 54 c-mblf)

The base of subunit 3B is comprised of dark grey (10 YR 4/1) to greyish brown (2.5 Y 5/2) silty clay with decimeter scale varves composed of fine silty clay and silt/sand layers in the lower parts (42 – 54 c-mblf) which gradually turn into lighter silty clays with thinner varves upwards. The uppermost part of subunit 3B (39 – 42 c-mblf) is a reddish brown (2.5 YR 5/2) silty clay with ~ 7 cm thick diffuse varve structures. The coarse fraction content (>63 µm) , and more notably the sortable silt content (10 – 63 µm), increases towards the top of the subunit (Fig. 6b and c).

At 39 c-mblf a distinct change from lighter to darker sediments, combined with changes in bulk density and magnetic susceptibility, marks the boundary between subunits 3B and 3A.

Subunit 3A (25 – 39 c-mblf)

The base of subunit 3A (31 – 39 c-mblf) is composed of brown (7.5 YR 5/2) to grey (7.5 YR 5/1) weakly laminated silty clays with grey (7.5 YR 5/1) silty layers and some sand lenses. An increase in the carbonate content seems to occur near the base of this subunit, with a decreasing amount of carbonate occurring up section (Fig. 6d). Above 31 c-mblf the colour of the sediment turns lighter towards reddish grey (2.5 YR 5/1) and close to the top of the subunit the sediments become a faint red (2.5 YR 4/2) with very thin, mm-scale varves (Fig. 5c). A 20 cm thick silt layer (27.65 – 27.85 c-mblf) occurs near the top of subunit 3A. The top of subunit 3A is marked by a very distinct change from mm-scale varved red clays into sulfide laminated dark grey (10 YR 4/1) to dark greenish grey (GLEY 2 3/2BG) silty clay. The top of subunit 3A is manifested by a strong reflector in the synthetic seismogram as well as in the seismic Line 14, reflector R4 (Fig. 9).

Unit 2 (15 – 25 c-mblf), Postglacial clay

The transition between unit 3 and unit 2 is characterized by a distinct colour change from red/brown to sulphide laminated dark greenish grey (GLEY 2 3/5BG) silty clay occurring across a 2 cm sand layer (Fig. 11). The black sulphide laminations at the base of Unit 2 (subunit 2B) are between 5-15 mm thick and become much less pronounced, and even absent at ~21 c-mblf, the onset of subunit 2A. The 2A/2B boundary is marked by a colour change from the dark greenish grey silty clay to dark grey clay (5Y 4/1) with streaks of brown clay (7.5 YR 5/3). This colour change is clearly represented in the RGB data, and is accompanied by an increase in bulk density and magnetic susceptibility (Fig. 4a-c). However, discrete sample analyses indicate higher coarse fraction and silt contents in subunit 2B. Subunit 2A shifts color occasionally to brownish grey (2.5Y 5/1) and to olive grey (5Y 5/4) before it returns to dark grey (10 YR 4/1) in the upper meter of Unit 2. Subunit 2A sediments have lower and less variable carbonate content than sediments in subunit 2B, and low and relatively uniform TOC content, as seen in the discrete sample analyses (Fig. 6d-e)

Throughout subunit 2B there are signs of extreme sediment deformation e.g. compressed laminations and microfaults (Fig. 11a). The most notable of these are captured at the same interval in cores from 2 different boreholes (cores D2 and E10), and strongly argue against drilling disturbances as the underlying cause. The highly faulted sulphide laminated sediments only found in subunit 2B occur above the 2 cm sand layer (Fig. 12) in cores D2 and E10 that marks the base of Unit 2.

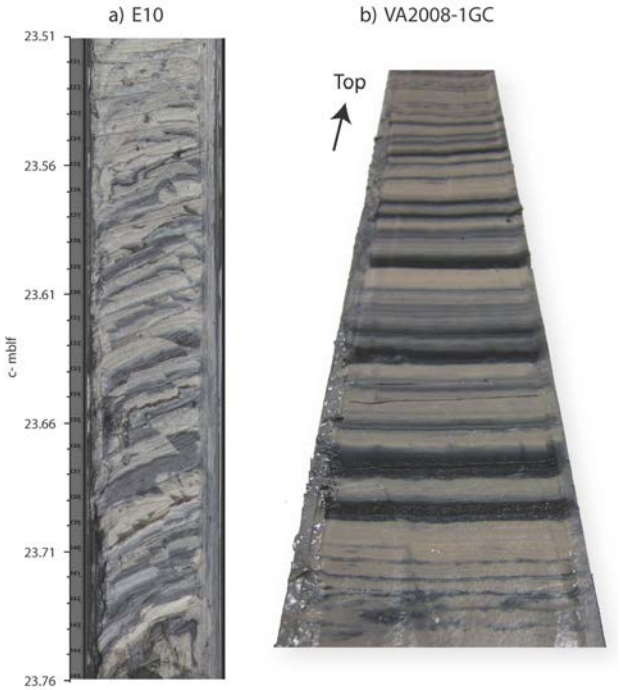

Fig. 11. a) Disturbed laminated sediment at 23.45-23.70 c-mblf (Hole E core 10 section 2) with microfaults and compressional structures. b) Contemporary core section from VA2008-1GC (undisturbed) showing the same lithology with black sulfide laminated greenish grey silty clay.

Unit 1 (0 – 15 c-mblf), Gyttja clay

The Unit 1/ 2 boundary (15 c-mblf) is marked by a change from dark grey (10 YR 4/1) to grey (7.5 YR 5/1) and brown (7.5 YR 5/2) silty clay. Sediment grain density begins to decrease at

the base of Unit 1, together with a trend of increasing TOC content towards the lake floor. Unit 1 is subdivided into subunits 1A and 1B based upon the grain density data, which illustrates a gradual reduction in grain density through subunits 1B and a low and uniform grain density (2.54 g/cm^3) in subunit 1A. Furthermore, at the 1A/1B boundary, fine, parallel and undisturbed laminations become clearly visible in the recovered gyttja clay (Fig. 13).

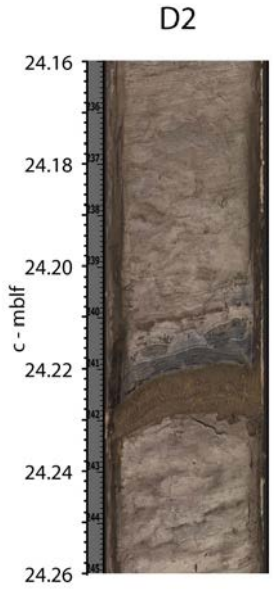

Fig. 12. Sand layer at 23.66-23.68 c-mblf contemporary with the BIL drainage and the Na pore water peak (Hole D core 2 section 2).

Paleo-environmental significance

In this section we outline the main themes we can interpret from the sediment record. The three lithostratigraphic units are interpreted as glacial clay, postglacial clay and gyttja clay. This sequence records, at a first order, the withdrawal of ice from the Vättern basin at the end of the last glacial period, and subsequent development of the modern lake system. Within this sequence we identify: a period of ice grounding; ice margin oscillations; drainage episodes of the BIL; a brackish phase in the lake´s environment; and Lake Vättern´s subsequent isolation from the Yoldia Sea.

Glacial Dynamics

Within Unit 3 several variables point at an increasingly distal location with respect to the retreating Scandinavian ice sheet: The decrease in varve thickness from the bottom (decimeter scale varves) to the top (millimeter scale varves) of Unit 3 indicates a decreasing water run-off in the catchment area pointing to a general withdrawal of the ice margin. Bedrock in the Lake Vättern region is mainly non-calcareous and low carbonate content in the sediment is expected if the deposited material is of local origin. In Unit 3, the carbonate data is scattered (0.1 – 0.9%) but displays a first order decrease towards the top of the unit (Fig. 6d). This likely reflects the contribution of detrital carbonates from the retreating ice sheet. This is supported by the relatively low carbonate content in the postglacial clays, (10 – 25 c-mblf, 0.05 – 0.1%) and absence of carbonates in the gyttja clay above 10 c-mblf.

Grounded glacial ice existed at the drilling site in Southern Lake Vättern at the top of subunit 3C, at 54 c-mblf. Below this horizon, sediments are highly deformed and composed of thick, cm- to decimeter scale intervals of clays with intercalating silt and sand lenses which indicates a proglacial lake environment, which has been overridden by a readvancing ice sheet at least once. The lowermost recovered sequence (72.9 – 74.3 c-mblf) contains a broad (~1 dm) coarse sand layer including larger clasts (∅ 2 cm) which indicates either a very proximal ice margin with strong glacifluvial influence or the presence of interbedded tills and glacial clays deposited during ice margin oscillations. This sequence composes the upper part of thicker coarse sediment seen in seismic data from the Vättern basin (Fig. 9, reflectors R2-R3). Based on the available data it is not possible to reliably distinguish discrete ice margin advances between 54 and 74 c-mblf.

It is reasonable to assume that the last ice grounding horizon at 54 c-mblf, must be equivalent to or younger than the first major ice recession in the southern part of the lake, <14.0 cal. ka BP (Björck, 1995; Lundqvist and

Wohlfarth, 2000). According to onshore investigations in the Jönköping area Waldermarsson (1986) suggested two major readvances after the first retreat of the ice margin. These are assumed to corresponden

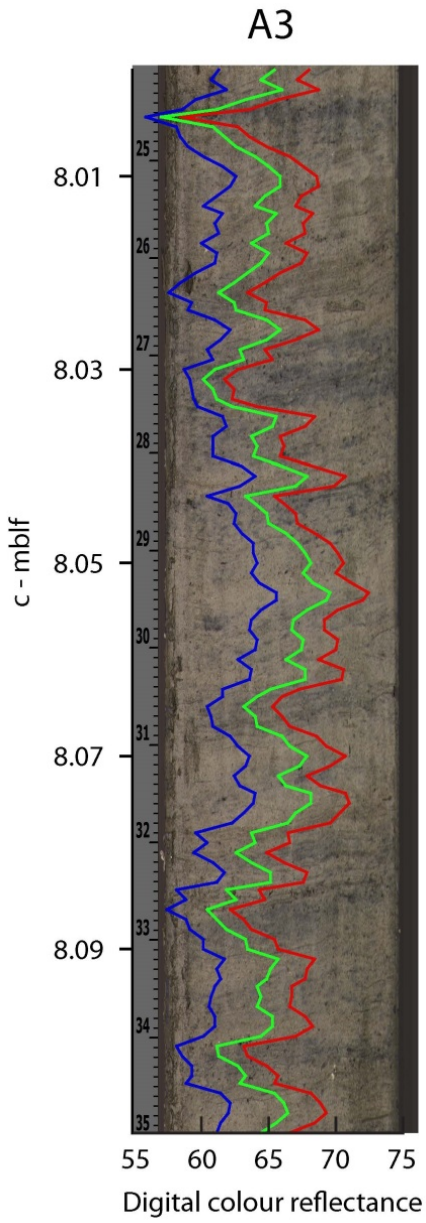

to the

Fig. 13 (right) Laminated gyttjaclay at 7.99-8.10 c-mblf (Hole A core 3 section 2) with overlying colour reflectance. Brighter sediment color – higher reflectance.

regional marginal moraine ridges (Levene and Younger Dryas – Skövde respectively) formed by the ice recession in southern Sweden (Lundqvist and Wohlfarth, 2001) (Fig. 1b). We could therefore associate the grounding event identified in the lake sediment record with either a ~13.4 cal. ka BP or ~12.2 cal. ka BP readvance interpreted from the onshore record.

The glacial clays overlying the grounding event are varved, and although the thicknesses of the varves vary greatly throughout Unit 3, the couplets retain the same compositional and grain size contrasts, with darker, generally coarser grained intervals having higher Ca contents alternating with lighter finer grained intervals having lower Ca content (Fig. 5a and b). Although the general upward decrease in varve thickness in Unit 3 implies an increasingly distal ice margin we also notice intervals with thicker varves, silt and sand layers, and dropstones within the glacial clay that punctuate the overall trend, e.g. the top of subunit 3B and 3A. These potentially reflect readvance(s) of the ice margin within the basin without ice grounding as far south as the drill site. Current ice margin reconstructions show the ice front remained in the Northern part of Lake Vättern until after the Younger Dryas. Oscillations of this ice front could deliver the observed dropstones either via iceberg rafting or meltout from a floating ice tongue near to the drilling site.

The final drainage of the BIL

The color change at the Unit 2 – Unit 3 transition has been reported in areas close to Lake Vättern by several authors; from Lake Örlen and Lake Viken west of Lake Vättern (Björck et al., 2001) and west of Mt. Billingen (Johnson et al., 2013). This transition has been tied to the final drainage of the BIL (e.g. Strömberg, 1992, Brunnberg, 1995 and Andrén et al., 1999) and occurred at the very end of the Younger Dryas cold interval ~11.7 cal. ka BP (Björck et al., 1996; Andrén et al., 2002). A further age constraint on Unit 2 is provided by gravity core VA2008-1GC retrieved from the deep strait between Visingsö and Gränna c. 24 km NNE of the 2012 drill site (Fig. 1b). Sediments in VA2008-1GC are greenish silty clays with distinct cm-scale black sulphide laminations, and are lithological

similar to the sediments within subunit 2B (Fig. 11a and b). Pollen analysis in VA2008-1GC (Jakobsson et al., 2014) revealed the characteristic pollen zone of the Younger Dryas-Preboreal transition (for definition of the pollen zone see Berglund, 1966). This indicates an age of ~11.5 cal. ka BP for the undisturbed laminated sequence within this core (Jakobsson et al., 2014). VA2008-1GC was recovered from on top of seismically disturbed sediments, and was used to date the end of neotectonic activities in the Vättern basin (Jakobsson et al., 2014). The undisturbed laminations in VA2008-1GC were deposited directly after the earthquake event(s) whereas the laminations in E10 and D2 from this study are disturbed (Fig. 11a and b). The age of the base of subunit 2B is therefore considered to be >11.5 cal. ka, due to the combination of the specific lithological imprint together with the seismically disturbed structures (see discussion below). It is therefore most likely that the distinct color transition between Unit 2 and Unit 3 together with the accompanying 2 cm sand layer is a marker of the catastrophic drainage of the BIL (~11.7 cal. ka BP).

Coarsening of sediments within subunit 2B (Fig. 6) may reflect the ~40 meter lowering of the lake level during the Yoldia stage (Norrman, 1964), which followed the deglaciation of the basin and northwards retreat of ice. This lake level change is connected to a rapid uplift in the southern part of the lake in parallel with the ice recession in the north. The distances from the shores to the deeper parts of the lake were shorter during this period and coarse abraded material were deposited along the slopes and in the deeper sub basins of Lake Vättern (Norrman and Köunigsson, 1972).

Marine incursion(s) into Lake Vättern

The pore water data indicates one or more marine incursion(s) into the Vättern basin during deposition of the varved glacial clays of Unit 3 as well as during the deposition of the post-glacial clay of Unit 2 (Fig. 8). Although likely impacted significantly by diffusion, the general shape of the pore water salinity reveals a peak at 33.4 c-mblf. The peak salinity, derived from Cl data, is only 0.15 ppt, but likely represents a fraction of the true salinity which later diffused into the overlying water column and surrounding sediments. The offset between the peaks of the two major constituents of marine water (Na and Cl) is striking but can be explained in terms of different diffusion constants for the ions together with cation exchange between the dissolved ions in pore water and the surrounding clay minerals. While chloride ions are conservative under most conditions, cations will exchange more or less due to various types of clay minerals and various concentration of different cations (Sayles and Mangelsdorf Jr, 1977). In addition, the ratio between Na/Cl in the pore water is higher (from 1 to 8 by weight) than observed ratios in sea water (molar ratio 0.9, and by weight 0.6). This suggest that Na is weak proxy for revealing sea water input in this system since a major source for Na is also mineral weathering. However, the Na and Cl concentration depth profiles in general follow each other with the exception of the peak concentrations and the concentration profile below 35 mblf. These discrepancies can be a result of weathering input for Na together with difference in diffusion rates.

Traditionally, the period ascribed to saline waters within Lake Vättern is the Yoldia Sea stage, which followed the final drainage of the BIL and, according to Svensson (1989) lasted c. 1000 years and had three main phases: an initial fresh water phase followed by a brackish phase and finally yet another fresh water phase. The first phase lasted c. 300 years before pulses of sea water entered the Baltic basin via the Närke straight (Andrén et al., 1999). For Lake Vättern Björck et al. (2001) analyzed sediment cores (0-1.3 c-mblf) from the northern part (Sjöboda) and found peak carbonate content at 1.6% in a dated (~11 000 cal. ka BP) post glacial reddish clay with an upward decline to 0.1% in the overlying varved grey clay layer. The carbonate peak together with the finding of the marine bivalve mollusk *Portlandia arctica (yoldia)* led Björck et al. (2001) to assign this clay layer to a saline Yoldia stage in Lake Vättern. Using varve measurements, pollen analysis and

radiocarbon dating Björck et al. (2001) dated this marine incursion to ~250 years after the final drainage of the BIL.

Our chloride pore water data instead indicate an earlier marine incursion (Fig. 8) and we connect it to the suggested first drainage of the BIL (Björck, 1979, 1981; Björck and Digerfeldt, 1984; Svensson, 1991) at ~12.8 cal. ka BP. Recent data from the Arkona basin suggest a lowering of the Baltic Ice Lake by 20 meters during late Alleröd, which is in the same magnitude as the shore level displacement during the final drainage of the BIL (Bennike and Jensen, 2013). This drainage may have been a result of either a deglaciation during the end of the Alleröd warming period or subglacial drainage somewhere at the northern tip of Mount

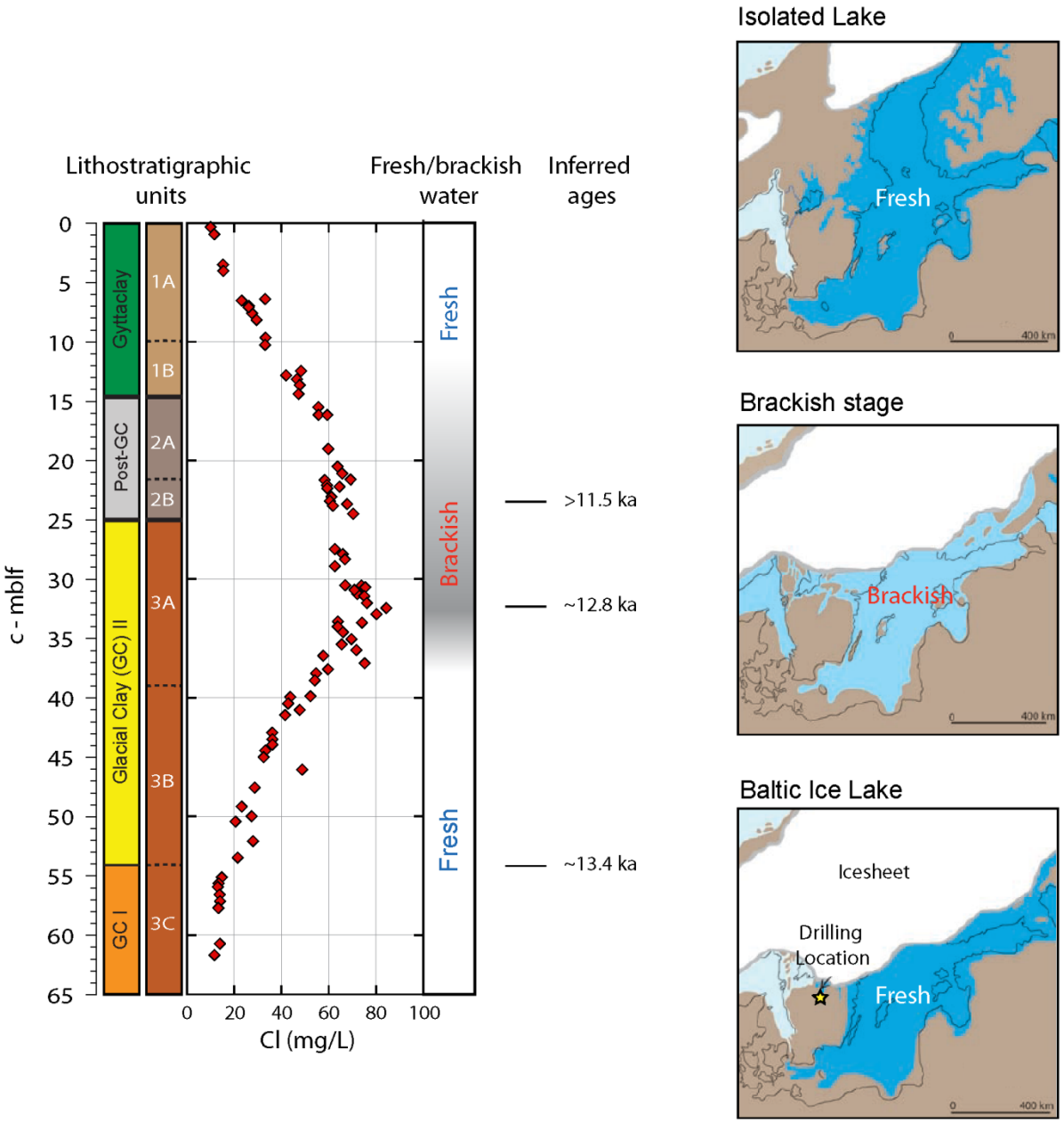

Fig. 14 Lithostratigraphic units along with pore water chlorinity and estimated positions of fresh water/brackish water transitions. Inferred ages for significant sedimentological imprints and corresponding stages of the Baltic Sea are presented to the right in the figure. Maps are modified from Björck (1995).

Billingen (Björck, 1995). The pore water data strengthens the idea of an earlier drainage of the BIL, and indicate that it would have occurred due to deglaciation rather than subglacial drainage, since marine incursion via subglacial routes seems implausible. The broad plateau in the pore water data (22 – 33 c-mblf) infers a prolonged incursion or several incursions at different times and it is possible that new pulses of saline water intruded Lake Vättern after the final drainage of the BIL.

The marine incursion is positioned well above the 54 c-mblf ice grounding position which argues against a Younger Dryas age for the 54 c-mblf horizon. On the basis of these arguments, we suggest that the grounding event corresponds to a pre-Younger Dryas ice advance.

Time constraints from varves

To further constrain the age of the different events seen in the sediment cores we used the cyclic variations in bulk densities found in the glacial clay to estimate a time between the ice – grounding (54 c-mblf) and the most notable marine incursion (33 c-mblf). We assumed that one varve is the distance between two consecutive bulk density peaks. Where possible to resolve, the number of varves/meter were counted, across data gaps linear interpolation was used to provide an estimate of the total number of varves within the glacial sequence. Approximately 300 varves were found in the glacial clay between 33 – 54 c-mblf (see supplementary material). Varves thinner than the bulk density resolution (1 cm) were not captured in the counting procedure. Therefore 300 varves are seen as a minimum estimate. Assuming that the peak in chlorinity at 33 c-mblf marks the first drainage of the BIL at ~12.8 cal. ka BP, the estimated 300 varves found between 33 and 54 c-mblf place the ice grounding horizon at ~13.1 cal. ka BP. This is reasonably close to the Levene moraine ridge age (~13.4 cal. ka BP). It is therefore likely that during the ice readvance that formed the Levene moraine ridge, grounded glacial ice also existed in southern Lake Vättern.

The Isolation of Lake Vättern

The Yoldia Sea stage is usually taken to have lasted ca. 1000 years (Svensson, 1989), but Lake Vättern was probably isolated before the end of the Yoldia stage due to local isostatic rebound. Between 9 and 15 c-mblf the sediment gradually changes colour, with a concomitant decrease in grain density and increase in TOC towards the core-top, reflecting higher input or preservation of organic material. We connect this change to the lake isolation. After the isolation of Lake Vättern the depositional environment attained its present condition, with undisturbed laminated gyttja clay containing thin sulfide laminations (Fig. 13) indicating oscillating oxygen supply to the bottom waters. The smooth decrease in pore water salinity throughout Unit 1 is most likely a diffusion-dominated signal. More rigorous sedimentation-diffusion modeling, coupled to a firm chronostratigraphy for the recovered sequence, may help resolve how the bottom water salinity of Lake Vättern changed prior to and throughout the Yoldia Sea stage.

Neotectonic activity in the Vättern Basin

Mörner (1985) highlighted sedimentological indications of neotectonic activity in northern Lake Vättern, and found displacements of up to 20 m in the soft sediment together with slumps and distal turbidities. Recent research has revealed soft sediment displacements of similar size in the middle and southern part of the Vättern basin (Jakobsson et al., 2014). These displacements (~17 m) are centered along the old fracture of the Vättern basin (Fig 1b) and are suggested to be related to large neotectonic activity following the retreat of the Scandinavian ice sheet. Bathymetry and subbottom data also reveal numerous subaqueous slope failures on the margins of Lake Vättern that may be linked to this neotectonic activity.

Throughout the cored sequence there are numerous and recurrent intervals of core disturbance. Drilling disturbances appear most common near the top of each core, but cannot explain down-core structures. Core deformation below 54 c-mblf (Fig. 10) is

interpreted as glaciotectonic in origin (O'Regan et al., in prep). In Unit 3B and 3A, evidence of disturbance to the varved sediments is likely a combination of coring disturbances and deformation related to post glacial seismic activity, or numerous smaller seismic events. The most spectacular disturbances, evident as compressional microfaults, are found at the base of unit 2 (Fig. 11a). These types of microfaults and their relation to palaeoseismicity were described by Mörner (1985). We connect these microfaults to the major seismic event in the Vättern basin described by Jakobsson et al. (2014) which is dated by pollen analysis to ~11.5 cal. ka BP.

Above 21 c-mblf the sulfide laminations within Unit 2 are absent and the sediment turns into homogenous grey silty clay. Above 8.00 c-mblf, sediments are clearly undisturbed, and the laminated gyttjaclay is nicely preserved (Fig. 13); this provides a conservative estimate for the depth of the last tectonically induced deformations.

Conclusions

- Three main lithostratigraphic regimes: a glacial clay unit, a post-glacial clay unit and a gyttjaclay unit, were identified in the upper 74 m of sediments recovered from southern Lake Vättern (Fig. 14).
- Below 54 c-mblf the glacial clay has been overridden by a readvancing ice sheet, most likely associated with the emplacement of the terrestrial Levene ice marginal moraine (~13.4 cal. ka BP).
- A brackish phase in the Vättern basin is clearly revealed in pore water chlorinity data. It occurs during the deposition of the glacial clay unit deposited before the Younger Dryas-Pre Boreal transition. This provides evidence in support of an earlier drainage event for the BIL (~12.8 cal. ka BP) (Fig. 14).
- The final drainage of the BIL is exhibited in the sediment as the transition between the glacial clay and the post-glacial clay. This transition is dated by correlation to neighboring cores to >11.5 cal. ka BP (Fig. 14).
- The lower post-glacial sediments (21-24 c-mblf) exhibit obvious signs of neotectonic activity with microfaults and compressed structures, and are connected to the major post-glacial earthquake episode in the Vättern basin described by Jakobsson et al., (2014).

Acknowledgements

We are grateful to Asera Mining Ltd. for providing us with the opportunity to use their drilling platform to core; we thank CEO Ove Göting and Steen Sörensen and the drill crew. We also thank Måns Lindell, County Administrative Board, Jönköping, for supporting the project. For laboratory help we thank Carina Johansson who ran the ITRAX analysis, Pär Hjelmqvist at ITM who successfully performed the pore water chlorinity analysis, Heike Siegmund and Malin Söderman at SIL for the TOC and carbonate analysis and Tina Varga for the help in the core laboratory at IGV.

Financial support to H. Swärd was provided by the Stockholm University Research School focusing on Natural Hazards financed by the Swedish Research Council VR. Stockholm University scientists are affiliated with the Bert Bolin Centre for Climate Research, supported through a grant from the Swedish Research Council Formas. R. Ananayev and D. Chernykh were supported by the Government of the Russian Federation under Grant #2013-220-04-157.

References

Adkins, J. F., and D. P. Schrag (2001), Pore fluid constraints on deep ocean temperature and salinity during the last glacial maximum, Geophys. Res. Lett. 28(5), 771–774.

Andréasson, P.-G., Rodhe, A., 1990. Geology of the Protogine Zone south of Lake Vättern, southern Sweden: A reinterpretation. Geologiska Föreningen i Stockholm Förhandlingar 112, 107-125.

Andrén, T., Björck, J., Johnsen, S., 1999. Correlation of Swedish glacial varves with the Greenland (GRIP) oxygen isotope record. Journal of Quaternary Science 14, 361-371.

Andrén, T., Lindeberg, G., Andrén, E., 2002. Evidence of the final drainage of the Baltic Ice Lake and the brackish phase of the Yolida Sea in glacial varved from the Baltic Sea. Boreas 31, 226 - 238.

Bakke, J., Lie, O., Heegaard, E., Dokken, T., Haug, G.H., Birks, H.H., Dulski, P., Nilsen, T., 2009. Rapid oceanic and atmospheric changes during the Younger Dryas cold period. Nature Geoscience 2, 202-205.

Bennike, O., & Jensen, J. (2013). A Baltic Ice Lake lowstand of latest Allerod age in the Arkona Basin, southern Baltic Sea. Geological Survey Of Denmark And Greenland Bulletin 28, 17-20.

Berglund, B.E. (1966a). Late-Quaternary vegetation in eastern Blekinge, southeastern Sweden. A pollen-analytical study. I. Late-Glacial time. Opera Botanica 12(1), 180 pp.

Berglund, B.E. (1966b). Late-Quaternary vegetation in eastern Blekinge, southeastern Sweden. A pollen-analytical study. II. Post-Glacial time. Opera Botanica 12(2), 190 pp.

Bingen, B., Andersson, J., Söderlund, U., Möller, C., 2008. The Mesoproterozoic in the Nordic countries. Episodes 31, 29-34.

Björck, S., 1979. Late Weichselian stratigraphy of Blekinge,Sweden, and water level changes in the Baltic Ice Lake. Thesis, University of Lund, Department of Quaternary Geology 7, 248 pp.

Björck, S., 1981. A stratigraphic study of Late Weichseliandeglaciation, shore displacement and vegetation history in southeastern Sweden. Fossils and Strata 14, 93 pp.

Björck, S., Digerfeldt, G., 1981. New 14-C dates from Hunneberg supporting the revised deglaciation chronology of the Middle Swedish endmoraine zone. Geologiska Föreningen i Stockholm Förhandlingar 103, 395-404.

Björck, S., 1995. A review of the history of the Baltic Sea, 13.0-8.0ka BP. Quaternary International 27, 19-40.

Björck, S., Kromer, B., Johnsen, S., Bennike, O., Hammarlund, D., Lemdahl,G., Possnert,G., Rasmussen,T.L., Wohlfarth,B., Hammer,C.U., Spurk,M., 1996. Synchronized terrestrial–atmospheric deglacial records around the North Atlantic. Science 274(5290), 1155–1160.

Brunnberg, L., 1995. Clay-varve Chronology and Deglaciation During the Younger Dryas and Preboreal in the Easternmost Part of the Middle Swedish Ice Marginal Zone. Department of Quaternary Research PhD thesis, Stockholm University.

Croudace, I.W., Rothwell, R.G., Rindby, A., 2006. ITRAX: Description and evaluation of a new multi-function X-ray core scanner. In *New Techniques in Sediment Core Analysis*, R. Rothwell G (ed.). Geological Society of London, London, 51–63.

De Geer, G., 1940. Geochronologia Suecica Principles. Kungliga Svenska Vetenskapsakademiens handlingar Ser III 18(6), 367 p.

Dickens, G.R., Koelling, M., Smith, D.C., Schnieders, L., 2007. Rhizon Sampling of Pore Waters on Scientific Drilling Expeditions: An Example from the IODP Expedition 302, Arctic Coring Expedition (ACEX), Scientific Drilling, 22-25.

Duncan, J.M., Wright, S.G., 2005. Soil strength and slope stability. John Wiley & Sons, Inc., Hoboken, New Jersey.

Gorbatschev, R., 1980. The Precambrian development of southern Sweden. Geologiska Föreningen i Stockholm Förhandlingar 102, 129-136.

Jakobsson, M., Björck, S., Alm, G., Andrén, T., Lindeberg, G., Svensson, N.-O., 2007. Reconstructing the Younger Dryas ice dammed lake in the Baltic Basin: Bathymetry, area and volume. Global and Planetary Change 57, 355-370.

Jakobsson, M., Björck, S., O´Regan, M., Flodén, T., Greenwood, S.L., Swärd, H., Lif, A., Ampel, L., Koyi, H., Skelton, A., 2014. Major earthquakes at the Pleistocene-Holocene transition in Lake Vättern, southern Sweden. Geology 42, 379-382.

Johnson, M.D., Kylander, M.E., Casserstedt, L., Wiborgh, H., Björck, S., 2013. Varved glaciomarine clay in central Sweden before and after the Baltic Ice Lake drainage: a further clue to the drainage events at Mt Billingen. GFF 135, 293-307.

Kylander, M.E., Klaminder, J., Wohlfarth, B. and Löwemark, L., 2013. Geochemical responses to paleoclimatic changes in southern Sweden since the late glacial: the Hässeldala Port lake sediment record. Journal of Paleolimnology 50(1), 57-70.

Koinig, K.A., Shotyk, W., Lotter, A.F., Ohlendorf, C. and Sturm, M., 2003. 9000 years of geochemical evolution of lithogenic major and trace elements in the sediment of an alpine lake - The role of climate, vegetation, and land-use history. Journal of Paleolimnology 30(3), 307-320.

Lundqvist, J., Wohlfarth, B., 2001. Timing and east–west correlation of south Swedish ice marginal lines during the Late Weichselian. Quaternary Science Reviews 20, 1127-1148.

McDuff, R.E., 1985. The chemistry of interstitial waters, deep sea drilling project leg 86, Initial Report of the DSDP 86, 675-687.

Månsson, A.G.M., 1996. Brittle reactivation of ductile basement structures; a tectonic model for the lake Vättern basin, southern Sweden. GFF 118(4), 19-19.

Mörner, N.-A., 1985. Paleoseismicity and geodynamics in Sweden. Tectonophysics 117, 139-153.

Norrman, J.O., 1964. Lake Vättern - Investigations on shore and bottom morphology, Institute of Geography PhD thesis. Uppsala University, p. 238.

Norrman, J.O., Köunigsson, L.-K., 1972. The Sediment Distribution in Lake Vättern and some Analyses of Cores from its Southern Basin. Geologiska Föreningen i Stockholm Förhandlingar 94, 489-513.

Sayles, F.L., Mangelsdorf Jr, P.C., 1977. The equilibration of clay minerals with sea water: exchange reactions. Geochimica et Cosmochimica Acta 41, 951-960.

STANDARDS, J.P.O.O.T.A., 1966. International oceanographic tables. UNESCO Publications Center, New York, p. 118.

Strömberg, B. , 1969. Den mellansvenska israndzonen. Översiktlig naturvårdsinventering med hänsyn till kvartärgeologisk-naturgeografiska värden. Stockholms Universitet, Naturgeografiska Institutionen, Forskningsrapport 6. 56pp.

Svensson, N.-O., 1989. Late Weichselian and early Holocene shore displacement in the central Baltic, based on stratigraphical and morphological records from eastern Småland and Gotland, Sweden, Department of Quaternary Geology PhD thesis. Lund University,p.

Vaasma, T., 2008. Grain-size analysis of lacustrine sediments: a comparison of pre-treatment methods. Järvesetete terasuuruse analüüsid: eeltöötlusmeetodite võrdlus 57, 231-243.

Waldemarson, D., 1986. Weichselian lithostratigraphy, depositional processes and deglaciation pattern in the southern Vättern basin, south Sweden. LUNDQUA Thesis, Vol. 17, 128pp.

Walker, M., Johnsen, S., Rasmussen, S.O., Popp, T., Steffensen, J.-P., Gibbard, P., Hoek, W., Lowe, J., Andrews, J., Björck, S., Cwynar, L.C., Hughen, K., Kershaw, P., Kromer, B., Litt, T., Lowe, D.J., Nakagawa, T., Newnham, R., Schwander, J., 2009. Formal definition and dating of the GSSP for the base of the Holocene using the Greenland NGRIP ice core, and selected auxiliary records. Journal of Quaternary Science 24, 3-17.

Supplementary material:

a) Complete list of cores from holes A-E with offsets for the composite meter below depth scale

b) Varve counting from cyclic bulk density variations

c) Results from the piecewise linear interpolation of varves

Vättern coring 2012

Hole A						
Core	*Section 1 Length (cm)*	*Section 2 Length (cm)*	*mblf (top)*	*mblf (base)*	*Offset for Composite Depth (Cmblf)*	*Cmblf (top)*
A-1			0.25	0.25	0	0.25
A-2			3.25	3.25	0	3.25
A-3	150	87	6.25	8.62	0.01	6.26
A-4	42.5		9.25	9.675	0	9.25
A-5	124		12.25	13.49	0	12.25
A-6	123		15.25	16.48	-0.02	15.23
A-7	93		18.25	19.18	0	18.25

Hole B						
Core	*Section 1 Length (cm)*	*Section 2 Length (cm)*	*mblf (top)*	*mblf (base)*	*Offset for Composite Depth (Cmblf)*	*Cmblf (top)*
B-1			3.25	3.25	0	3.25
B-2			6.25	6.25	0	6.25
B-3			9.25	9.25	0	9.25
B-4			12.25	12.25	0	12.25
B-5	28		15.25	15.53	0	15.25
B-6	46		18.25	18.71	0	18.25
B-7	62		21.25	21.87	0	21.25
B-8	54		24.25	24.79	0	24.25
B-9	18		25.75	25.93	0	25.75
B-10	17		27.25	27.42	0	27.25
B-11	120		30.25	31.45	0	30.25
B-12	28		33.25	33.53	0	33.25
B-13	28		36.25	36.53	0	36.25

Hole C						
Core	*Section 1 Length (cm)*	*Section 2 Length (cm)*	*mblf (top)*	*mblf (base)*	*Offset for Compsoite Depth (cmblf)*	*Cmblf (top)*
C-1			18.25	18.25	0	18.25
C-2	10		21.25	21.35	0	21.25
C-3	12		24.25	24.37	0	24.25
C-4	0		27.25	27.25	0	27.25
C-5	93		30.25	31.18	0.29	30.54
C-6	106	54	33.25	34.85	-0.68	32.57
C-7	27		36.25	36.52	-0.02	36.23
C-8	140		39.25	40.65	-0.49	38.76
C-9	36		42.25	42.61	0	42.25
C-10	0		45.25	45.25	0	45.25
C-11	0		48.25	48.25	0	48.25
C-12	156	151	51.25	54.25	-0.04	51.21
C-13	58	85	54.25	55.68	0.02	54.27
C-14	56		57.25	57.85	0	57.25
C-15	150	89	60.25	62.53	0.27	60.52
C-16	150	29	63.25	64.95	0	63.25
C-17	77		66.25	67.02	0	66.25
C-18	72		69.25	69.98	0	69.25
C-19			72.25	74.39	0	72.25

Hole D						
Core	*Section 1 Length (cm)*	*Section 2 Length (cm)*	*mblf (top)*	*mblf (base)*	*Offset for Compsoite Depth (cmblf)*	*Cmblf (top)*
D-1	30		18.25	18.55	0	18.25
D-2	155	153	21.25	24.25	0.56	21.81
D-3	22		24.25	24.47	0.57	24.82
D-4	135	64	27.25	29.24	0	27.25
D-5	146	150	30.25	33.19	0	30.25
D-6	156	150	33.25	36.25	-0.05	33.2
D-7	152	150	36.25	39.25	0	36.25
D-8	149	150	39.25	42.24	0.01	39.26
D-9	148	150	42.25	45.24	0	42.25
D-10	151	150	45.25	48.25	0	45.25
D-11	156	151	48.25	51.25	0.01	48.26
D-12	70		51.25	53.2	0.07	51.32
D-13	156	150	54.25	57.25	0	54.25
D-14	155	150	57.25	60.25	0.06	57.31
D-15	97	140	60.25	62.61	0.11	60.36

Hole E						
Core	*Section 1 Length (cm)*	*Section 2 Length (cm)*	*mblf (top)*	*mblf (base)*	*Offset for Compsoite Depth (cmblf)*	*Cmblf (top)*
E-1	29		-5.75	-5.46	0	0
E-2			-2.75	-2.75	0	0
E-3	81		0.25	1.06	0	0.25
E-4	109		3.25	4.35	0	3.25
E-5	126		6.25	7.52	0	6.25
E-6	156		9.25	10.82	0	9.25
E-7	95	152	12.25	14.7	0	12.25
E-8	120		15.25	16.55	0	15.25
E-9	155	151	18.25	21.25	0	18.25
E-10	155	152	21.25	24.25	0.06	21.31

Varves from cyclical bulk density variations M.V. = missing varves

CoreID	Section	Section length (m)	Cmblf top	Cmblf bottom	Number of varves	Sed. rate (cm/year)	Varves/m
C13	2	0.8	54.85	55.65	9	9	11.25
C13	1	0.58	54.27	54.85	M.V.		
C12	2	1.5	52.77	54.27	M.V.		
C12	1	1.56	51.21	52.77	M.V.		
D12	1	0.7	51.32	52.02	M.V.		
D11	2	0.1	49.83	49.93	M.V.		
D11	2	0.28	49.93	50.21	3	9	10.71
D11	2	1.12	50.21	51.33	M.V.		
D11	1	0.5	48.26	48.76	M.V.		
D11	1	0.9	48.76	49.66	10	9	11.11
D11	1	0.16	49.66	49.82	M.V.		
D10	2	1.5	46.76	48.26	M.V.		
D10	1	0.3	45.25	45.55	M.V.		
D10	1	0.32	45.55	45.87	3	11	9.38
D10	1	0.88	45.87	46.75	M.V.		
D9	2	0.56	43.72	44.28	9	6	16.07
D9	2	0.18	44.28	44.46	M.V.		
D9	2	0.76	44.46	45.22	12	6	15.79
D9	1	0.44	42.25	42.69	M.V.		
D9	1	0.62	42.69	43.31	8	8	12.90
D9	1	0.14	43.31	43.45	M.V.		
D9	1	0.27	43.45	43.72	2	14	7.41
D8	2	0.5	40.73	41.23	6	8	12.00
D8	2	1	41.23	42.23	M.V.		
D8	1	1.02	39.26	40.28	15	7	14.71
D8	1	0.45	40.28	40.73	M.V.		
D7	2	1.49	37.76	39.25	M.V.		
D7	1	1.51	36.25	37.76	M.V.		
D6	2	1.45	34.75	36.2	M.V.		
D6	1	0.42	33.2	33.62	M.V.		
D6	1	1.13	33.62	34.75	19	6	16.81
D5	2	1.5	31.7	33.2	M.V.		
D5	1	0.3	30.25	30.55	M.V.		
D5	1	0.66	30.55	31.21	6	11	9.09
D5	1	0.49	31.21	31.7	M.V.		
D4	1	1.33	27.25	28.58	M.V.		
E10	1 and 2	3.06	21.31	24.37	M.V.		
E9	1 and 2	3	18.25	21.25	M.V.		
E8	1	1.25	15.25	16.5	M.V.		
E7	2	0.58	13.1	13.68	M.V.		
E7	2	0.34	13.68	14.02	8	4	23.53
E7	1	0.95	12.25	13.2	M.V.		
E6	1	1.6	9.25	10.85	M.V.		
E5	1	1.26	6.25	7.51	M.V.		
E4	1	1.05	3.25	4.3	M.V.		
E3	1	0.8	0.25	1.05	M.V.		

Piecewise linear-interpolation of varves

Cmblf top	varves/m	Cmblf top	Piecewise linear-interp. (varves/m).
13.68	23.52941176	13	23.52941176
14.02	23.52941176	14	23.42878771
30.55	9.090909091	15	22.67340858
31.21	9.090909091	16	21.79993594
33.62	16.81415929	17	20.92646331
34.75	16.81415929	18	20.05299067
39.26	14.70588235	19	19.17951803
40.28	14.70588235	20	18.3060454
40.73	12	21	17.43257276
41.23	12	22	16.55910013
42.69	12.90322581	23	15.68562749
43.31	12.90322581	24	14.81215486
43.45	7.407407407	25	13.93868222
43.72	7.407407407	26	13.06520958
43.73	16.07142857	27	12.19173695
44.28	16.07142857	28	11.31826431
44.46	15.78947368	29	10.44479168
45.22	15.78947368	30	9.571319041
45.55	9.375	31	9.226757227
45.87	9.375	32	11.62259692
48.76	11.11111111	33	14.82726505
49.66	11.11111111	34	16.79108568
49.93	10.71428571	35	16.68268415
50.21	10.71428571	36	16.22982533
54.85	11.25	37	15.76235816
55.65	11.25	38	15.29489099
		39	14.84088687
		40	14.56036601
		41	12.18159546
		42	12.47635882
		43	12.23256101
		44	14.08536967
		45	15.02751196
		46	9.518512214
		47	10.05382545
		48	10.65455594
		49	11.09080642
		50	10.83620411
		51	10.80549569
		52	10.92095135
		53	11.03640702
		54	11.15186268
		55	11.24292834

Core description
VÄTTERN 2012

VAT-12-C12 Sec: 1

Coring date: 2012-11-04 **MBLF (m):** 51.25 **Position:** N 57:49:59.89
E 14:11:02.90

Described by: Pedro Preto

Stockholm University

Core depth (cm) | Image | RGB 50 60 70 80 | ρ_B (g/cm^3) 1.7 1.9 | MS x10^{-5} SI 24 34 44 | Lithology | Description

0
10
20
30
40
50
60
70
80
90
100
110
120
130
140
150

Dark greyish brown silty clay with varves. Intercalation of greyish and brownish layers make up varves.

Dark greyish sand layer

Dark greyish brown silty clay with varves. Intercalation of greyish and brownish layers make up varves.

Dark greyish brown sand layer

Dark greyish brown silty clay with varves. Intercalation of greyish and brownish layers make up varves.

Core description
VÄTTERN 2012

VAT-12-C12 Sec: 2

Coring date: 2012-11-04 **MBLF (m):** 51.25 **Position:** N 57:49:59.89
E 14:11:02.90

Described by: Pedro Preto, Henrik Swärd

Stockholm University

Core depth (cm) | Image | RGB 54 64 74 | ρ_B (g/cm^3) 1.8 1.9 | MS x10^{-5} SI 30 35 40 45 50 | Lithology | Description

156
166
176
186
196
206
216
226
236
246
256
266
276
286
296
306

Grey silty clay

Grey low angle parallell bedded silt

Grey low angle parallell bedded silt

Grey high angle parallell bedded silt

Grey silty clay varves with thin layers of silt and spots with pebbles. Thin (few mm to 1 cm wide) sand layer at 17 and 106 cm. Grey sandstones at 5, 33, 91 and 95-98 cm.

Core description
VÄTTERN 2012

VAT-12-C13 Sec: 1

Coring date: 2012-11-04 **MBLF (m):** 54.25 **Position:** N 57:49:59.89
E 14:11:02.90

Described by: Henrik Swärd

Stockholm University

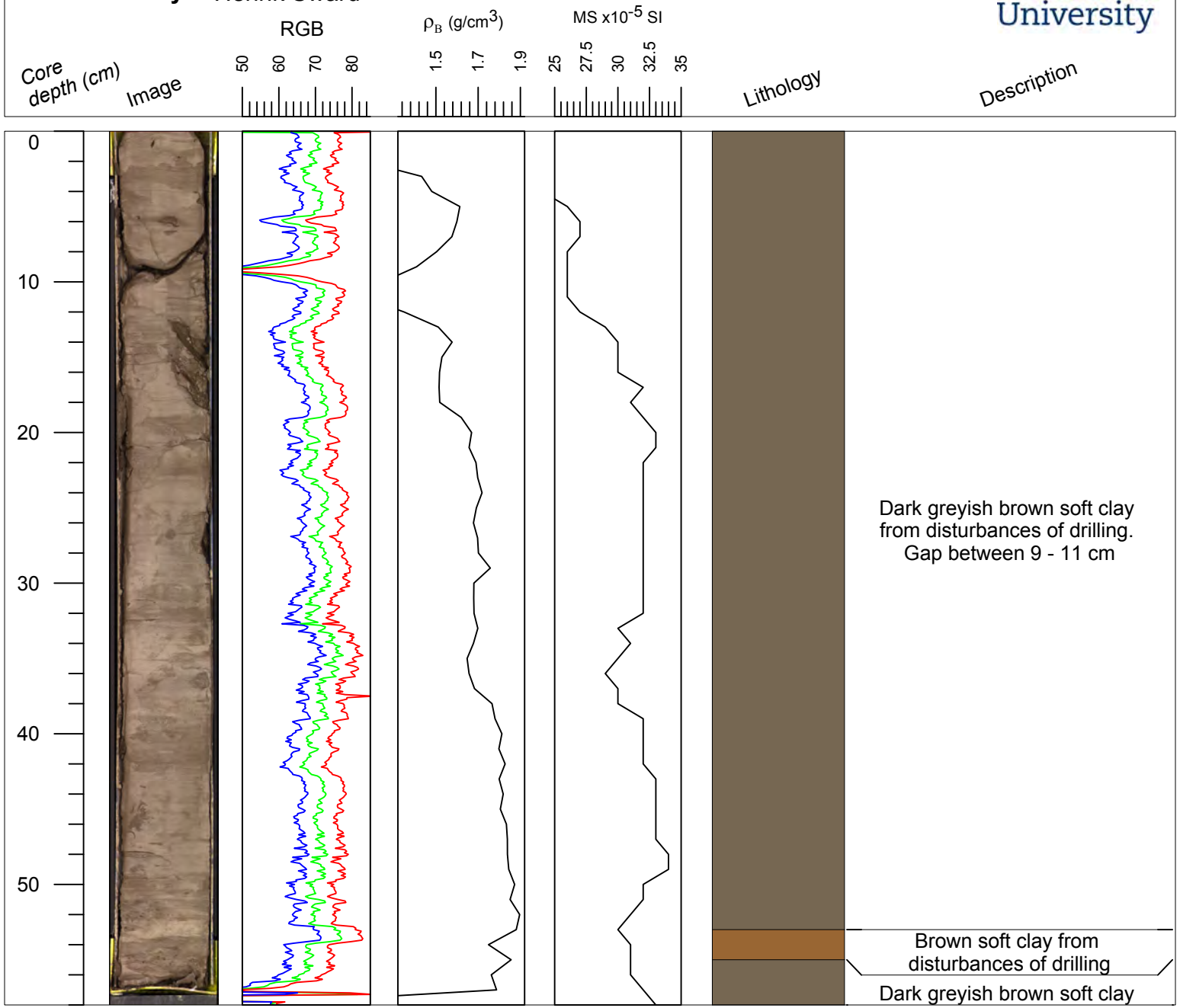

Core description
VÄTTERN 2012

VAT-12-C13 Sec: 2

Coring date: 2012-11-04 **MBLF (m):** 54.25 **Position:** N 57:49:59.89
E 14:11:02.90

Described by: Pedro Preto

Stockholm University

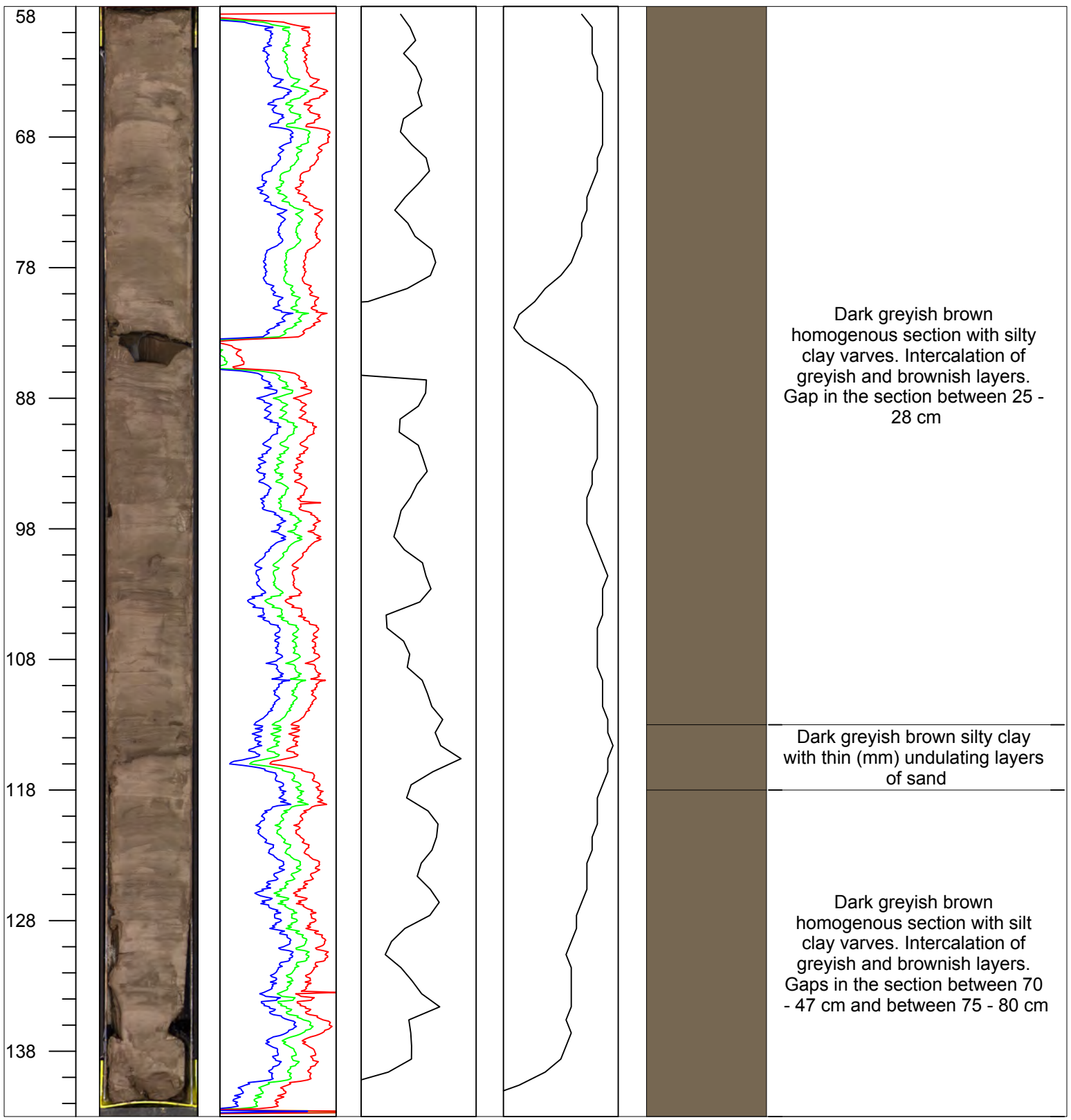

Core description
VÄTTERN 2012

VAT-12-C14 Sec: 1

Coring date: 2012-11-04 **MBLF (m):** 57.25 **Position:** N 57:49:59.89
E 14:11:02.90

Described by: Pedro Preto

Stockholm University

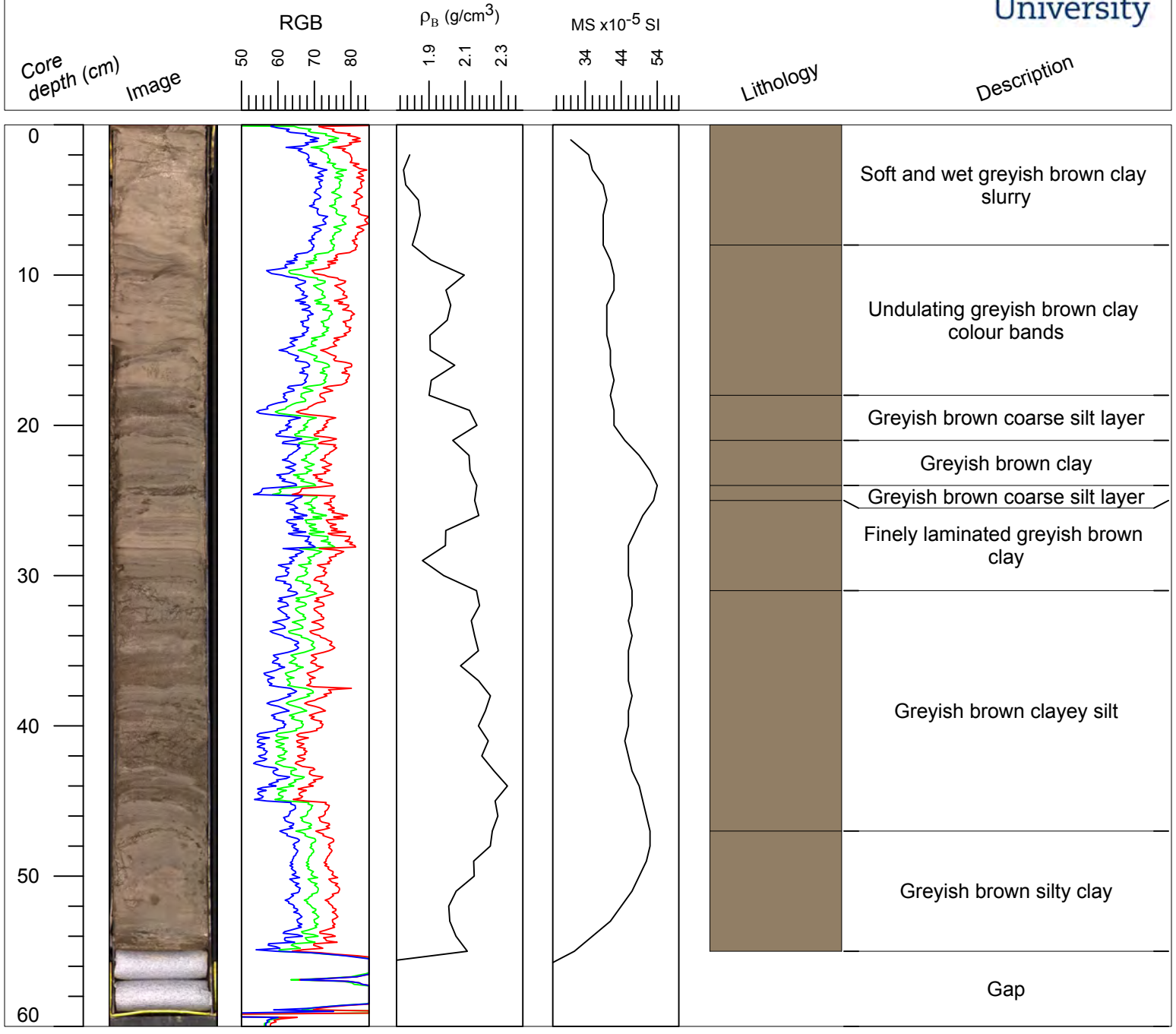

Core description
VÄTTERN 2012

VAT-12-C15 Sec: 1

Coring date: 2012-11-04 **MBLF (m):** 60.25 **Position:** N 57:49:59.89
E 14:11:02.90

Described by: Svante Björck

Stockholm University

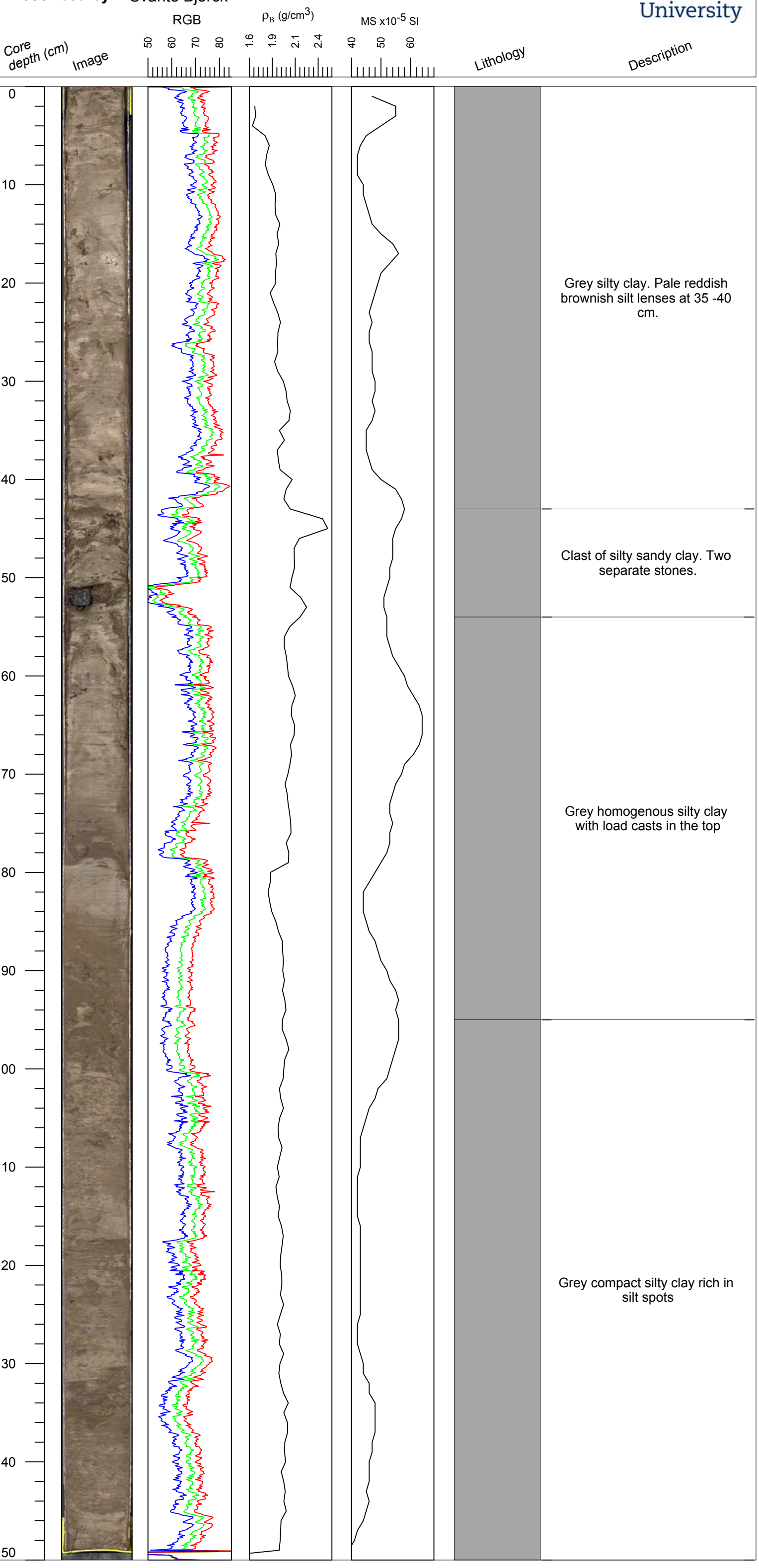

Core description
VÄTTERN 2012

VAT-12-C15 Sec: 2

Coring date: 2012-11-04 **MBLF (m):** 60.25 **Position:** N 57:49:59.89
E 14:11:02.90

Described by: Svante Björck

Stockholm University

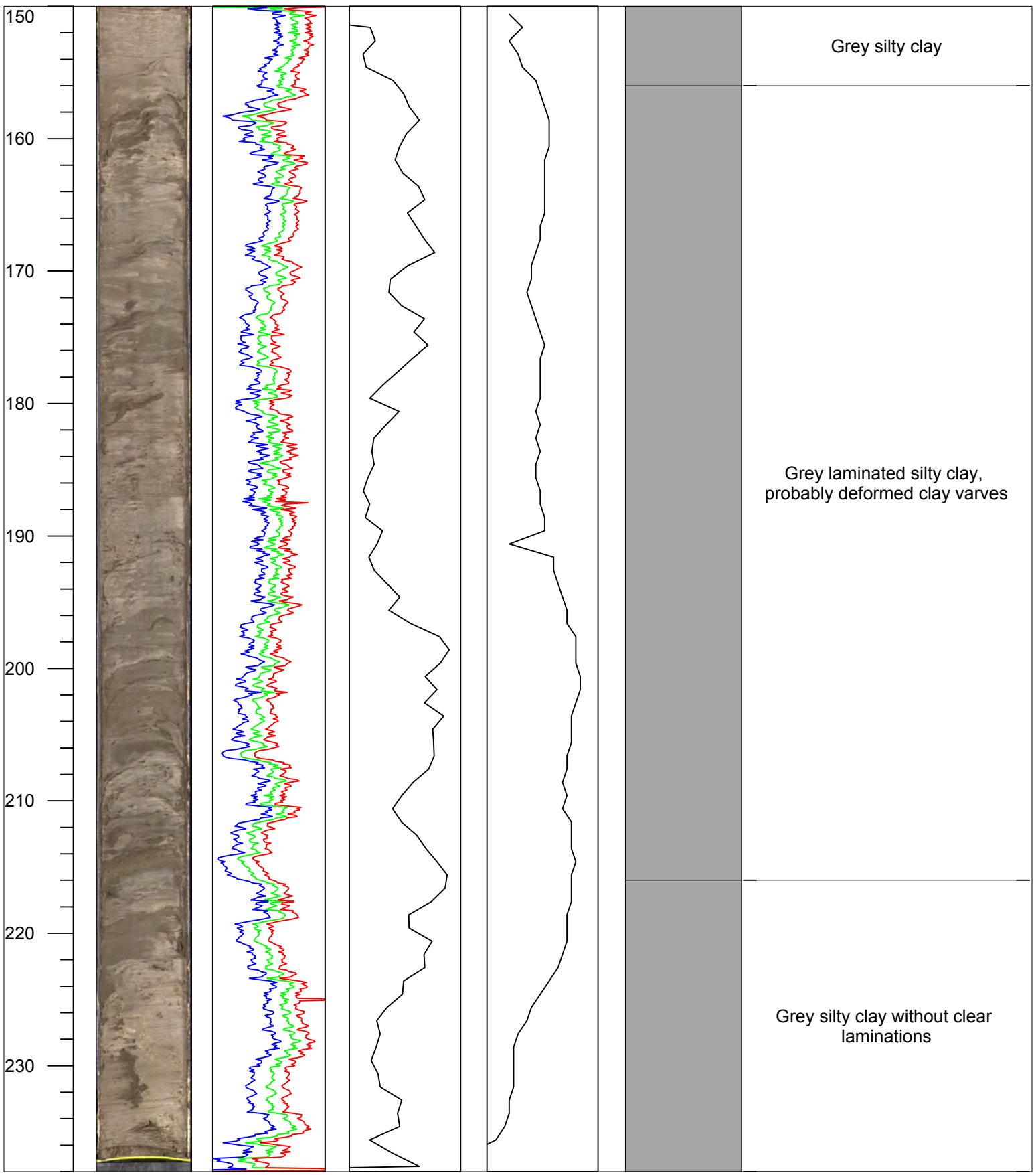

Core description
VÄTTERN 2012

VAT-12-C16 Sec: 1

Coring date: 2012-11-04 **MBLF (m):** 63.25 **Position:** N 57:49:59.89
E 14:11:02.90

Described by: Pedro Preto

Stockholm University

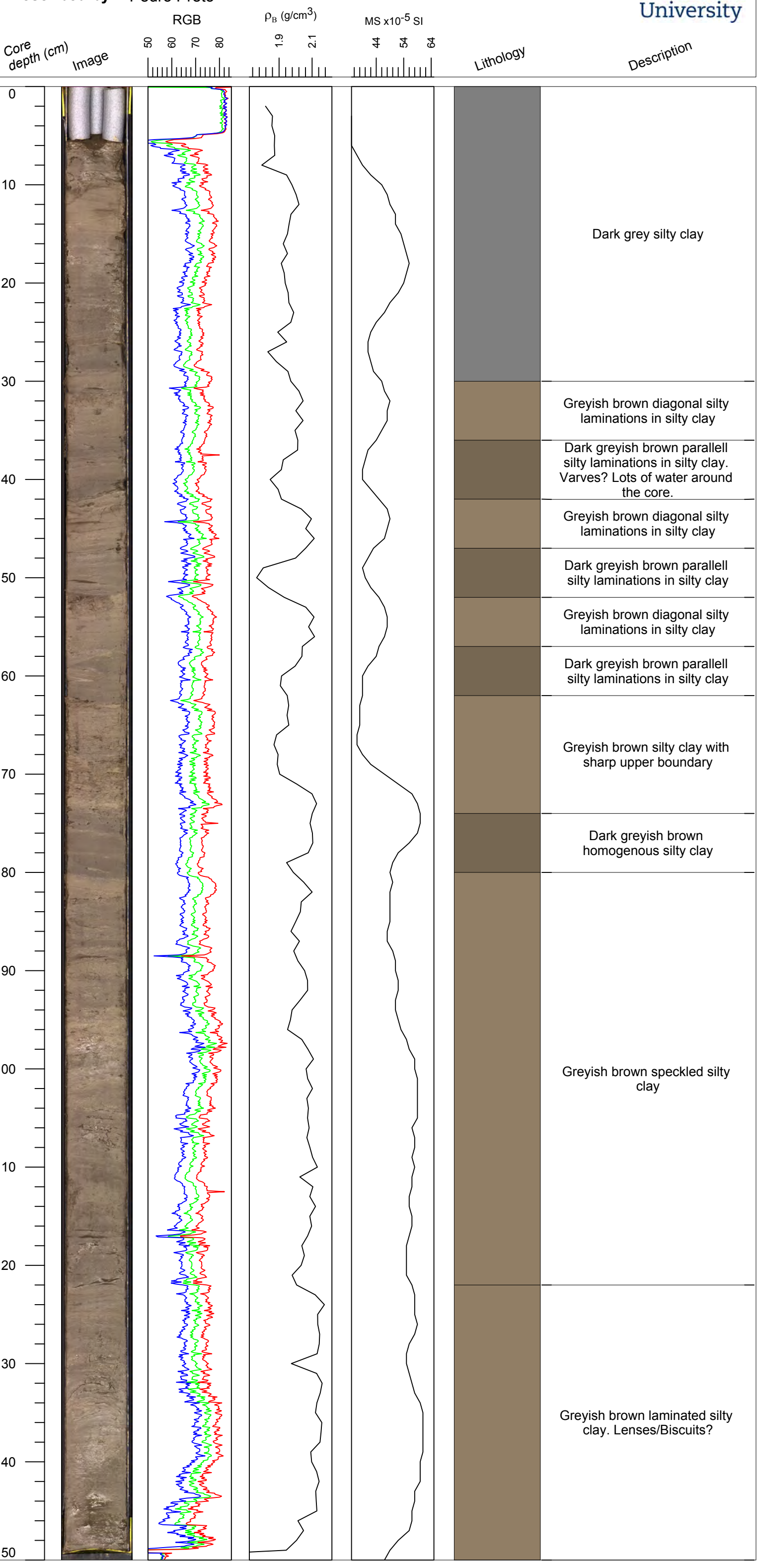

Core description
VÄTTERN 2012

VAT-12-C18 Sec: 1

Coring date: 2012-11-05 **MBLF (m):** 69.25 **Position:** N 57:49:59.89
E 14:11:02.90

Described by: Pedro Preto

Stockholm University

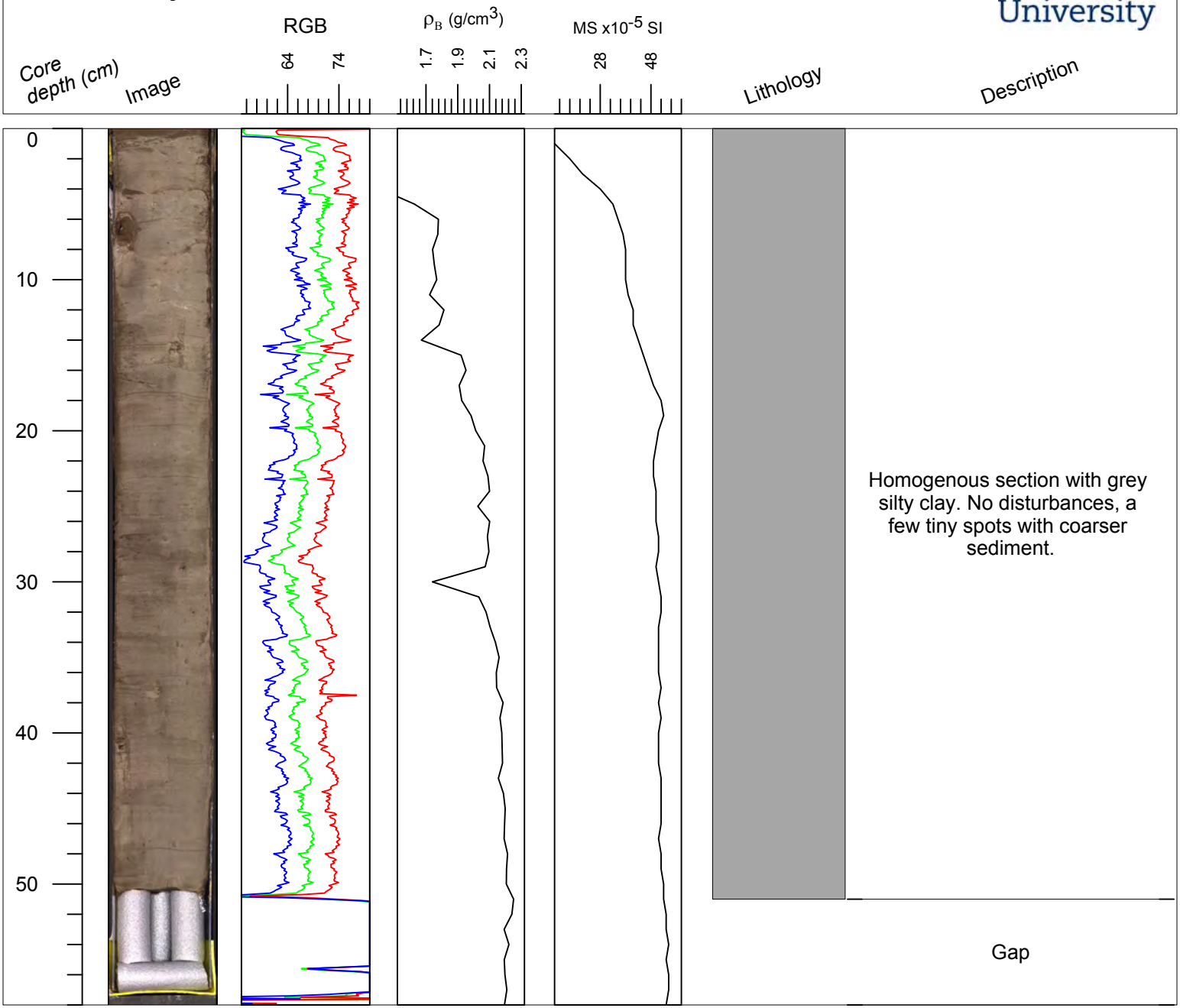

Core description
VÄTTERN 2012

VAT-12-C19 Sec: 2

Coring date: 2012-11-05 **MBLF (m):** 72.25 **Position:** N 57:49:59.89
E 14:11:02.90

Described by: Helena Alexandersson

Stockholm University

RGB ρ_B (g/cm^3) MS x10^{-5} SI

Core depth (cm)	Image	48 68 88	1.7 1.9	24 34 44	Lithology	Description
67–77						Grey sandy clay with clast and gravel. Diamict
77–97						Grey silty clay with sand grains
97–107						Grey clay with clast. 4 cm clast at 62 cm.
107–117						Grey fine sand
117–137						Grey mixed clayey sandy silt
137–147						Grey coarse well sorted sand. 2 cm clast
147–157						Dark grey sandy clayey silt with clast
157–167						Dark grey folded/deformed sandy silty clay. Light band at 139 cm, dark band at 145 cm
167–177						Dark grey laminated? Sandy clayey silt
177–187						Dark grey highly compacted deformed? Silty clay with colour shift. Small gravel at 127 cm.
187–197						Dark grey deformed highly compacted laminated silty clay. Mottled with lighter spots.
197–207						

Core description
VÄTTERN 2012

VAT-12-D4 Sec: 1

Coring date: 2012-11-06 **MBLF (m):** 27.25 **Position:** N 57:49:59.62
E 14:11:03.48

Described by: Helena Alexandersson

Stockholm University

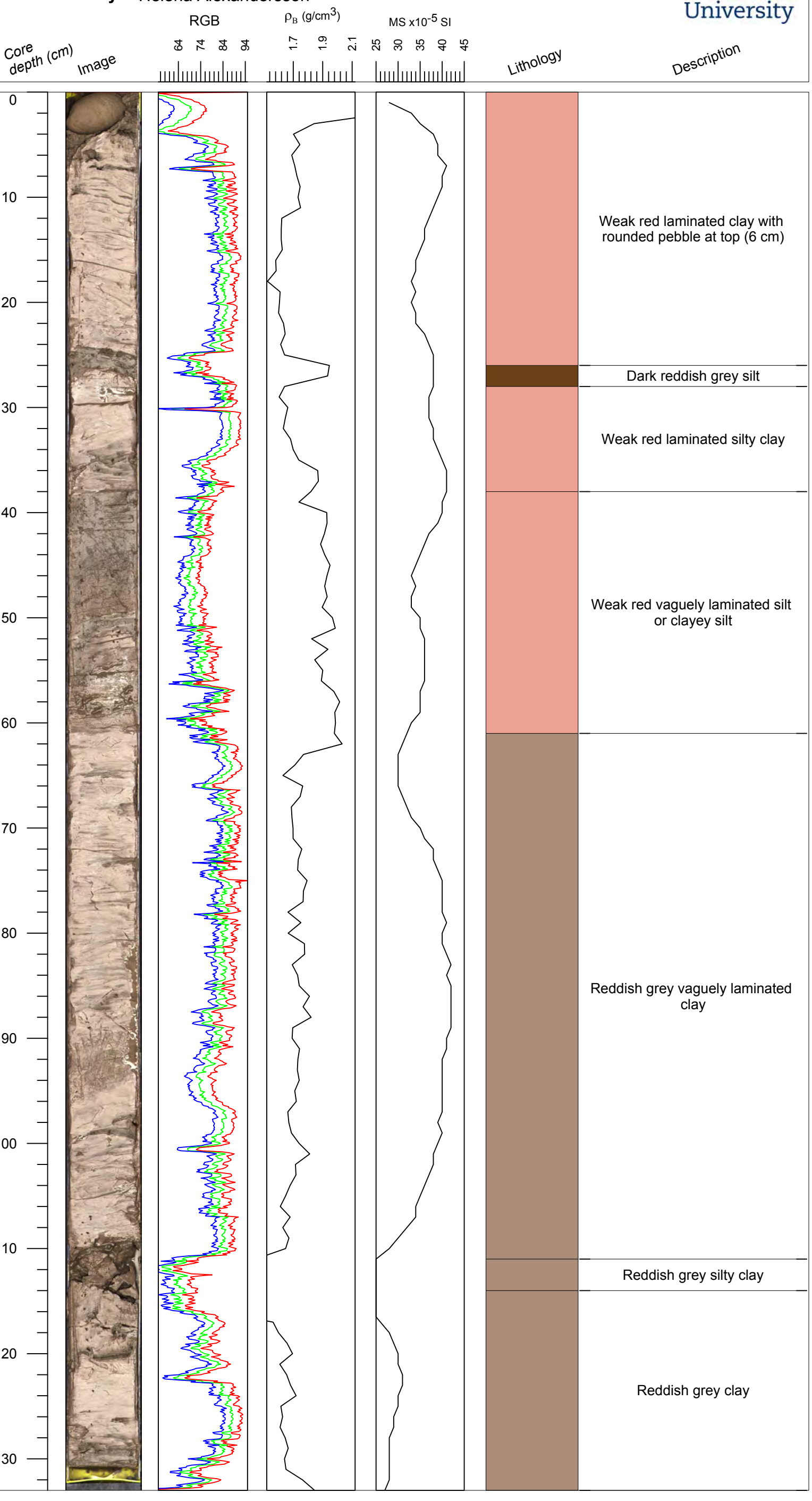

Core description
VÄTTERN 2012

VAT-12-D5 Sec: 1

Coring date: 2012-11-06 **MBLF (m):** 30.25 **Position:** N 57:49:59.62
E 14:11:03.48

Described by: Pedro Preto

Stockholm University

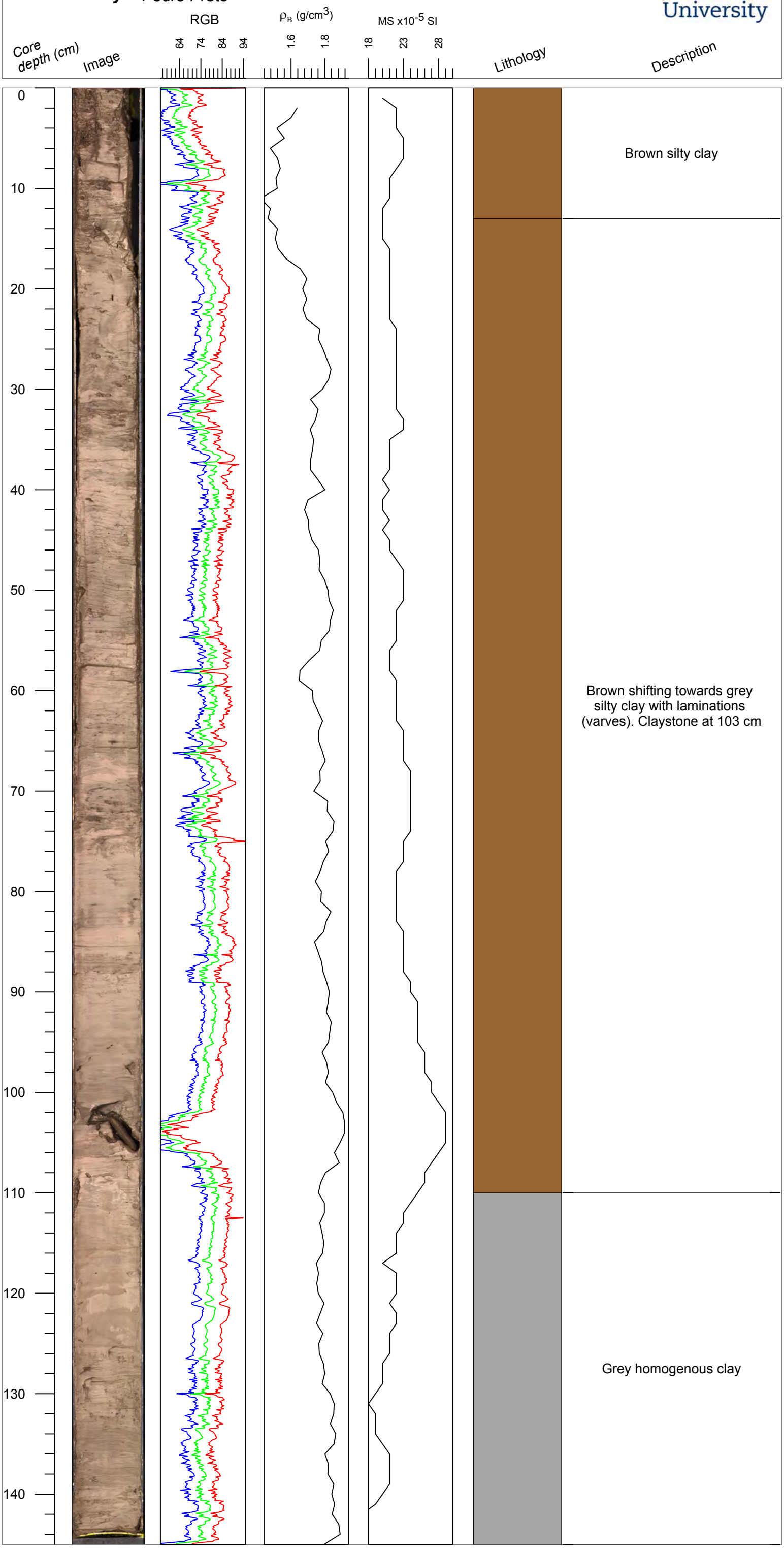

Core description
VÄTTERN 2012

VAT-12-D5 Sec: 1

Coring date: 2012-11-06 **MBLF (m):** 30.25 **Position:** N 57:49:59.62
E 14:11:03.48

Described by: Pedro Preto

Stockholm University

Core depth (cm) | Image | RGB 64 84 | ρ_B (g/cm^3) 1.7 1.9 | MS x10^{-5} SI 20 25 30 35 40 | Lithology | Description

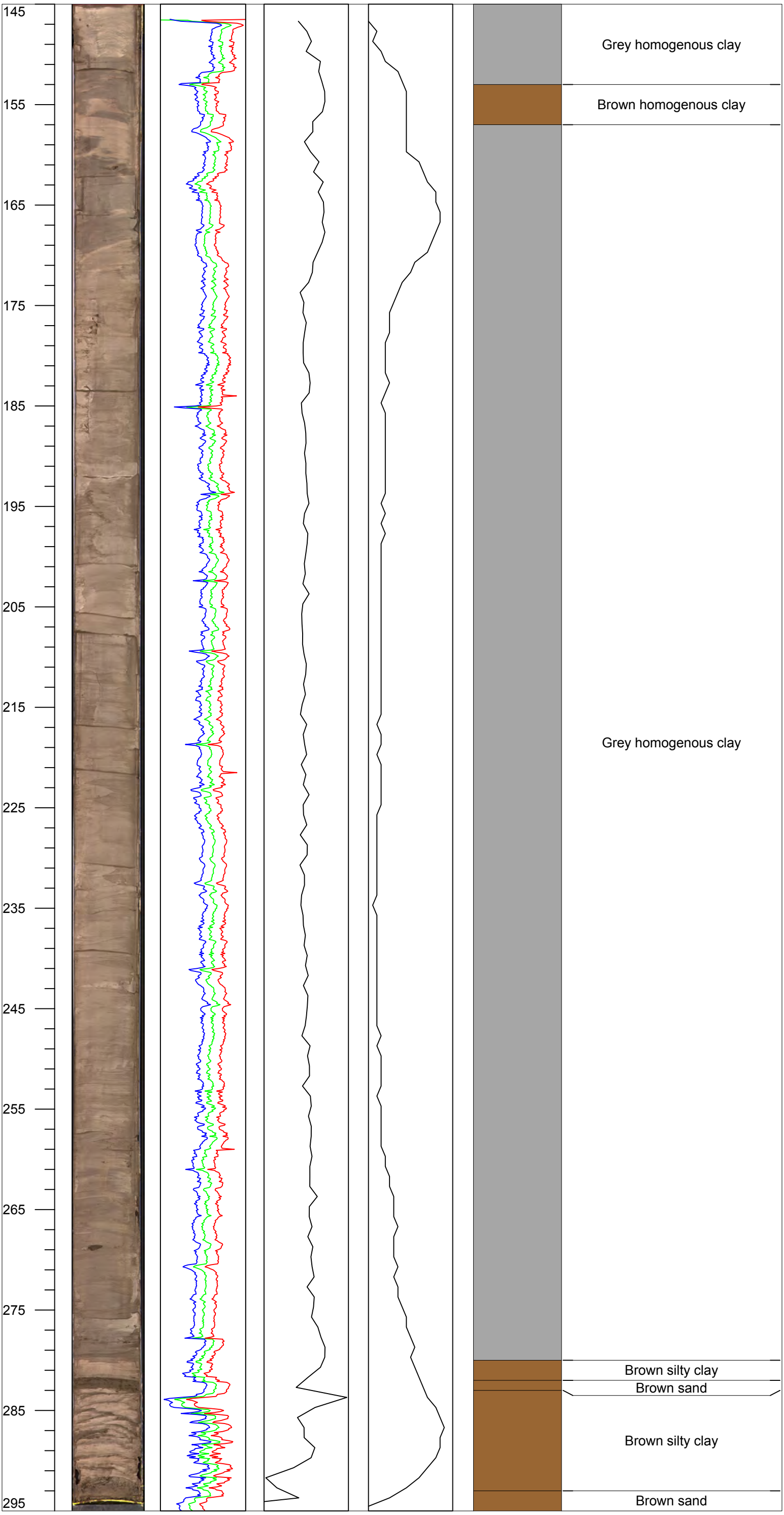

Core description
VÄTTERN 2012

VAT-12-D6 Sec: 1

Coring date: 2012-11-07 **MBLF (m):** 33.25 **Position:** N 57:49:59.62
E 14:11:03.48

Described by: Pedro Preto

Stockholm University

Core depth (cm) | Image | RGB 50 60 70 80 | ρ_B (g/cm^3) 1.7 1.9 | MS x10^{-5} SI 31 36 41 | Lithology | Description

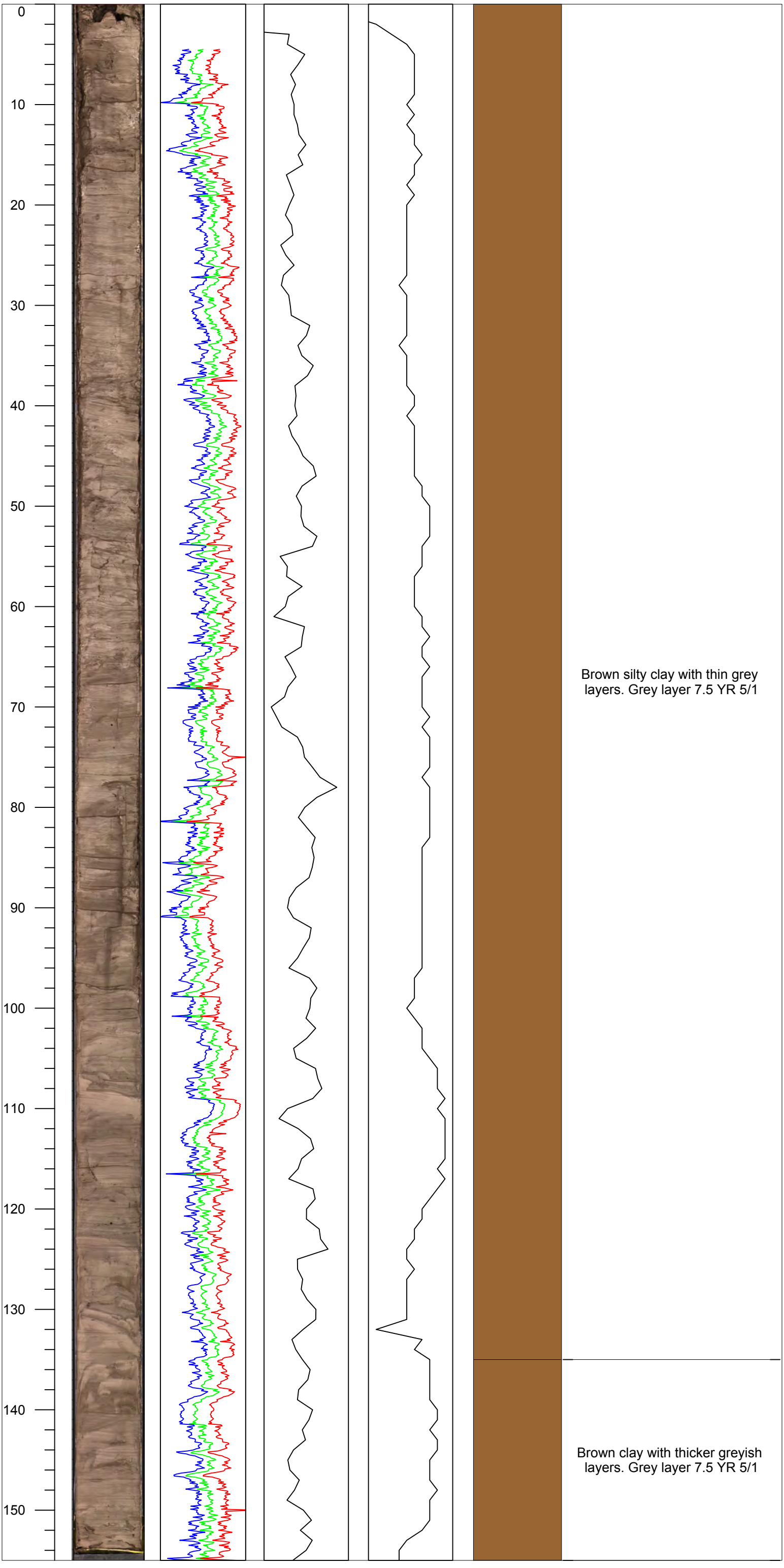

Brown silty clay with thin grey layers. Grey layer 7.5 YR 5/1

Brown clay with thicker greyish layers. Grey layer 7.5 YR 5/1

Core description
VÄTTERN 2012

VAT-12-D6 Sec: 2

Coring date: 2012-11-06 **MBLF (m):** 33.25 **Position:** N 57:49:59.62
E 14:11:03.48

Described by: Pedro Preto

Stockholm University

Core depth (cm) | Image | RGB 50 60 70 80 90 | ρ_B (g/cm^3) 1.7 1.8 1.9 | MS x10^{-5} SI 25 30 35 40 45 | Lithology | Description

155
165
175
185
195
205
215
225
235
245
255
265
275
285
295

Homogenous section with intercalation of grey silty layers in brown clay. Grey layer 7.5 YR 5/1

Core description
VÄTTERN 2012

VAT-12-D7 Sec: 1

Coring date: 2012-11-07 **MBLF (m):** 36.25 **Position:** N 57:49:59.62
E 14:11:03.48

Described by: Pedro Preto

Stockholm University

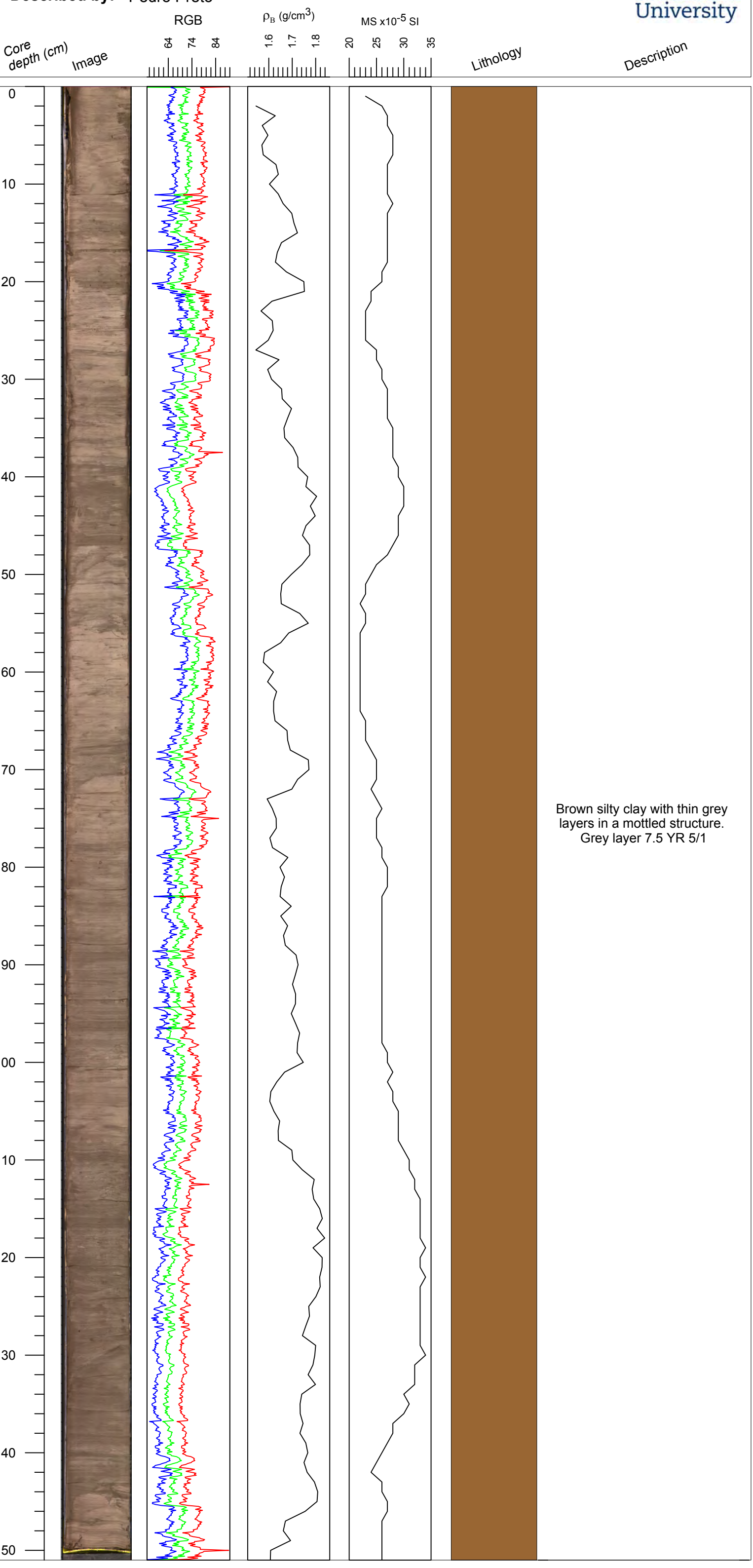

Core description
VÄTTERN 2012

VAT-12-D7 Sec: 2

Coring date: 2012-11-07 **MBLF (m):** 36.25 **Position:** N 57:49:59.62
E 14:11:03.48

Described by: Henrik Swärd

Stockholm University

Core depth (cm) | Image | RGB 64 74 84 | ρ_B (g/cm^3) 1.7 1.8 1.9 | MS x10^{-5} SI 22 27 32 | Lithology | Description

151
161
171
181
191
201
211
221
231
241
251
261
271
281
291

Mottled brown to grey clay. Grey parts 7.5 YR 7/2. At 111 - 117 cm light wave band pattern are present (2.5YR 5/1)

Core description
VÄTTERN 2012

VAT-12-D8 Sec: 1

Coring date: 2012-11-07 **MBLF (m):** 39.25 **Position:** N 57:49:59.62
E 14:11:03.48

Described by: Svante Björck

Stockholm University

Core depth (cm) | Image | RGB 64 74 84 94 | ρ_B (g/cm^3) 1.7 1.9 2.1 | MS x10^{-5} SI 32 34.5 37 39.5 | Lithology | Description

0
10
20
30
40
50
60
70
80
90
100
110
120
130
140

Faintly reddish-brown diffusedly silty varved clay, less compacted possibly thick varves. Sharp lower boundary

Reddish brown compact silty clay with very diffuse varve structures. Grey parts 7.5 YR 7/2. At 111 - 117 cm light wave band pattern are present (2.5YR 5/1)

Core description
VÄTTERN 2012

VAT-12-D8 Sec: 2

Coring date: 2012-11-07 **MBLF (m):** 39.25 **Position:** N 57:49:59.62
E 14:11:03.48

Described by: Svante Björck

Stockholm University

Core depth (cm) | Image | RGB 64 74 84 | ρ_B (g/cm^3) 1.7 1.8 1.9 2 | MS x10^{-5} SI 34 44 | Lithology | Description

147
157
167
177
187
197
207
217
227
237
247
257
267
277
287
297

Reddish brown silty clay with very diffuse varves. Compact to very compact. 2 cm large clast stone at 17 cm

Core description
VÄTTERN 2012

VAT-12-D9 Sec: 1

Coring date: 2012-11-07 **MBLF (m):** 42.25 **Position:** N 57:49:59.62
E 14:11:03.48

Described by: Henrik Swärd

Stockholm University

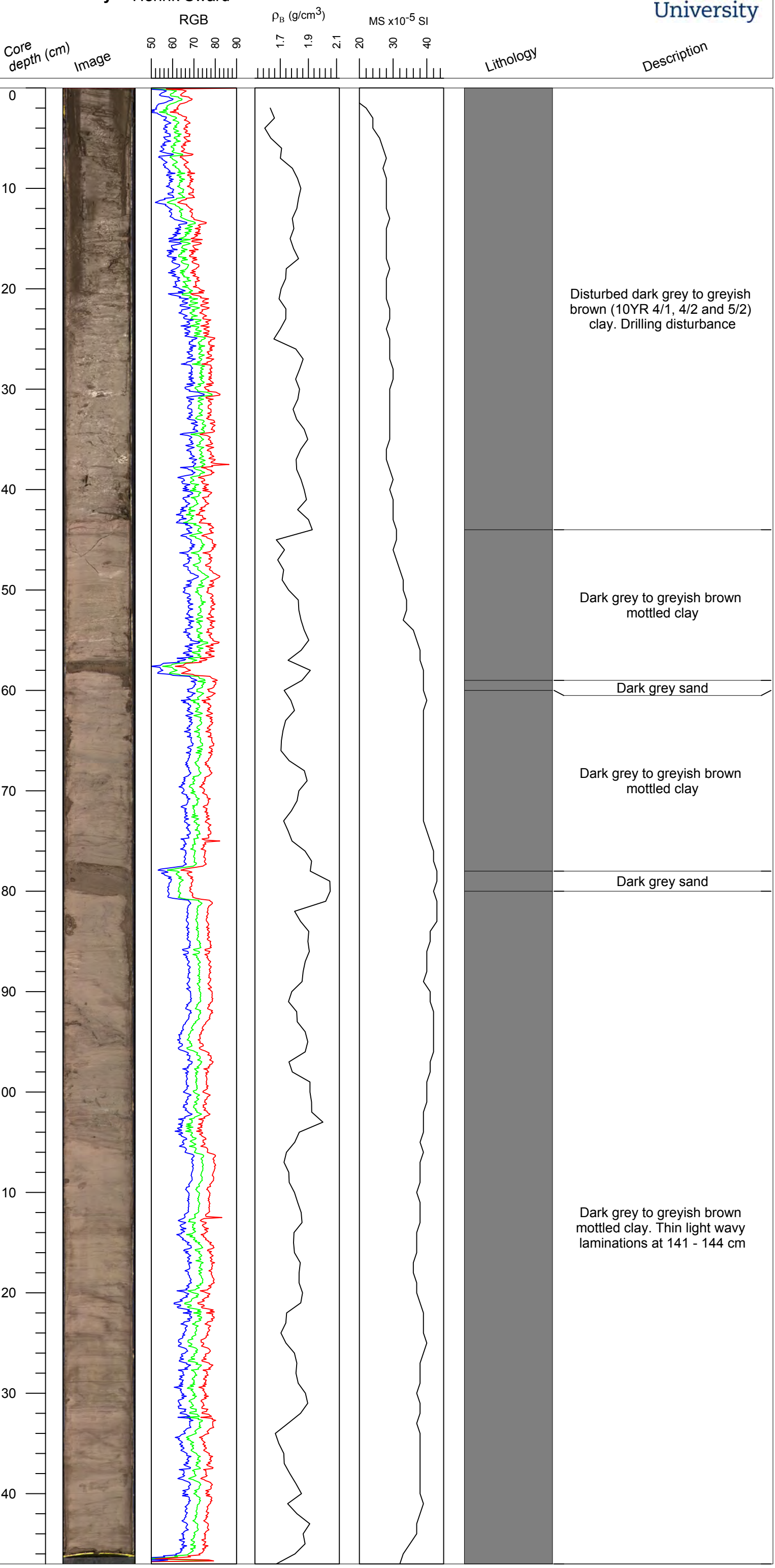

Core description
VÄTTERN 2012

VAT-12-D9 Sec: 2

Coring date: 2012-11-07 **MBLF (m):** 42.25 **Position:** N 57:49:59.62
E 14:11:03.48

Described by: Pedro Preto

Stockholm University

Core depth (cm) | Image | RGB 40 60 80 | ρ_B (g/cm^3) 1.7 1.9 | MS x10^{-5} SI 35 37.5 40 42.5 45 | Lithology | Description

147
157
167
177
187
197
207
217
227
237
247
257
267
277
287
297

Mottled brown (7.5YR 5/1) to grey (7.5YR 5/2) silty clay with lenses of sand interleaving the section. Sand related cracks at 4, 7, 17, 22 and 104 cm. Other thin sandy layers at 13, 20 - 22 and 38 cm.

Core description
VÄTTERN 2012

VAT-12-D10 Sec: 1

Coring date: 2012-11-07 **MBLF (m):** 45.25 **Position:** N 57:49:59.62
E 14:11:03.48

Described by: Henrik Swärd

Stockholm University

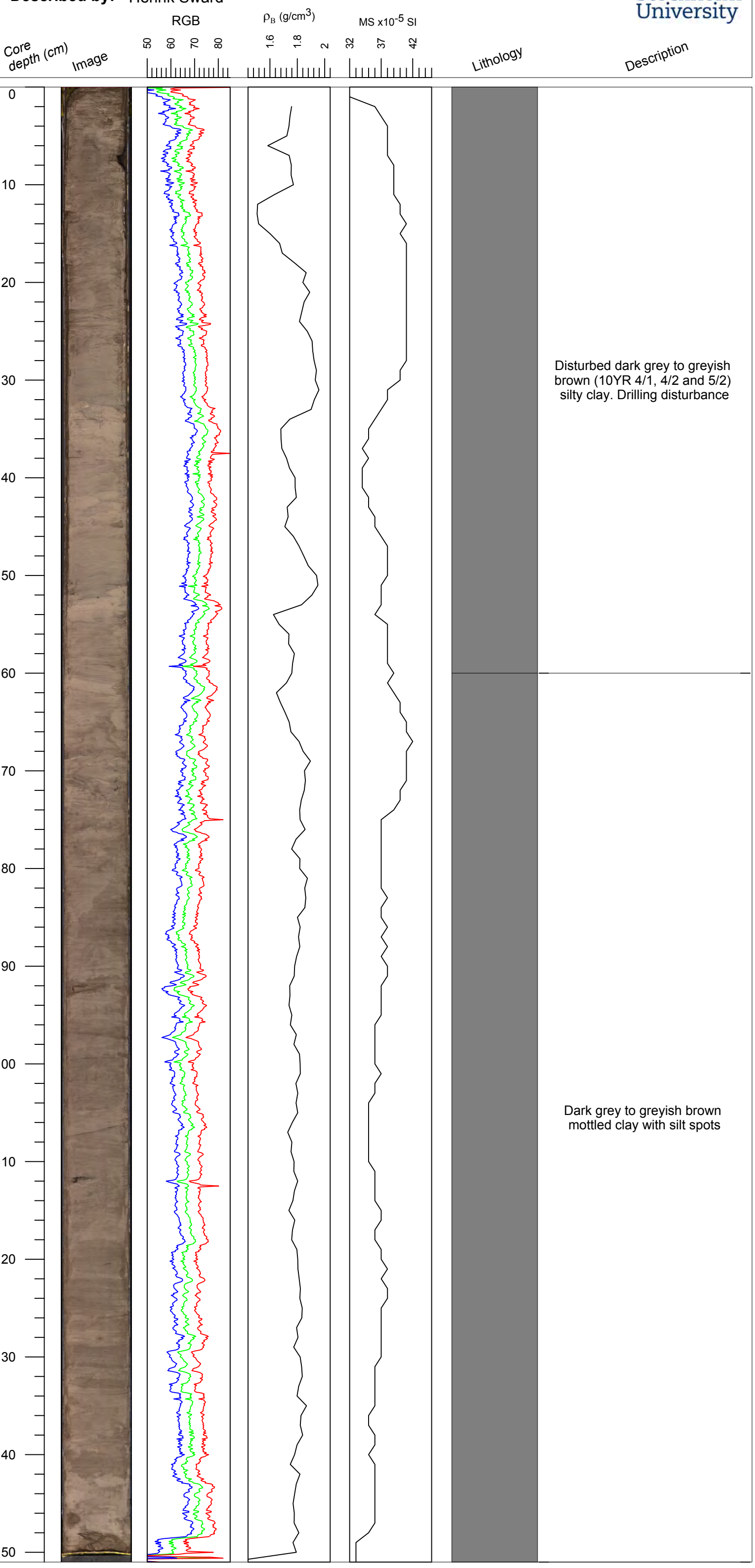

Core description
VÄTTERN 2012

VAT-12-D10 Sec: 2

Coring date: 2012-11-07 **MBLF (m):** 45.25 **Position:** N 57:49:59.62
E 14:11:03.48

Described by: Pedro Preto

Stockholm University

Core depth (cm) | Image | RGB 64 74 84 | ρ_B (g/cm^3) 1.7 1.8 1.9 2 | MS x10^{-5} SI 30 35 40 | Lithology | Description

151
161
171
181
191
201
211
221
231
241
251
261
271
281
291
301

Mottled grey to brown (7.5YR 5/1) silty clay layers (varves). 2 cm sand spot at 144 cm

Core description
VÄTTERN 2012

VAT-12-D11 Sec: 1

Coring date: 2012-11-07 **MBLF (m):** 48.25 **Position:** N 57:49:59.62
E 14:11:03.48

Described by: Pedro Preto

Stockholm University

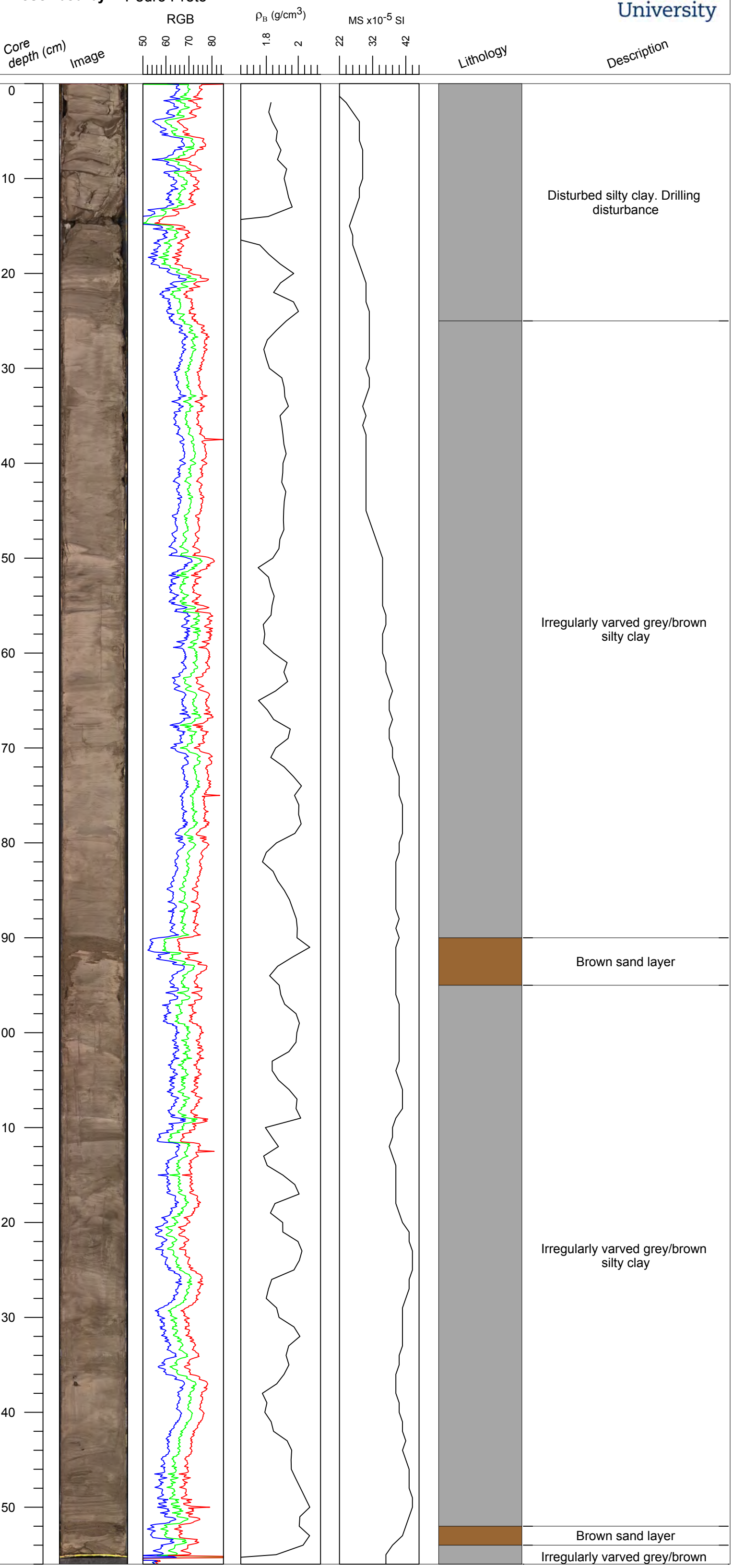

Core description
VÄTTERN 2012

VAT-12-D11 Sec: 2

Coring date: 2012-11-07 **MBLF (m):** 48.25 **Position:** N 57:49:59.62
E 14:11:03.48

Described by: Pedro Preto

Stockholm University

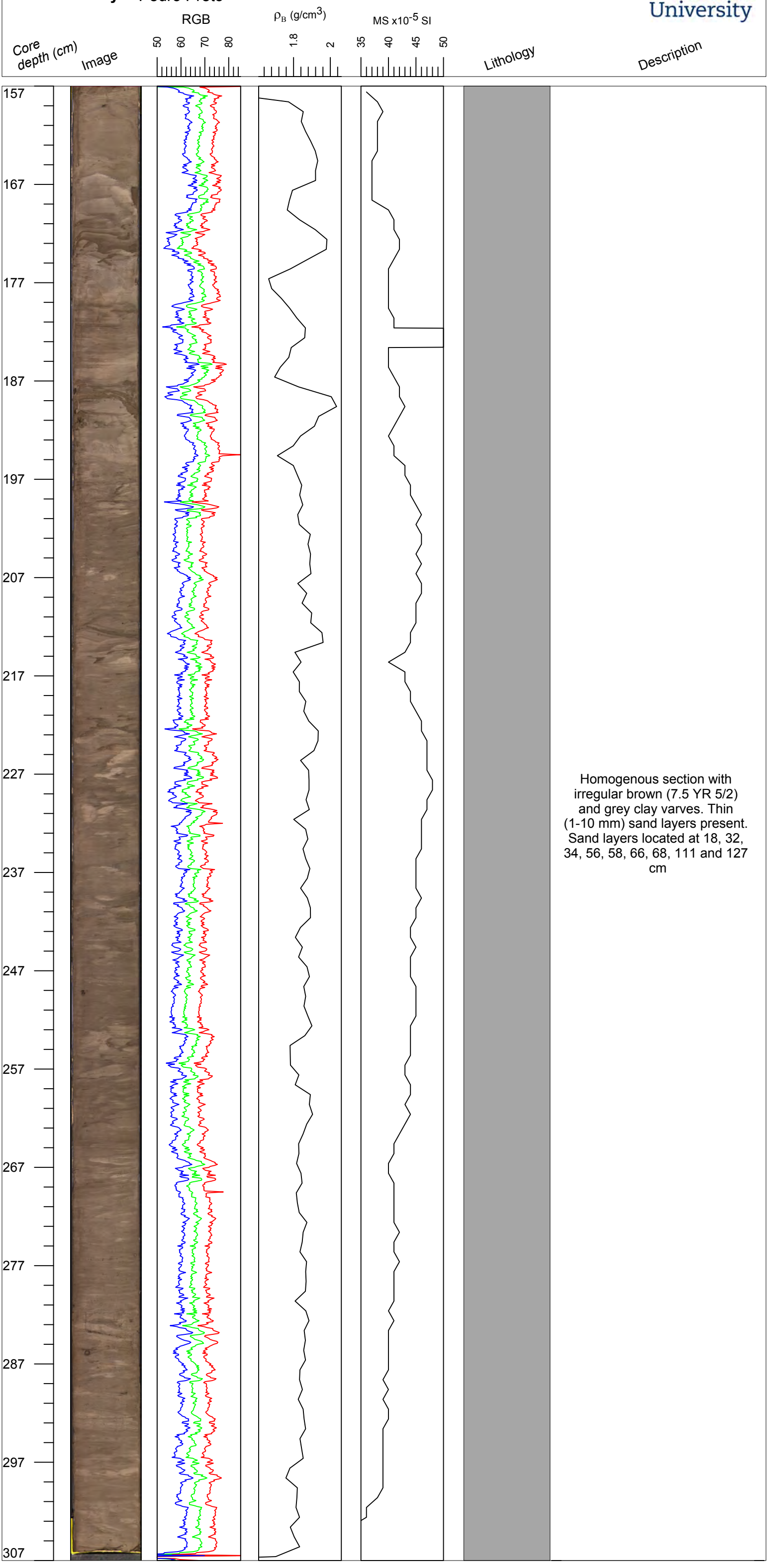

Homogenous section with irregular brown (7.5 YR 5/2) and grey clay varves. Thin (1-10 mm) sand layers present. Sand layers located at 18, 32, 34, 56, 58, 66, 68, 111 and 127 cm

Core description
VÄTTERN 2012

VAT-12-D12 Sec: 1

Coring date: 2012-11-07 **MBLF (m):** 51.25 **Position:** N 57:49:59.62
E 14:11:03.48

Described by: Pedro Preto

Stockholm University

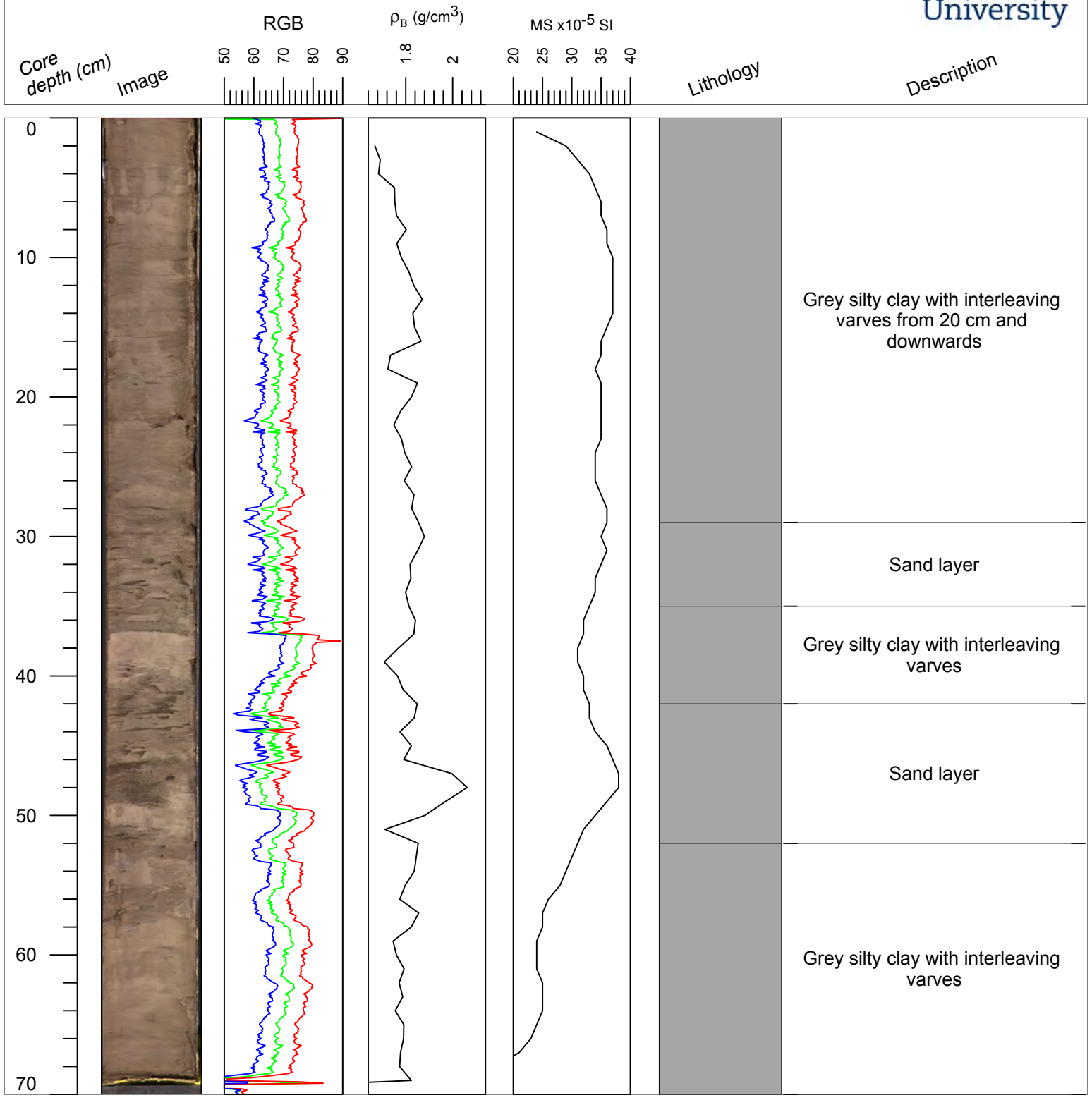

Core description
VÄTTERN 2012

VAT-12-D13 Sec: 1

Coring date: 2012-11-07 **MBLF (m):** 54.25 **Position:** N 57:49:59.62
E 14:11:03.48

Described by: Helena Alexandersson

Stockholm University

Core depth (cm) | Image | RGB 64 74 84 94 | ρ_B (g/cm^3) 1.8 2 | MS x10^{-5} SI 36 46 56 | Lithology | Description

0
10
20
30
40
50
60
70
80
90
100
110
120
130
140
150

Dark greyish brown clay

Dark greyish brown clayey silt

Dark greyish brown clay

Dark greyish brown clayey silt

Dark greyish brown clay

Dark greyish brown clayey silt

Dark greyish brown clay

Dark greyish brown deformed clayey silt with lamina

Dark greyish brown clay with thin silt streaks at top. Sharp lower boundary

Dark greyish brown laminated and deformed clayey silt withload casts

Dark greyish brown clay with silt streaks

Dark greyish brown laminated clayey silt

Dark greyish brown clay

Dark greyish brown laminated and deformed clayey silt

Dark greyish brown clay

Dark greyish brown laminated clayey silt

Dark greyish brown clay with irregular lower boundary

Dark greyish brown laminated clayey silt with silt/clay laminations

Grey clay

Grey deformed clayey silt

Core description
VÄTTERN 2012

VAT-12-D13 Sec: 1

Coring date: 2012-11-07 **MBLF (m):** 54.25 **Position:** N 57:49:59.62
E 14:11:03.48

Described by: Helena Alexandersson

Stockholm University

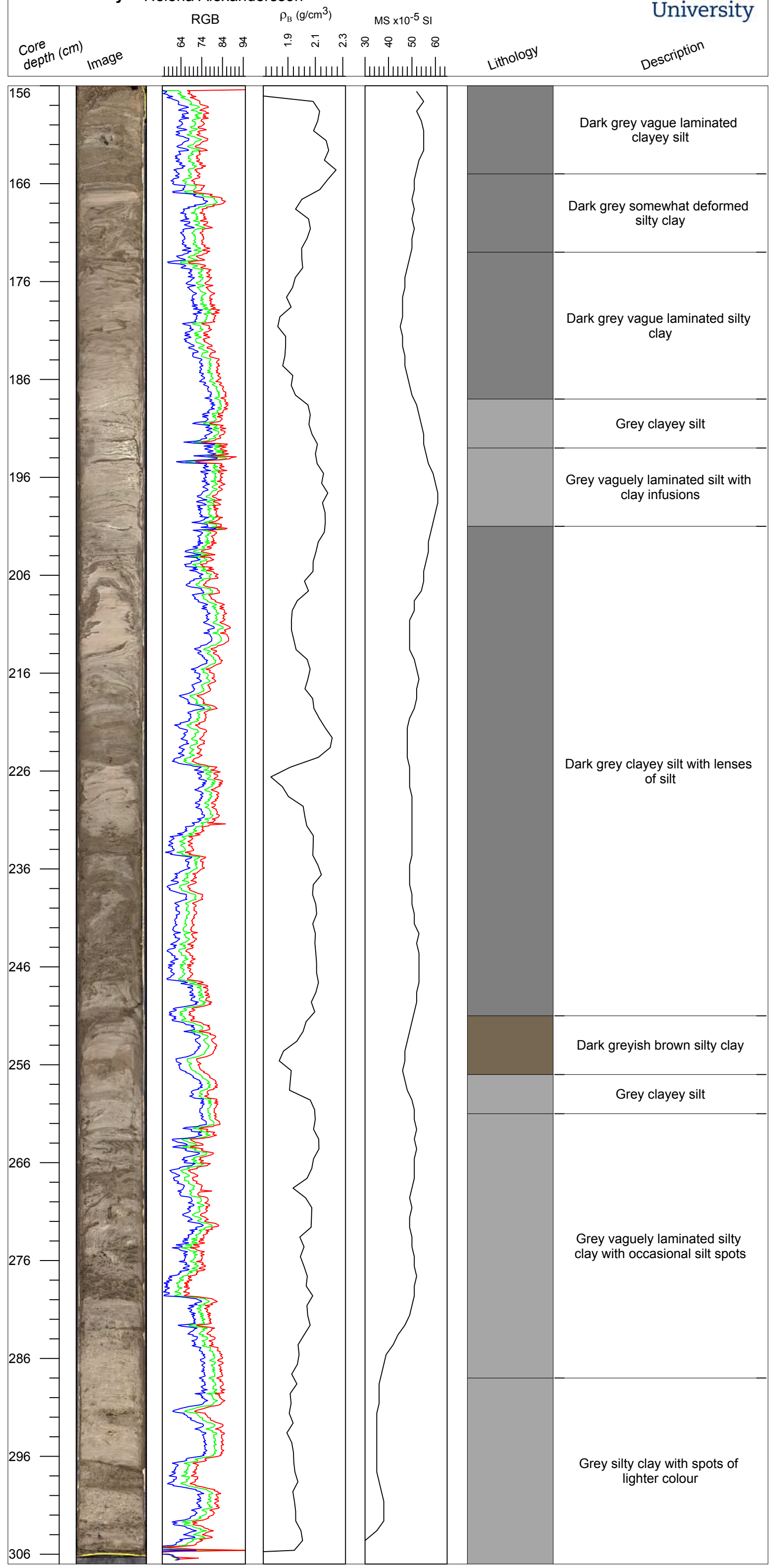

Core description
VÄTTERN 2012

VAT-12-D14 Sec: 1

Coring date: 2012-11-07 **MBLF (m):** 57.25 **Position:** N 57:49:59.62
E 14:11:03.48

Described by: Henrik Swärd

Stockholm University

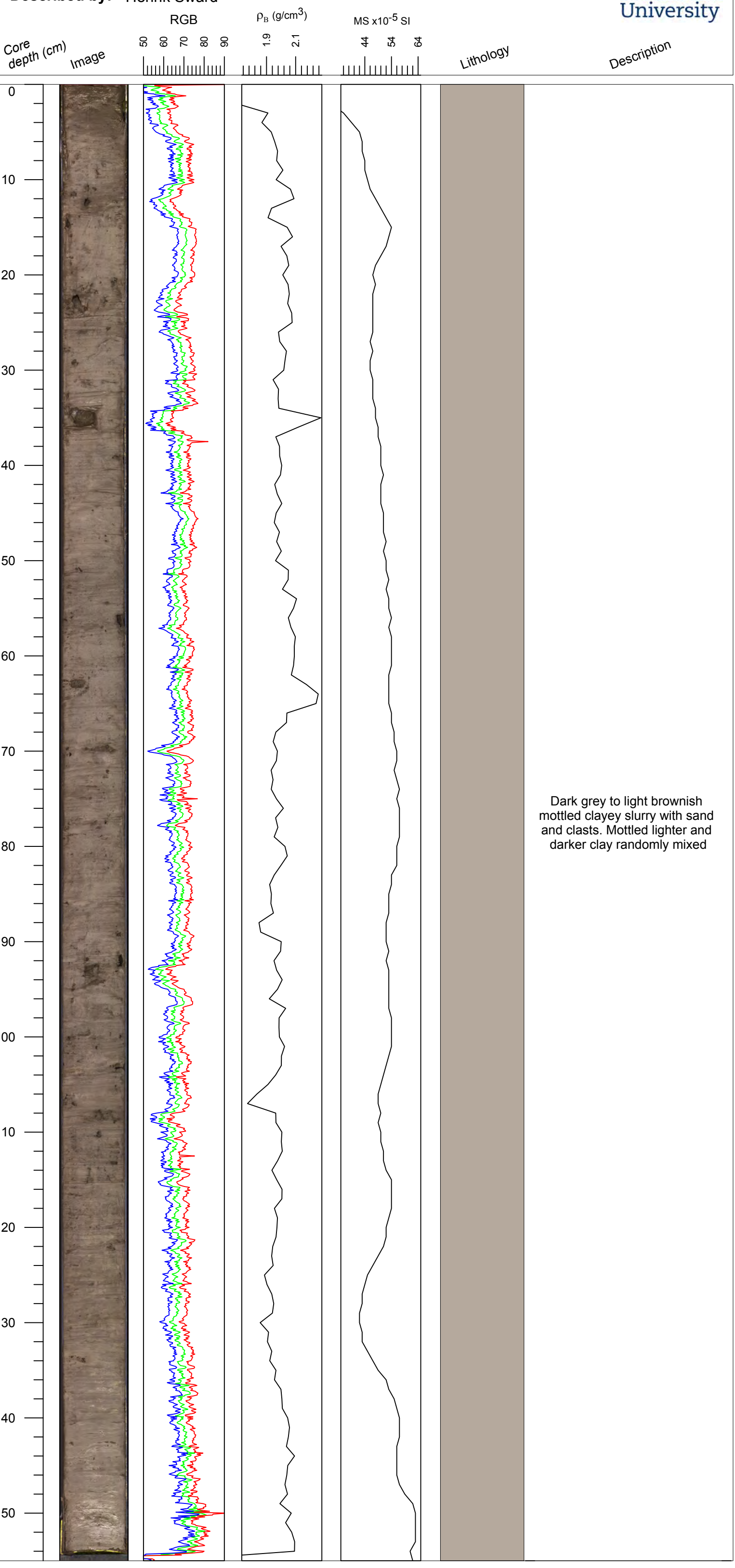

Core description
VÄTTERN 2012

VAT-12-D14 Sec: 2

Coring date: 2012-11-07 **MBLF (m):** 57.25 **Position:** N 57:49:59.62
E 14:11:03.48

Described by: Pedro Preto

Stockholm University

RGB ρ_B (g/cm^3) MS x10^{-5} SI

Core depth (cm) | Image | 40 60 80 | 1.8 1.9 2 2.1 | 46 56 66 | Lithology | Description

155
165
175
185
195
205
215
225
235
245
255
265
275
285
295
305

Very wet grey silty clay slurry

Wet silty clay with intercalation of greyish and brownish layers (varves) from 260 cm. With brown laminations

Core description
VÄTTERN 2012

E3-1

Sec: 1

Coring date: 2012-11-08 **MBLF (m):** 0.25 **Position:** N 57:49:59.60
E 14:11:03.53

Described by: Tina Varga

Stockholm University

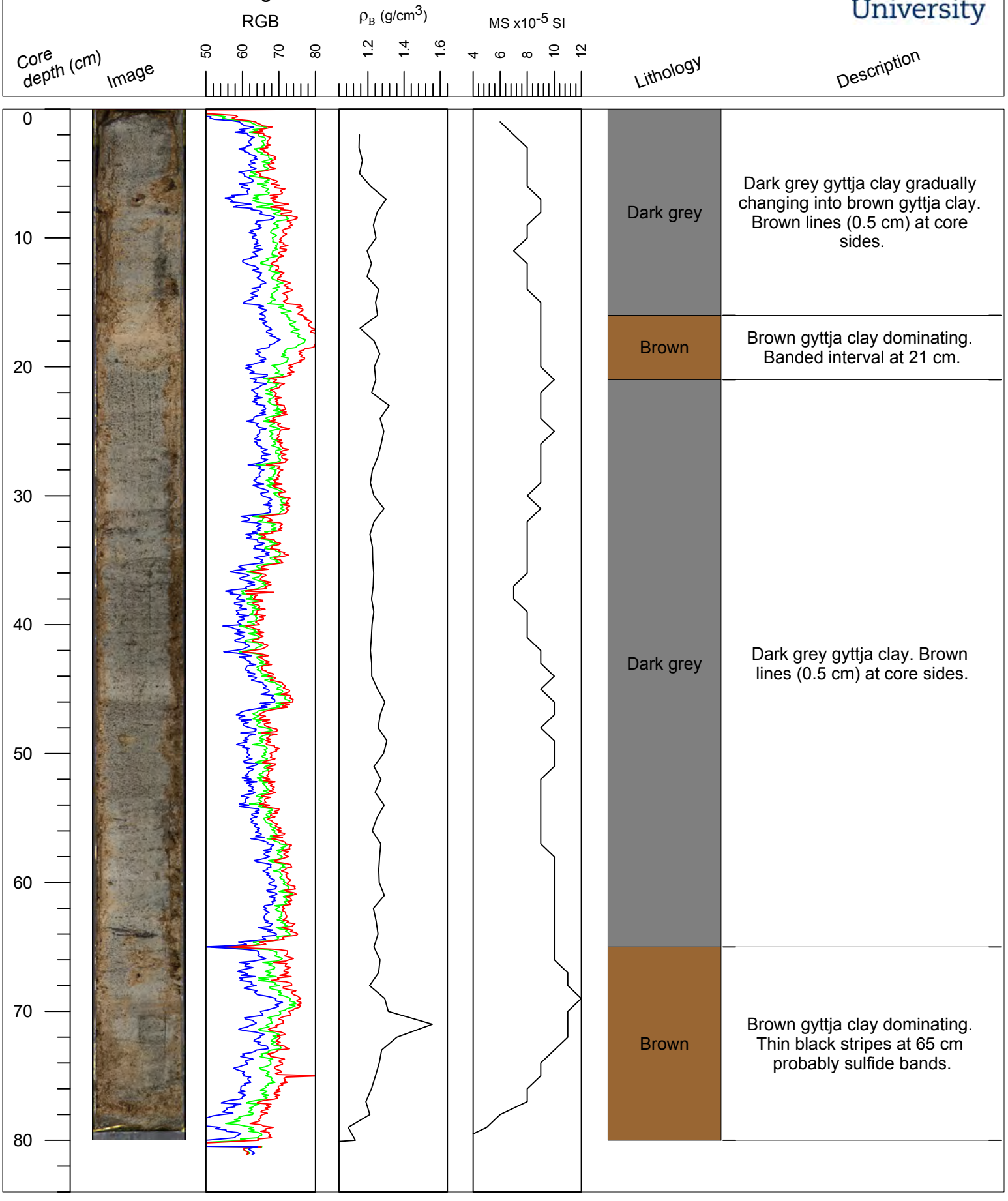

Core description
VÄTTERN 2012

VAT-12-E4 Sec: 1

Coring date: 2012-11-08 **MBLF (m):** 3.25 **Position:** N 57:49:59.60
E 14:11:03.53

Described by: Tina Varga

Stockholm University

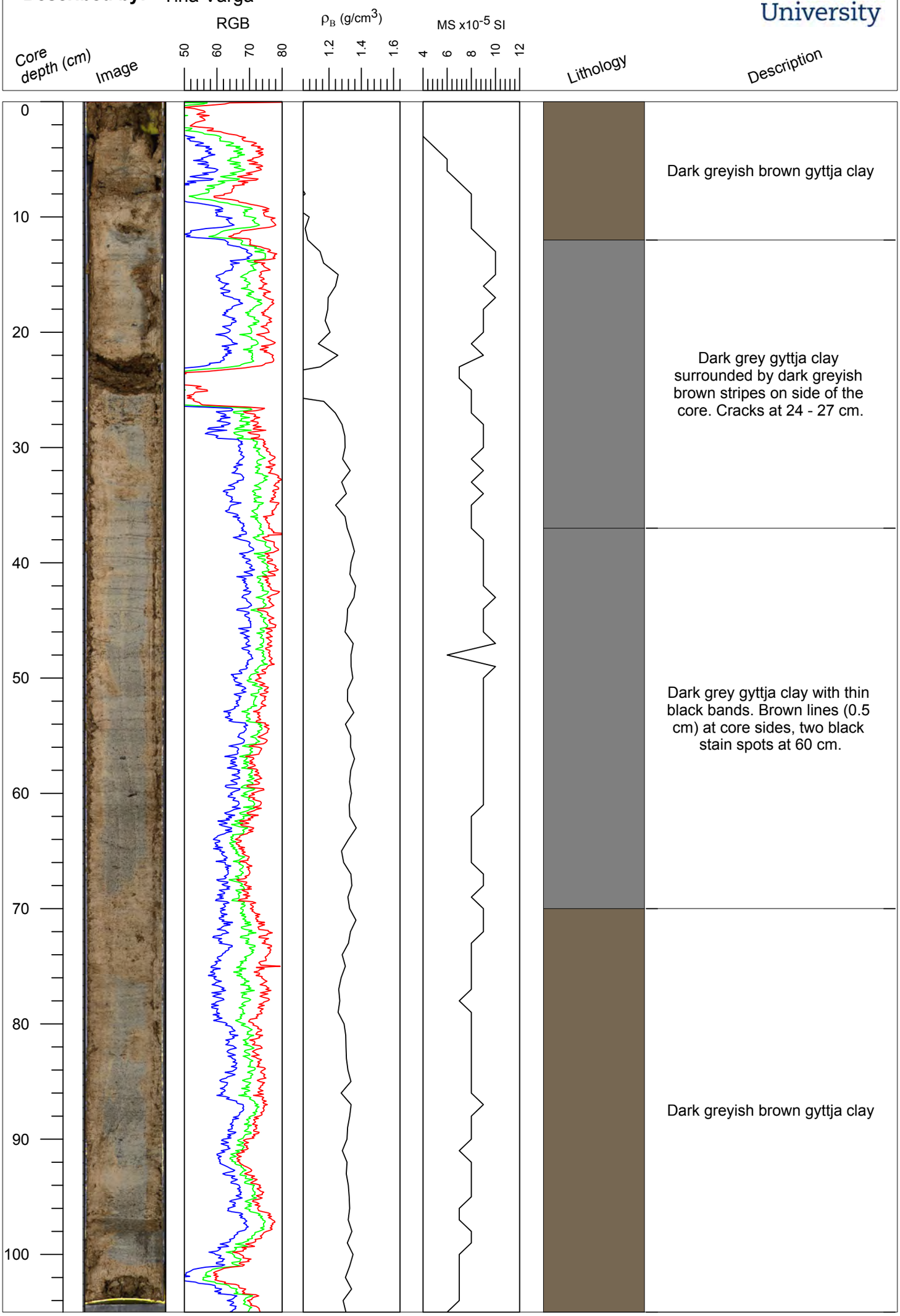

Core description
VÄTTERN 2012

E5-1

Sec: 1

Coring date: 2012-11-08 **MBLF (m):** 6.25 **Position:** N 57:49:59.60
E 14:11:03.53

Described by: Tina Varga

Stockholm University

Core depth (cm) | Image | RGB 50 60 70 80 | ρ_B (g/cm^3) 1.2 1.4 1.6 | MS x10^{-5} SI 4 6 8 10 12 | Lithology | Description

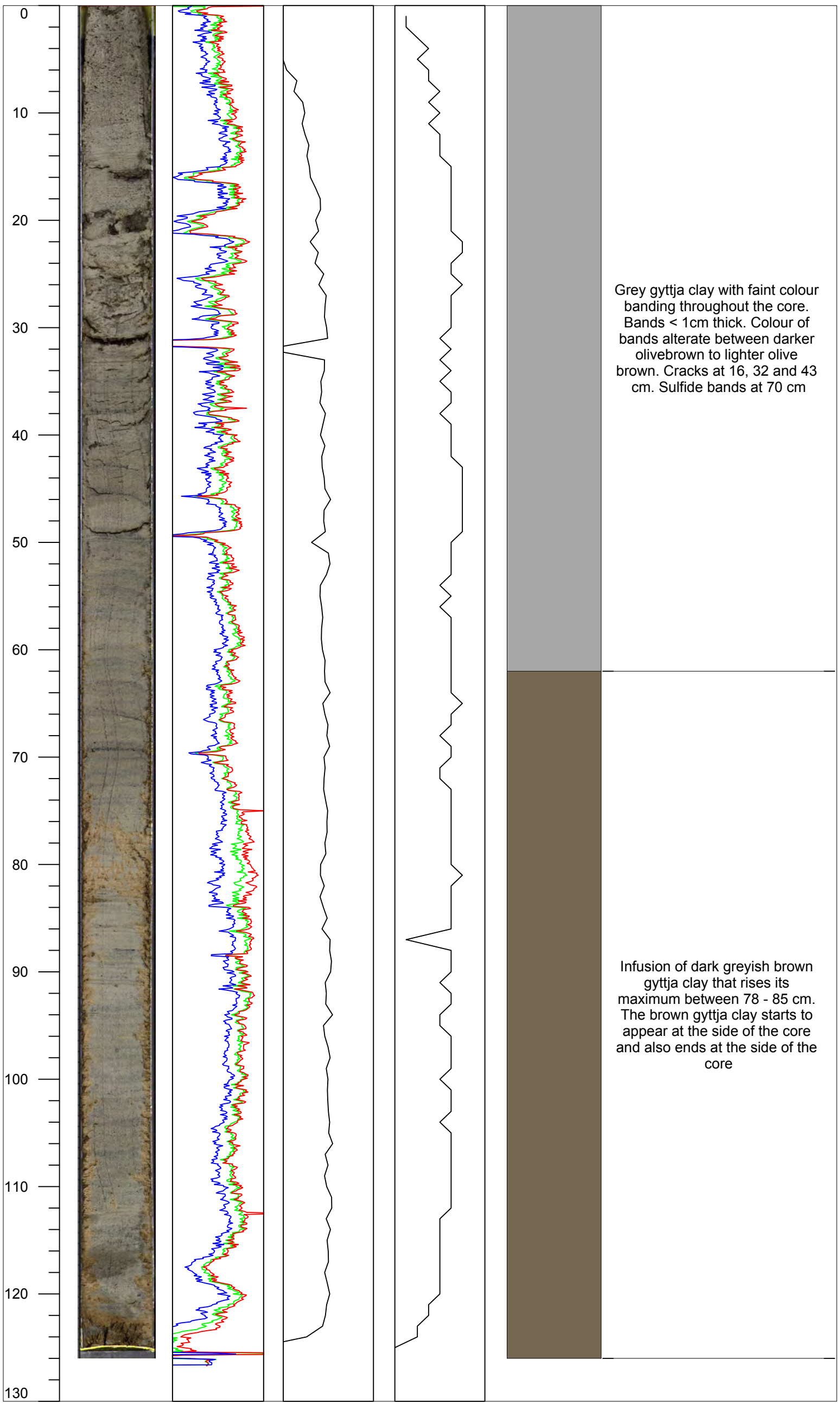

Grey gyttja clay with faint colour banding throughout the core. Bands < 1cm thick. Colour of bands alterate between darker olivebrown to lighter olive brown. Cracks at 16, 32 and 43 cm. Sulfide bands at 70 cm

Infusion of dark greyish brown gyttja clay that rises its maximum between 78 - 85 cm. The brown gyttja clay starts to appear at the side of the core and also ends at the side of the core

Core description
VÄTTERN 2012

VAT-12-E6 Sec: 1

Coring date: 2012-11-08 **MBLF (m):** 9.25 **Position:** N 57:49:59.60
E 14:11:03.53

Described by: Linda Ampel

Stockholm University

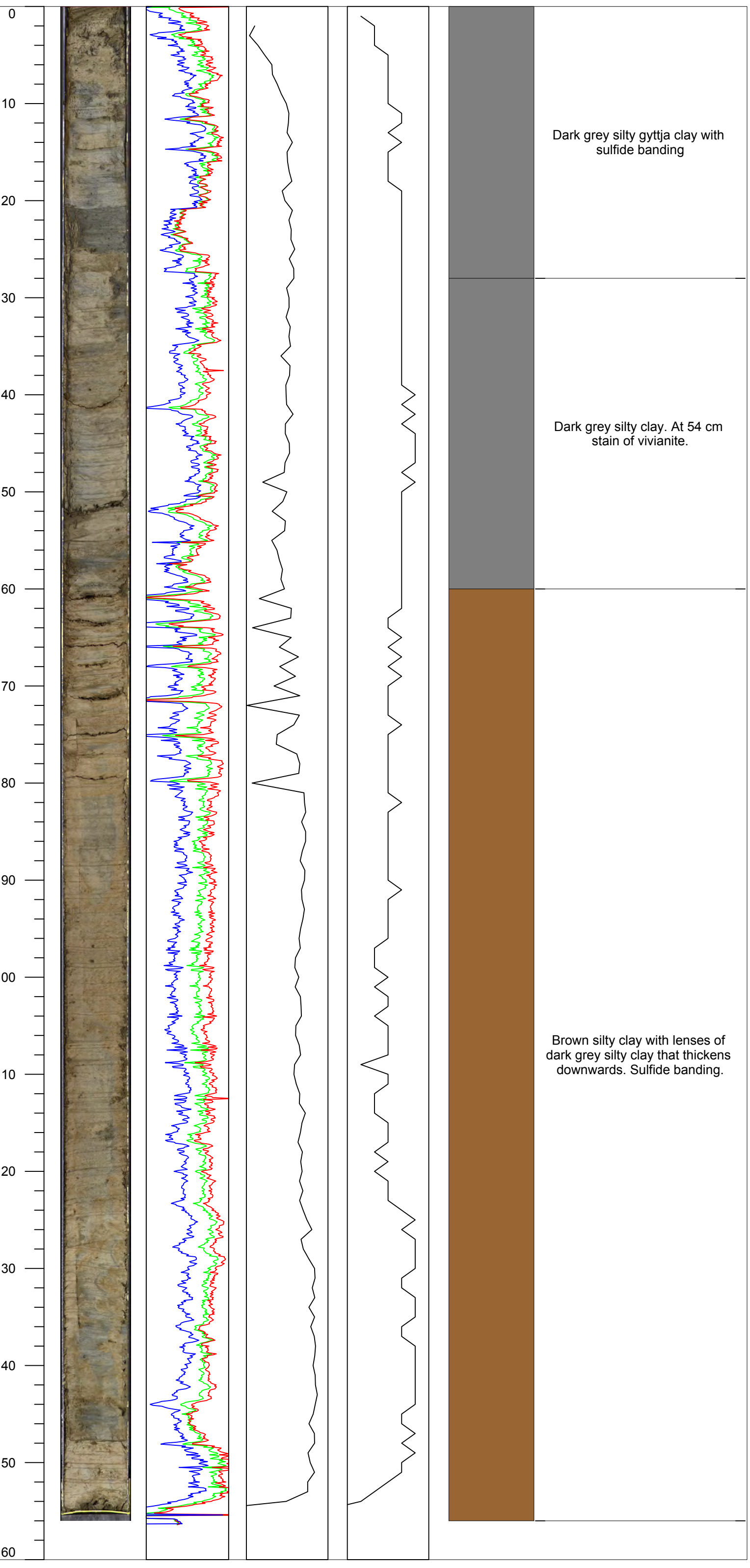

Core description
VÄTTERN 2012

VAT-12-E7 Sec: 1

Coring date: 2012-11-08 **MBLF (m):** 12.25 **Position:** N 57:49:59.60
E 14:11:03.53

Described by: Tina Varga

Stockholm University

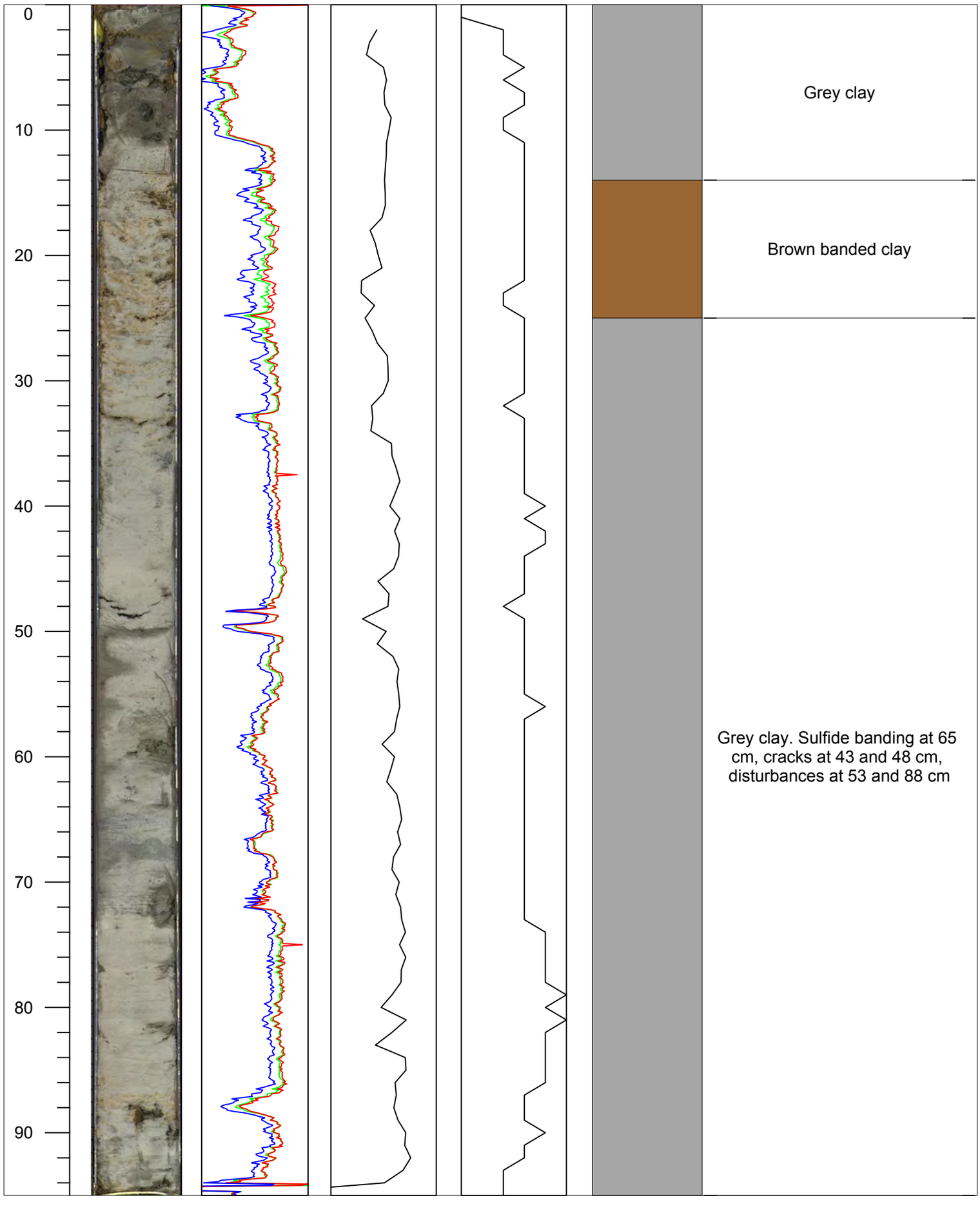

Core description
VÄTTERN 2012

VAT-12-E7 Sec: 2

Coring date: 2012-11-08 **MBLF (m):** 12.25 **Position:** N 57:49:59.60
E 14:11:03.53

Described by: Tina Varga

Stockholm University

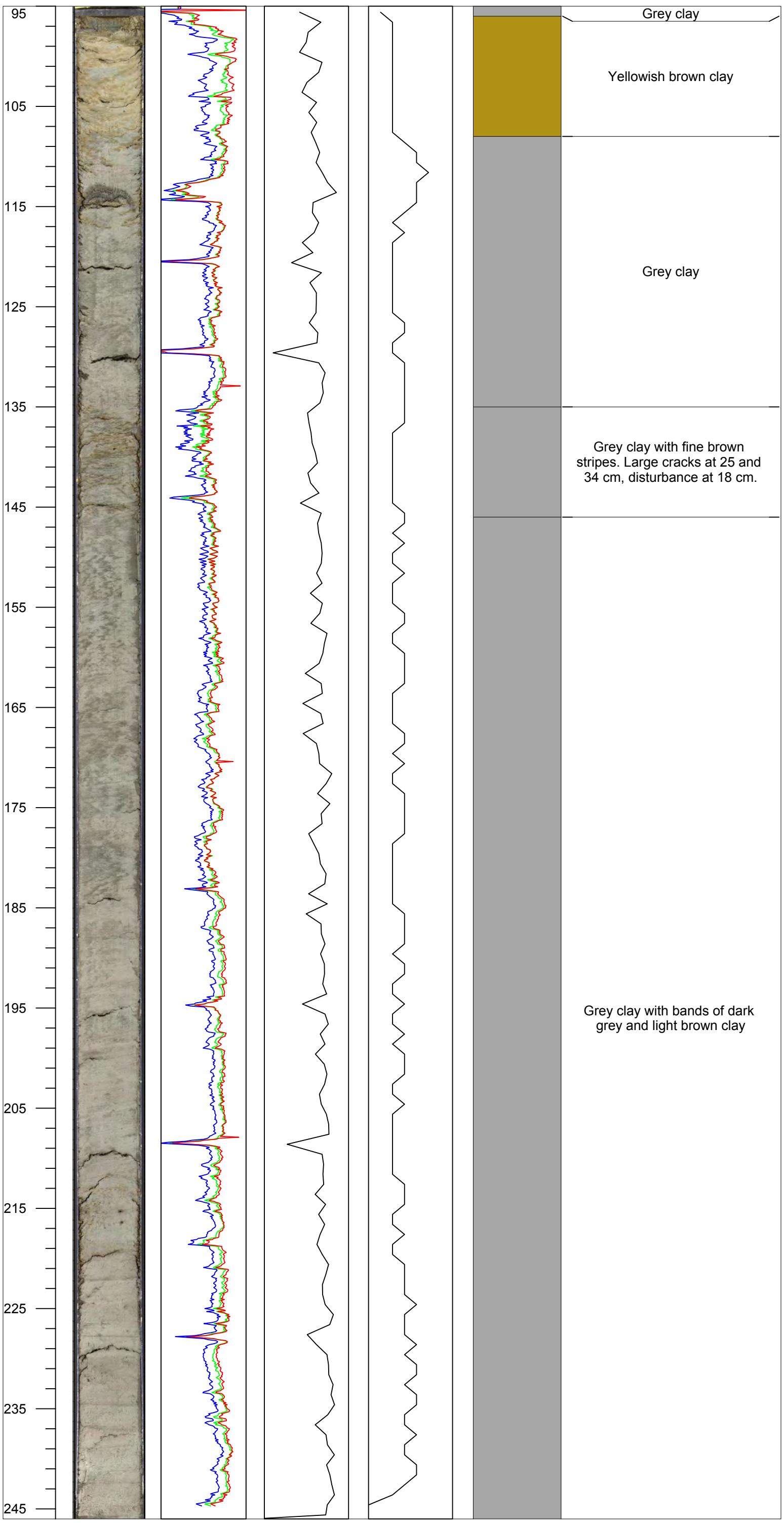

Core description
VÄTTERN 2012

VAT-12-E8 Sec: 1

Coring date: 2012-11-08 **MBLF (m):** 15.25 **Position:** N 57:49:59.60
E 14:11:03.53

Described by: Tina Varga

Stockholm University

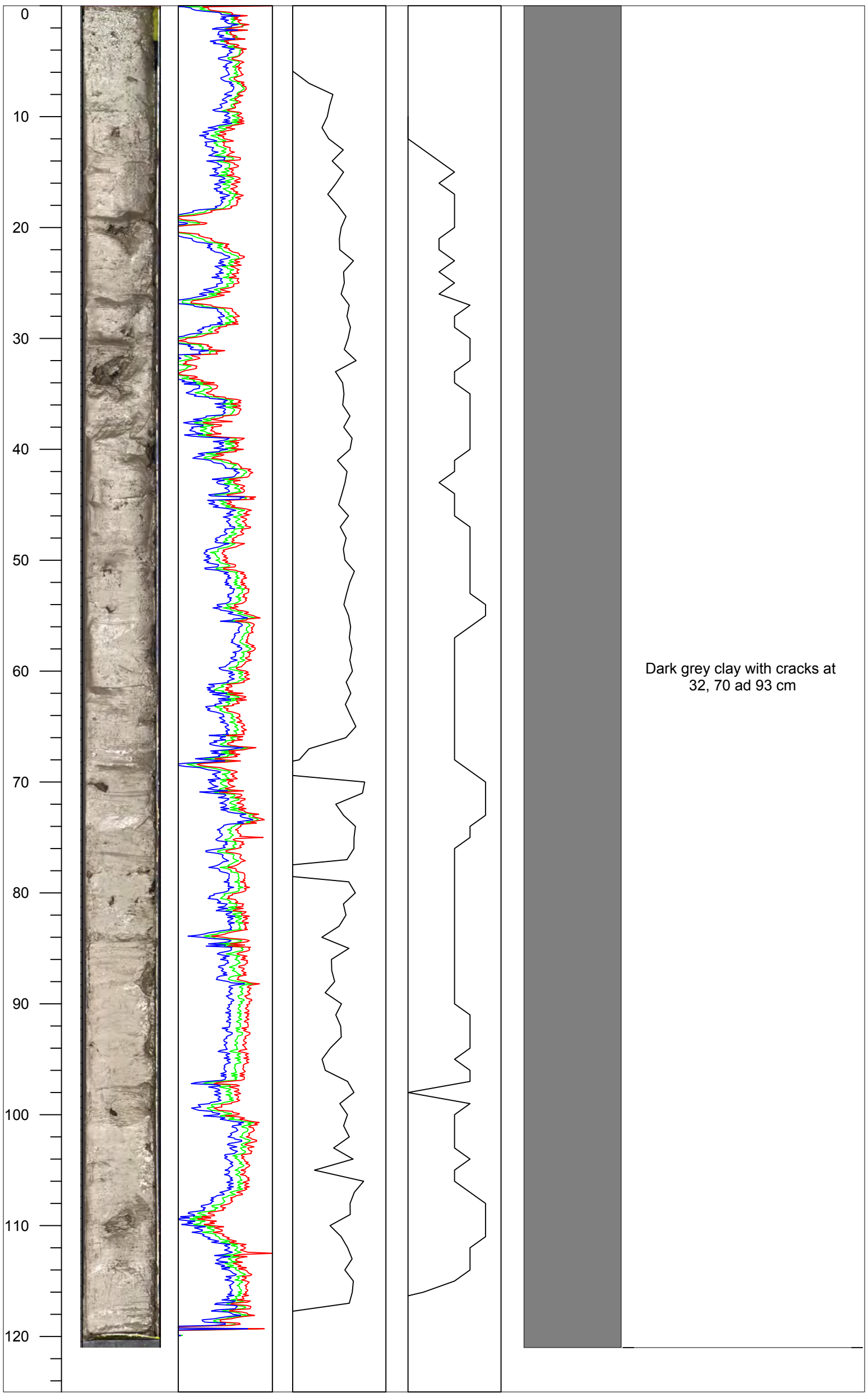

Core description
VÄTTERN 2012

VAT-12-E9 Sec: 1

Coring date: 2012-11-08 **MBLF (m):** 18.25 **Position:** N 57:49:59.60
E 14:11:03.53

Described by: Svante Björck

Stockholm University

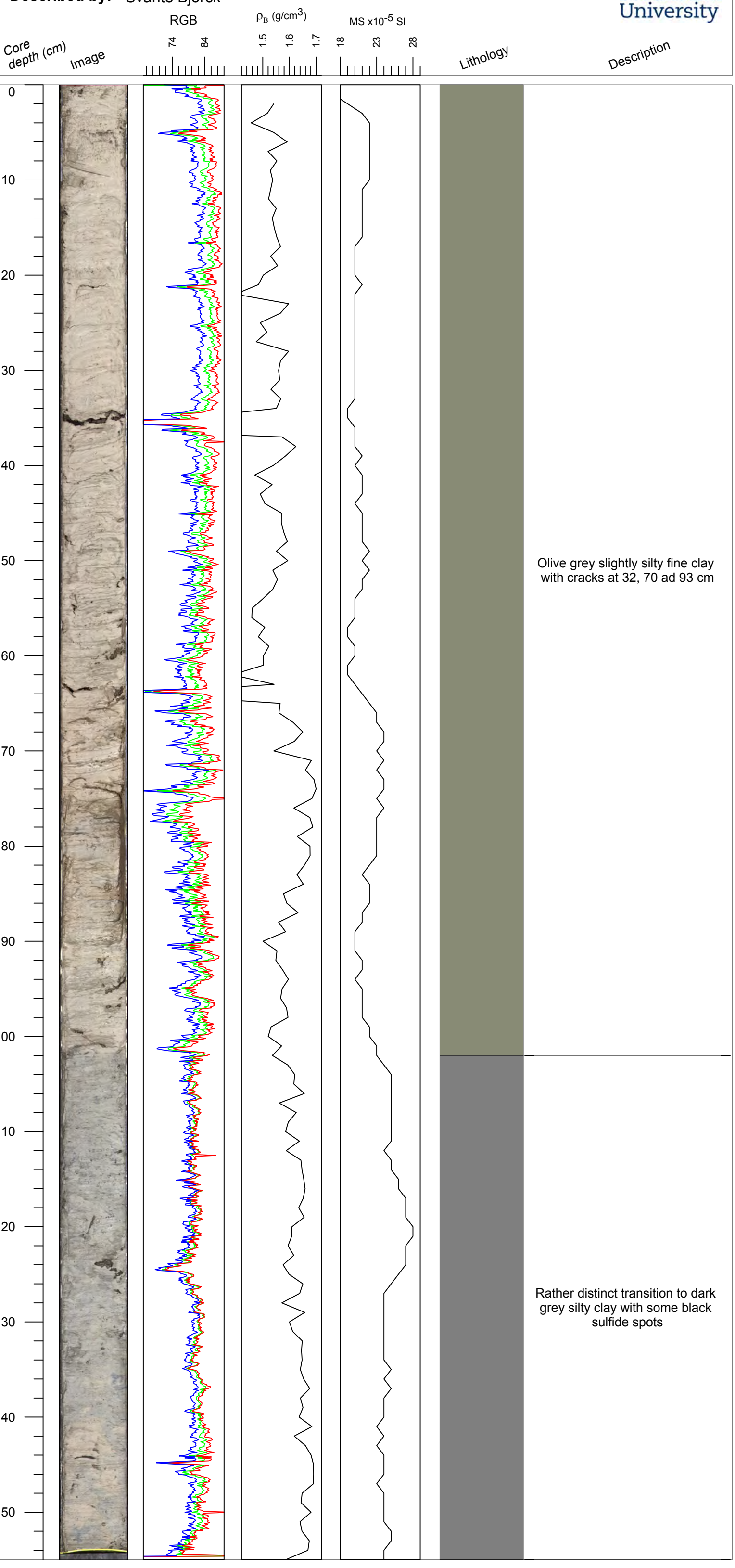

Core description
VÄTTERN 2012

VAT-12-E9 Sec: 2

Coring date: 2012-11-08 **MBLF (m):** 18.25 **Position:** N 57:49:59.60
E 14:11:03.53

Described by: Tina Varga

Stockholm University

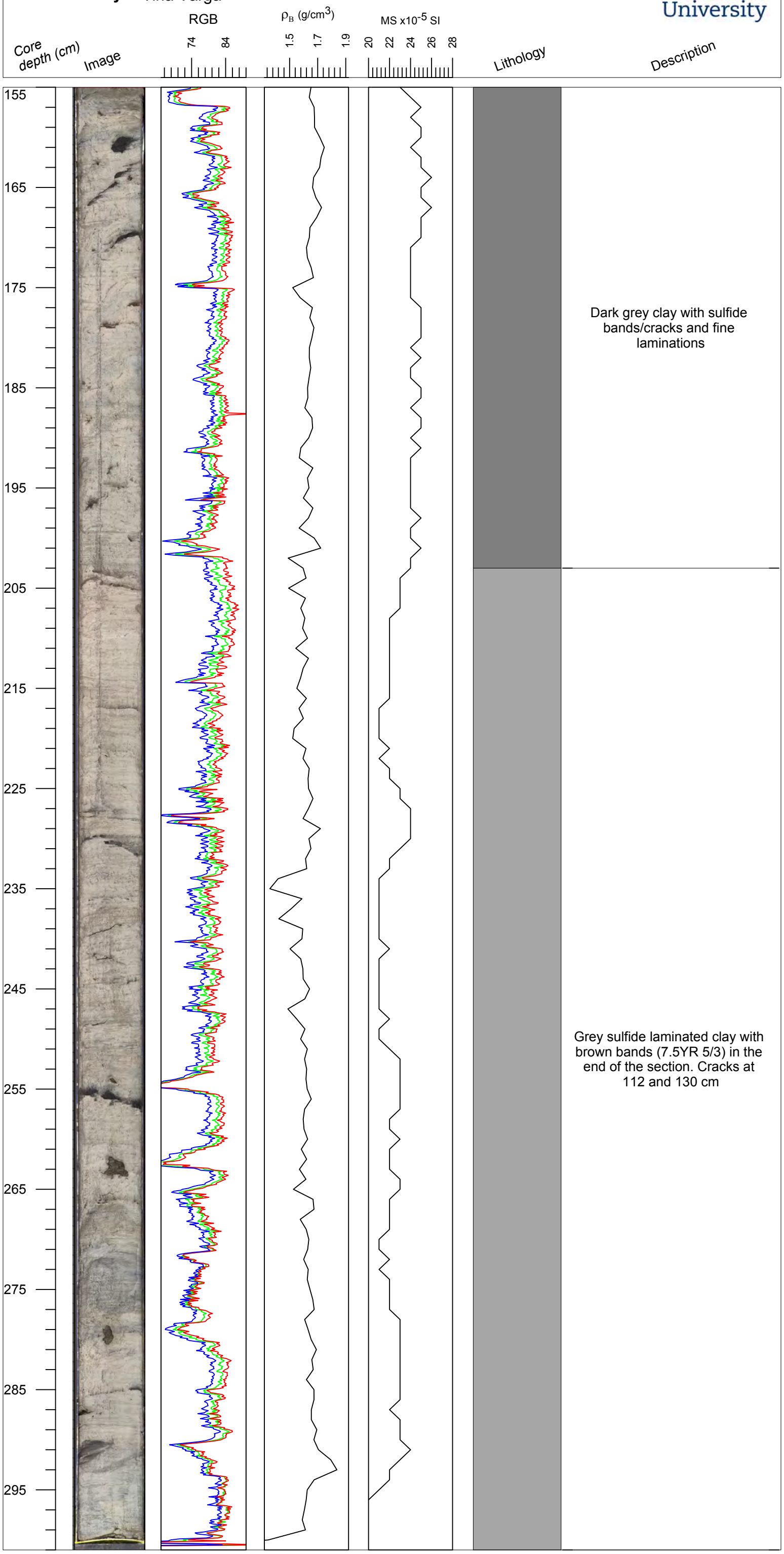

Core description
VÄTTERN 2012

VAT-12-E10 Sec: 1

Coring date: 2012-11-08 **MBLF (m):** 21.25 **Position:** N 57:49:59.60
E 14:11:03.53

Described by: Linda Ampel

Stockholm University

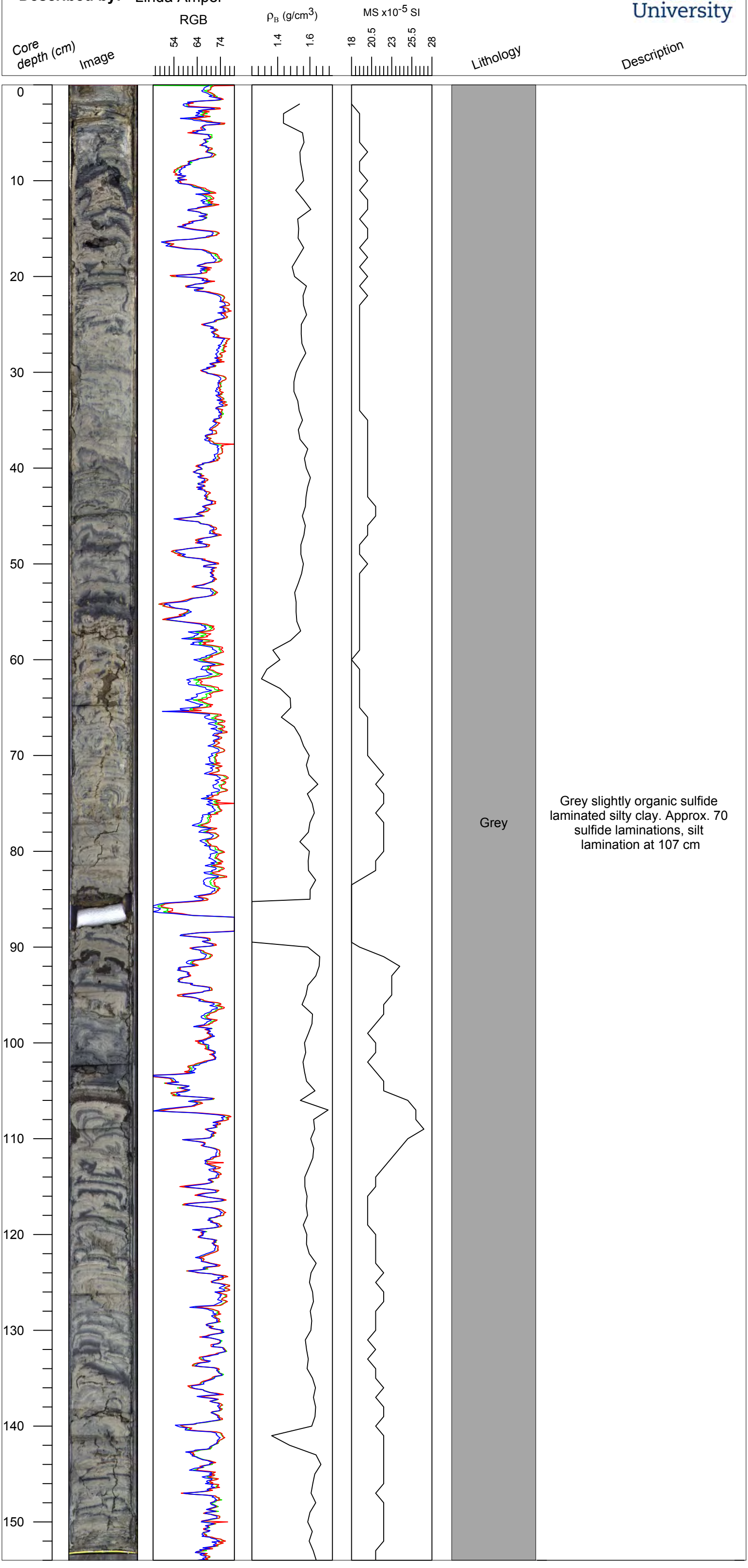

Core description
VÄTTERN 2012

VAT-12-E10 Sec: 2

Coring date: 2012-11-08 **MBLF (m):** 21.25 **Position:** N 57:49:59.60
E 14:11:03.53

Described by: Helena Alexandersson

Stockholm University

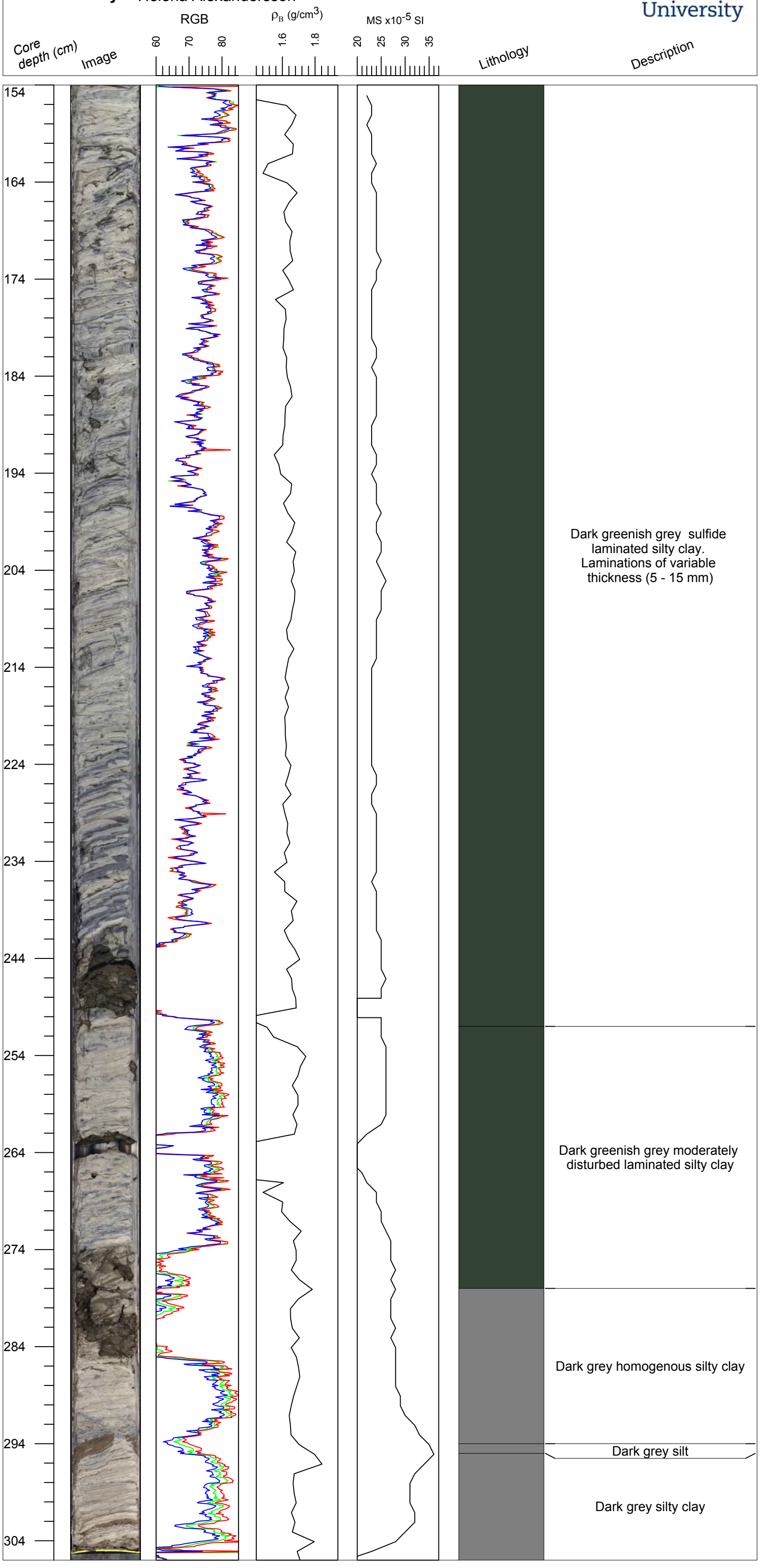

Core description
VÄTTERN 2012

VAT-12-PC2 Sec: 4

Coring date: 2012-06-29 **MBLF (m):** 0.00 **Position:** N 57:50:00.35
E 14:11:02.79

Described by: Henrik Swärd

Stockholm University

Core depth (cm) | Image | RGB (50, 60, 70, 80) | ρ_B (g/cm^3) (0.96, 1.2, 1.4) | MS x10^{-5} SI (10, 12, 14, 16) | Lithology | Description

Dark olive brown silty gyttja clay with black laminations and furthermore a dark/ligth alteration (varves?) ending up in a gradational boundary into the next unit

Olive brown silty gyttja clay with black laminations

Core description
VÄTTERN 2012

VAT-12-PC1 Sec: 4

Coring date: 2012-06-29 **MBLF (m):** 0.00 **Position:** N 57:50:00.35
E 14:11:02.79

Described by: Henrik Swärd

Stockholm University

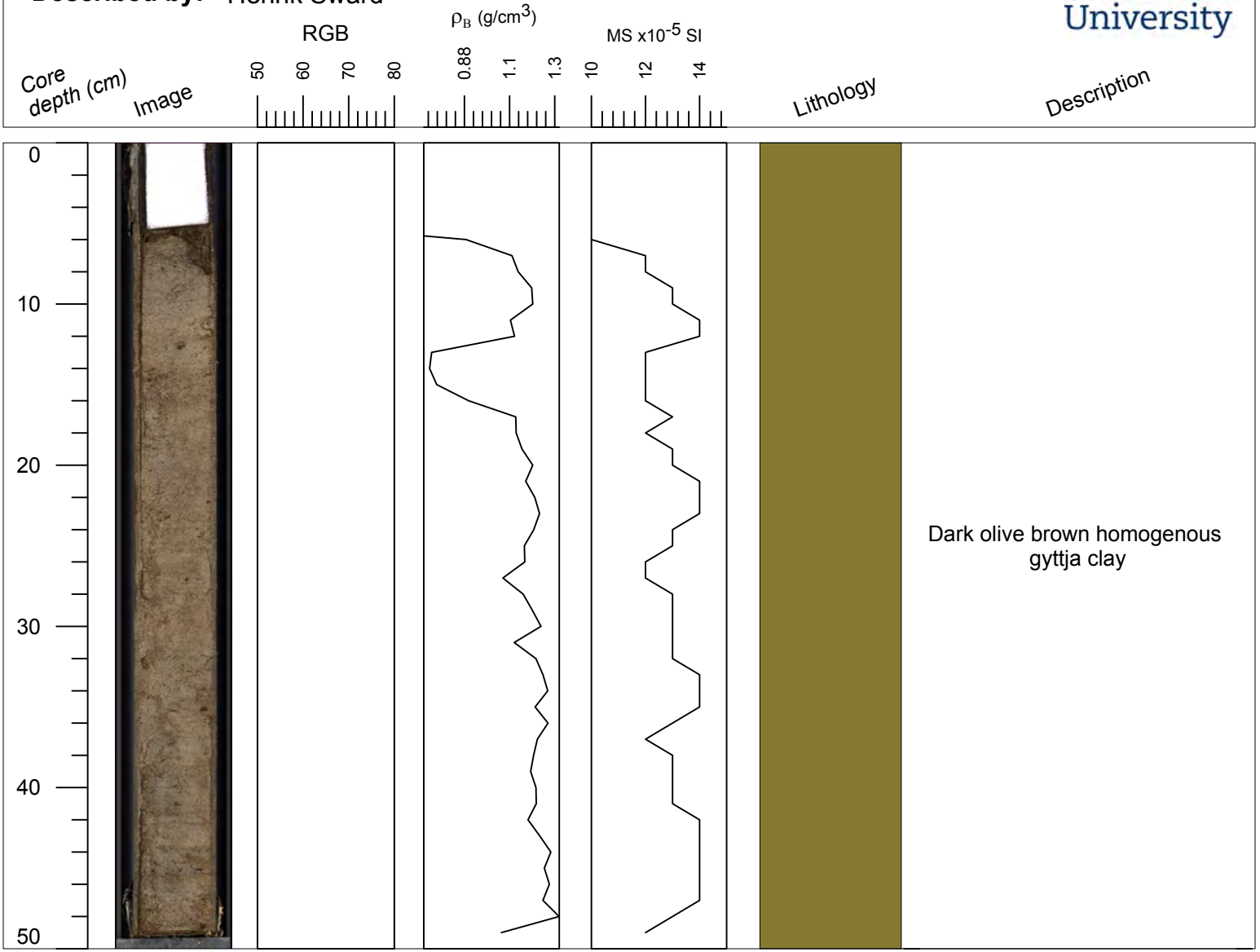

Core description
VÄTTERN 2012

VAT-12-PC1 Sec: 2

Coring date: 2012-06-29 **MBLF (m):** 0.00 **Position:** N 57:50:00.35
E 14:11:02.79

Described by: Henrik Swärd

Stockholm University

Core depth (cm) | Image | RGB 40 50 60 70 | ρ_B (g/cm^3) 1.2 1.4 | MS x10^{-5} SI 10 12.5 15 17.5 20 | Lithology | Description

200
210
220
230
240
250
260
270
280
290
300
310
320
330
340
350

Partly filled liner with olive brown silty clay

Olive brown silty clay with spots/lenses of dark yellowish brown (10YR 4/6) silty clay

No recovery

Olive brown silty clay with spots/lenses of dark yellowish brown (10YR 4/6) silty clay

Gap

Dark greyish brown silty clay with black stripes

Gap

Dark greyish brown silty clay with black stripes

Gap

Dark greyish brown silty clay with black stripes

Gap

Dark greyish brown silty clay with black stripes. Cracks at 103 and 107 cm

Gap

Dark greyish brown silty clay with black stripes. Lot´s of cracks

Core description
VÄTTERN 2012

VAT-12-PC1 Sec: 3

Coring date: 2012-06-29 **MBLF (m):** 0.00 **Position:** N 57:50:00.35
E 14:11:02.79

Described by: Henrik Swärd

Stockholm University

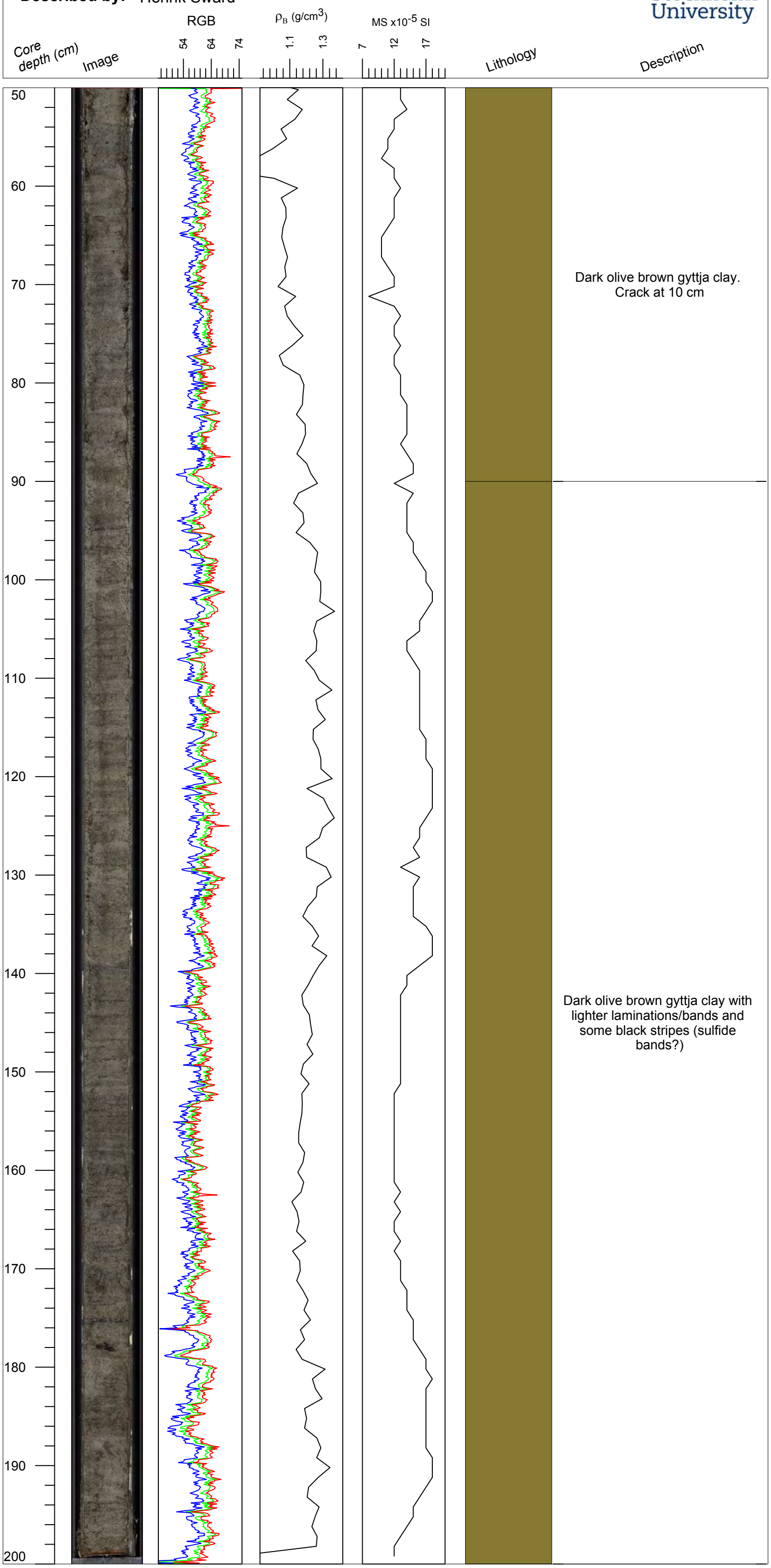

Core description
VÄTTERN 2012

VAT-12-PC1 Sec: 1

Coring date: 2012-06-29 **MBLF (m):** 0.00 **Position:** N 57:50:00.35
E 14:11:02.79

Described by: Henrik Swärd

Stockholm University